UNIVERSITY
OF THE
WITWATERSRAND
JOHANNESBURG

Patch Antenna Design

Gareth Louis Shaw

A dissertation submitted to the Faculty of Engineering and the Built Environment, University of the Witwatersrand, Johannesburg, in fulfilment of the requirements for the degree of Master of Science in Engineering.

Johannesburg, April 2005

Declaration

I declare that this is my own, unaided work, except where otherwise acknowledged. It is being submitted for the degree of Master of Science in Engineering at the University of the Witwatersrand, Johannesburg. It has not been submitted before for any degree or examination at any other university.

Signed this ________ day of ______________________________ 2005

____

Gareth Louis Shaw.

Abstract

This paper describes the formulation of a design procedure for the rectangular, probe-fed and rectangular, electromagnetically coupled patch antennas. The design procedure is presented in the form of design curves. The design curve data was generated by solving a bandwidth optimization problem subject to a specified minimum gain constraint. Given a particular performance requirement, an appropriate antenna geometry can be found using the design curves. An unavoidable tradeoff between the gain and impedance bandwidth performance parameters is evident from the design curves. The bandwidth and minimum gain configurations for design of the probe-fed patch range from 6.2% and 9.9dBi to 13.2% and 6.1dBi respectively. The bandwidth and minimum gain configurations for design of the electromagentically coupled patch range from 9.5% and 9.7dBi to 44% and 6.0dBi respectively.

Acknowledgements

I wish to thank the following people for their contributions to this MSc research project:

Prof. Alan Clark, for his supervision and guidance of this research.

OPTI-NUM solutions, for encouraging this MSc and supporting it financially.

Poynting Innovations and Poynting Software, for providing SUPERNECsoftware and hardware necessary for antenna measurements.

Dr. Grant Grobbelaar, for his insight, numerous helpful suggestions and always being willing to discuss MSc related issues during working hours.

Brandon Orchard, MSc Eng. (Elec.), for his help getting started with LaTeXand SUPERNEC.

James Longshaw, BSc Eng. (Elec.), for his patient assistance with performing patch antenna measurements.

Foreword

This dissertation is presented to the University of the Witwatersrand, Johannesburg, South Africa for the degree of Master of Science in Engineering.

The title of the dissertation is “Patch Antenna Design”. This research focuses on the generation of design curves for two basic patch antenna configurations: the rectangular probe-fed patch and the rectangular electromagentically coupled patch. Simulation of these antennas is investigated and correlation between the antenna’s geometrical and electrical parameters is quantified. Design curve data for these antennas is generated by solving an impedance bandwidth optimization problem subject to a particular minimum gain constraint over the frequency band of operation.

This document complies with the university’s so-called “paper model” format, and although the actual paper contains the essence of the research, the appendices present aspects of the work that are not covered in great detail in the main document.

Appendix A provides descriptions of commonly used terms associated with patch antennas. These terms are used regularly throughout the paper and other appendices.

Appendix B gives an introduction to the concept of patch antennas in general and describes the basic operation of these antennas via transmission line theory.

Appendix C explores simulation of the probe-fed patch and electromagentically coupled patch. The limitations of simulation and the errors encountered for the specific patches investigated are presented.

Appendix D presents a parameter study of the probe-fed patch and electromagentically coupled patch. This study uses the calculation of correlation between the various antenna parameters in order to establish which geometrical parameters are most significant when designing a particular patch.

Appendix E shows the design curves generated from solving an impedance bandwidth optimization problem subject to a constraint on the antennas minimum gain. The error associated with interpolation of design between the given design curve data points is quantified.

Appendix F provides a brief description of the contents of the CD associated with this dissertation. All code, data and documentation is provided on this CD.

Table of Contents

List of Figures

List of Tables

Patch Antenna Design

Gareth Louis Shaw

***Abstract*— This paper describes the formulation of a design procedure for the rectangular, probe-fed and rectangular, electromagnetically coupled patch antennas. The design procedure is presented in the form of design curves. The design curve data was generated by solving a bandwidth optimization problem subject to a specified minimum gain constraint. Given a particular performance requirement, an appropriate antenna geometry can be found using the design curves. An unavoidable trade-off between the gain and impedance bandwidth performance parameters is evident from the design curves. The bandwidth and minimum gain configurations for design of the probe-fed patch range from 6.2% and 9.9dBi to 13.2% and 6.1dBi respectively. The bandwidth and minimum gain configurations for design of the electromagentically coupled patch range from 9.5% and 9.7dBi to 44% and 6.0dBi respectively.**

I. Introduction

A patch antenna typically consists of a radiating plate suspended above a ground plane. Patch or microstrip antennas exhibit characteristics such as light weight and a low profile, which makes these antennas desirable for many applications, [1], [2], [10], [20]. Various approaches to patch antenna design exist, but these approaches may require a large degree of mathematical ability and knowledge of the technology's physics in order to produce an initial design for a particular patch configuration. Alternatively, design by simulation may require expensive simulation software and finding an appropriate design is a time-consuming, iterative procedure. As a result, all these approaches may require significant time and effort to produce an initial design. In contrast, an antenna configuration suitable for a particular application can be found rapidly using design curves.

This paper presents design curves for the rectangular probe-fed [3], [13] and electromagnetically coupled patch antennas [14] – [17]. Although the behaviour of the probe-fed patch and the effect of it's geometrical parameters on it's electrical parameters is widely known, a formal, quantified approach to this antenna's design does not seem to have been presented in the literature. For this reason it seems appropriate to develop design curves for this, the most fundamental patch antenna. The electromagentically coupled patch is also a logical design choice, given the improved bandwidth provided by this antenna's feed mechanism. The geometry of the probe-fed patch and electromagentically coupled patch can be seen in Figures 1 and 2.

Simulation is necessary for generating design curve data. The selected patch antenna simulation method is verified in Section II by comparing real and simulated patch antenna characteristics. Section III shows the results of a simulated patch antenna parameter study. The parameter study results allowed simplification of the design process presented in Section IV, as only the most relevant antenna parameters were actively used in the design.

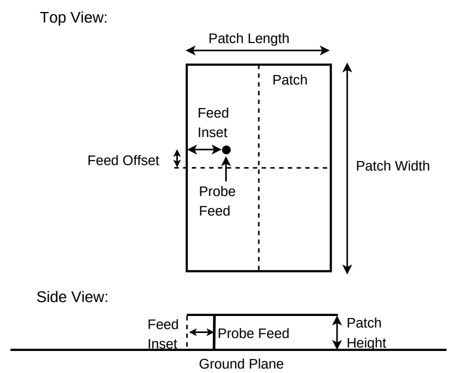

Fig. 1. Geometry of probe-fed patch.

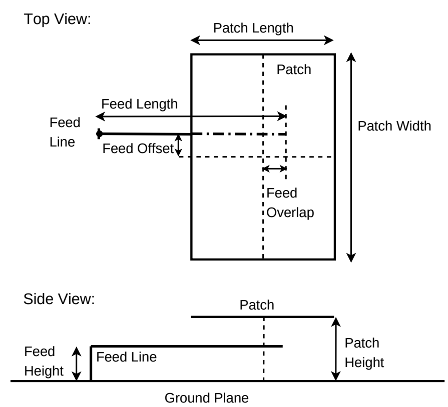

Fig. 2. Geometry of electromagentically coupled patch.

II. Patch Antenna Simulation

Patch antenna simulation is necessary for generating patch antenna design curve data. The SUPERNEC [29] simulation package, which uses a MoM solver, was selected for this purpose. SUPERNEC offers the flexibility to simulate arbitrary antenna geometries and provides connectivity with MATLAB [30], which allowed automation of simulations and easy analysis of simulation results. Figure 3 shows the SUPERNEC segmentation structure of the investigated antennas.

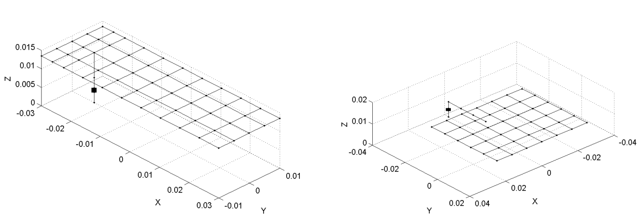

(a) Probe-fed patch. (b) Electromagnetically-fed patch.

Fig. 3. SUPERNEC model structure of investigated patch antennas.

This section investigates simulation of the rectangular probe-fed and electromagnetically-fed patch antennas in a qualitative manner. Sections II-A and II-B present the results for the probe-fed and electromagnetically-fed patches respectively. The conclusions from these results are presented in Section II-C. Further details of this study can be found in [21]. Definitions of the patch antenna terms used in this paper can be found in [20] and [18].

A. *Rectangular Probe-fed Patch Results*

The geometrical characteristics of the investigated probe-fed patch are: length 60mm (0.48λ), width 20mm (0.16λ), height 9mm (0.072λ), feed inset 3.5mm (0.028λ), feed offset 0mm, feed radius 0.4mm (0.032λ). Two physical antennas were constructed for comparison with the simulation. A comparison of the measured and simulated impedance results is shown in Figure 4. A comparison of the measured and simulated gain results is shown in Figure 5.

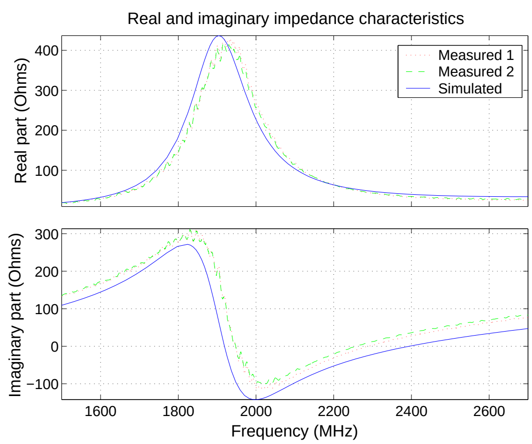

Fig. 4. Measured and simulated impedance characteristics for probe-fed patch

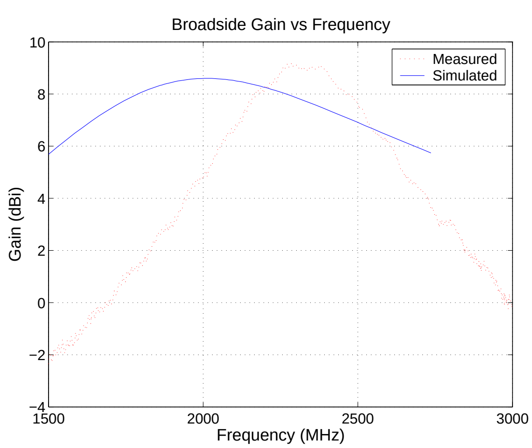

Fig. 5. Measured and simulated gain characteristics for probe-fed patch

The measured impedance showed good agreement with simulation, as seen in Figure 4. The measured gain, however, was found to be approximately 1dBi greater than the simulated gain over the operating frequency band (2.3GHz – 2.5GHz). The measured gain decreases rapidly outside the operating frequency band due to bad impedance matching with the network analyser used.

B. *Rectangular Electromagnetically Coupled Patch Results*

The geometrical characteristics of the investigated electromagnetically coupled patch are: length 40mm (0.33λ), width 50mm (0.41λ), patch height 11.2mm (0.093λ), feed length 23mm (0.19λ), feed overlap -14.5mm (0.12λ), feed height 7mm (0.058λ), feed diameter 2mm (0.017λ), feed offset 0mm. Two physical antennas were constructed for comparison with the simulation. A comparison of the measured and simulated impedance results is shown in Figure 6. A comparison of the measured and simulated gain results is shown in Figure 7.

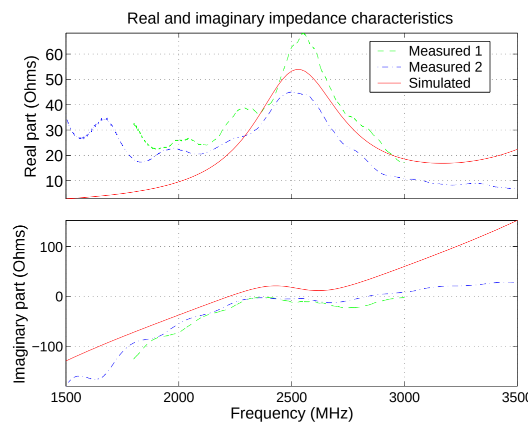

Fig. 6. Measured and simulated impedance characteristics for electromagnetically coupled patch.

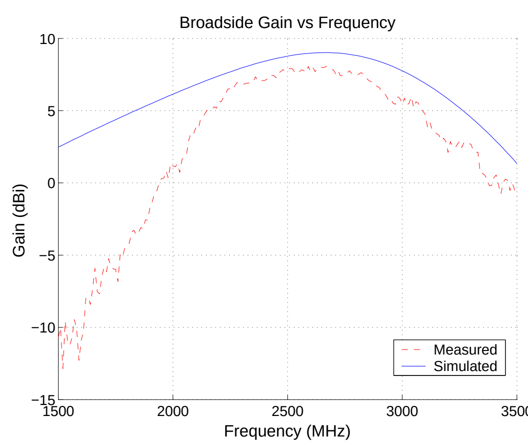

Fig. 7. Measured and simulated gain characteristics for electromagnetically coupled patch.

The measured results for impedance vary from values greater to values smaller than those predicted by the simulation. This implies that construction tolerances and error introduced by the measurement technique may be partly responsible for the discrepancy between measured and simulated results [21]. The antenna was enclosed in a protective plastic container which also effects the measured results [31]. The measured gain is seen to be approximately 1dBi less than the simulated gain (2.25 GHz – 2.75 GHz) over the operating frequency band (different network analyzers were used for the probe-fed and electromagnetically coupled patch mesurements).

C. Conclusions of Simulation and Measurement Comparison

Patches 1 and 2 from Sections II-A and II-B are constructed with the same geometrical specifications. Discrepancies between the measured results for the similar physical antennas, as well as between the simulated and measured results, immediately emphasizes the importance of construction tolerances and the need for good measurement equipment when producing an antenna. In particular, the discrepancy in measured and simulated gain results may have been introduced by the somewhat unreliable measurement equipment used during the two-antenna gain measurement procedure [21]. The simulation error, although not insignificant, is inline with that reported in the literature [12]. The effect of construction tolerances and measurement techniques, as well as other factors influencing simulation and measurement agreement, are discussed in [21] and have been commented on by [11].

Even though the SUPERNEC patch antenna simulations were not in total agreement with the measured results, the simulation error is comparable to that of other simulation and analysis techniques. It can be concluded that the simulation accuracy of SUPERNEC is sufficient for producing a first iteration of a practical antenna.

III. Patch Antenna Parameter Study

Patch antennas typically have many geometrical parameters. The parameter study presented in this section attempts to identify the most significant geometrical parameters belonging to the antennas of interest. This is achieved by varying a particular patch antenna's geometrical parameters to values 10% greater and smaller than their nominal values, and noting the effect this has on the antenna's performance parameters. The knowledge gained from this study allows simplification of the design procedure, as only the most important geometrical parameters are actively used in the design process presented in Section IV. The time taken to generate design curve data is also substantially decreased by this simplification.

The parameter study data set was generated by varying the geometrical characteristics of a number of preliminary design curve geometries, using SUPERNEC simulation. These geometries exhibited significant performance characteristics which are relevant to the design objective [22]. Data was recorded for the variation of every parameter when the antenna's other parameters were varied simultaneously. This required the generation of data for 2^{N} variations of each nominal geometry case, where N is the number of geometrical characteristics belonging to the antenna. The correlation between each parameter was calculated and an image of the correlation matrix for each of the antennas of interest can be seen in Figures 8 and 9. Strong positive or negative correlation is represented white elements in the image matrix.

The resonant frequency (F0), resonant resistance (R0), frequency of maximum resistance (Fmax) and maximum resistance (Rmax) parameters exhibit correlation characteristics consistent with that reported in other literature [18]. These parameters are presented in Figures 8 and 9 but not commented on in detail in the following parameter study, as the performance parameters are of primary interest for design purposes. The performance parameters are operating frequency (Fop), impedance bandwidth (BW), gain variation (GV), centre gain (CG) and minimum gain (MinG) [2].

A. Rectangular Probe-fed Patch Parameter Study

The probe-fed patch has the six geometrical parameters: the patch length (L), patch width (W), patch height (h), feed inset (FdInset), feed offset (FdOffset) and feed radius (FdRadius). Table I shows the maximum and minimum values between which the geometrical and performance parameters vary, for the fifteen cases considered. All nominal cases have a length of 0.03m and a feed offset of 0m. The study data set generated from the fifteen nominal cases consisted of 975 observations ($15 + 15 \times 2^6$).

TABLE I

Maximum and minimum parameter values for probe-fed patch study

Parameter	Maximum	Minimum
Width	0.047m	0.007m
Height	0.007.5m	0.0037m
Feed Inset	0.0041m	0.00075m
Feed Radius	0.00053m	0.00056m
Bandwidth	13.2%	6.2%
Minimum Gain	9.9dBi	6.1dBi

The correlation coefficient matrix calculated from the data set can be seen in Figure 8. The results for each performance parameter are analyzed below:

- *Frequency of operation:* The operating frequency shows a strong correlation with the patch length of -0.82. This result is consistent with that expected in p30 [1].
- *Bandwidth:* The bandwidth shows strongest correlation with the patch width (-0.64) and the patch height (+0.48). These results are also consistent with p42–44 [1]. The feed position is known to have a significant effect on the input impedance of the antenna, as shown by the fairly strong correlation between the feed inset and the maximum (+0.8) and resonant resistance (+0.8). Hence the feed position is important for feed matching purposes p13 [2]. This means that even though there was no strong positive or negative correlation between the feed inset and bandwidth, this value must still be chosen such that the maximum bandwidth is realised.
- *Center gain and minimum gain:* Both the center and minimum gain showed strong correlation with the patch width (+0.97). These results are expected from [1] p42–44. A strong negative correlation (-0.91) exists between the gain and the patch height. This indicates that increasing the patch height should decrease the gain. However, it is expected from the literature that increasing the patch height should result in more radiated power [10] p265. This contradictory result occurs due to the nature of the limited amount of patch configurations studied.
- *Gain variation:* The gain variation (defined in [19]) shows strongest correlation with the aspect ratio (-0.98). As the aspect ratio is a ratio of the length to the width this implies that increasing the width increases the gain variation percentage and indeed there is a strong correlation of +0.86 between the width and the gain variation.

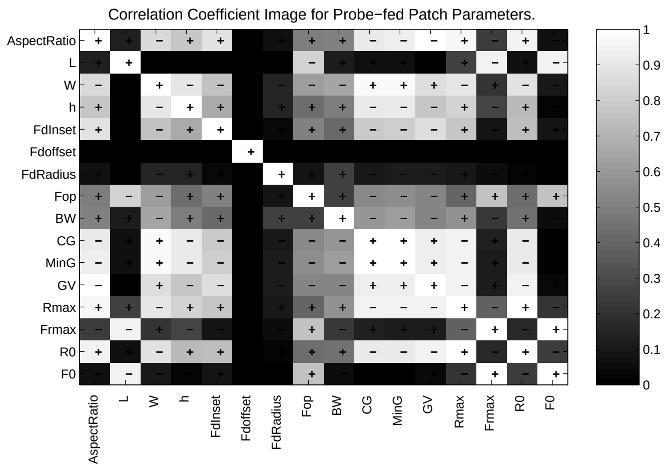

Fig. 8. Correlation coefficients of probe-fed patch.

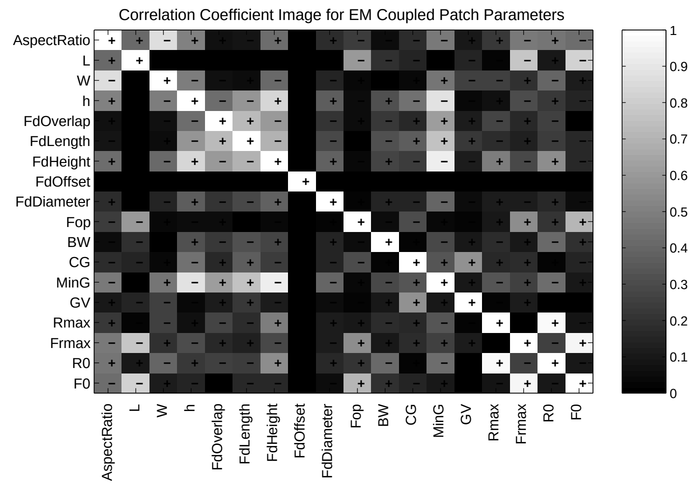

Fig. 9. Correlation coefficients of EM-fed patch.

The geometrical parameters which show the most significant correlation with the electrical parameters are length, width, height and feed inset. These parameters will be actively used for the generation of probe-fed patch design curves.

B. Rectangular Electromagnetically-fed Patch Parameter Study

The electromagentically coupled patch has eight geometrical parameters: length (L), width (W), height (h), feed overlap (FdOverlap), feed length (FdLength), feed height (FdHeight), feed offset (FdOffset) and feed diameter (FdDiameter). Table II shows the maximum and minimum values between which the geometrical and performance parameters vary, for the fourteen cases considered. All nominal cases have a length of 0.03m and a feed offset of 0m. The study data set generated from these fourteen nominal cases consisted of 3598 observations ($14 + 14 \times 2^8$).

TABLE II
MAXIMUM AND MINIMUM PARAMETER VALUES FOR EM-FED PATCH STUDY

Parameter	Maximum	Minimum
Width	0.0498m	0.0239m
Height	0.0116m	0.0061m
Feed Overlap	0.0007m	-0.0067m
Feed Length	0.0191m	0.0109m
Feed Height	0.0085m	0.0033m
Feed Diameter	0.0012m	0.001m
Bandwidth	43%	7.35%
Minimum Gain	9.62dBi	6.45dBi

The correlation coefficient matrix calculated from the study data set can be seen in Figure 9. The results for each performance parameter are analyzed below:

- *Frequency of operation:* The operating frequency shows a fairly strong correlation (-0.76) with the patch length. This result is consistent with that expected in [1] p30.
- *Bandwidth:* The bandwidth did not show strong correlation with any particular geometrical parameter. This implies that the bandwidth may be dependant on a combination of geometrical parameters. However, strongest correlation occurred with the patch height (+0.41), feed length (-0.44) and feed height (+0.46). This correlation is expected in [1] pp134–136.
- *Center gain:* The center gain showed strong correlation with the aspect ratio (-0.64) which is reflected in the width (+0.62). The patch height (-0.84) and the feed height (-0.77) also showed significant correlation. The explanation of the height correlation is analogous with that of the probe-fed patch, as given in Section III-A.
- *Minimum gain:* The minimum gain showed strong correlation with the patch height (-0.84), the feed length (+0.67) and the feed height (-0.77). In contrast to the results for the center gain, the minimum gain showed little correlation with the patch width (+0.36). This indicates a distinct difference between the behaviour of the electromagnetically-fed and probe-fed patch, which showed strong correlation between the minimum gain and the patch width. This result implies that different design curve data generation procedures will apply to each configuration when a minimum gain constraint is required for the antenna design.
- *Gain variation:* The gain variation showed little correlation with any particular geometrical parameter. This is expected when viewing the nominal gain variation data in Figure 40 of [22], which shows the gain variation to be fairly constant for the nominal configurations investigated. The gain variation did, however, appear to vary more for the cases that exhibited smaller gain characteristics and increased bandwidth [22].

The geometrical parameters which show the most significant correlation with the electrical parameters are length, width, height, feed overlap, feed length and feed height. These parameters will be actively used for the generation of electromagnetically coupled patch design curves.

IV. PATCH ANTENNA DESIGN

The design process presented in this section involves the selection of patch antenna geometrical characteristics such that a trade-off between the minimum gain over the antenna's frequency band of operation and impedance bandwidth exists. This trade-off is inherent to patch antenna design due to the nature of the antenna geometry. Increasing the antenna's minimum gain implies a reduction in impedance bandwidth and vice versa. The performance parameters for which design curves are generated are impedance bandwidth, minimum gain and operating frequency. The resulting centre (operating) frequency gain is also reported in the design curves, but the minimum gain was viewed as the constraining gain parameter and hence centre gain did not form an active part of the design curve data generation process. The design curves are generated with the assumption that the antenna will be fed by a 50Ω line as used in [15], [16], [24] – [28].

In general the design curve data was generated by solving a bandwidth optimization problem subject to a specified minimum gain constraint. The optimization problem was setup in MATLAB which used SUPERNEC for simulating the antenna configuration's characteristics. The results of the design curve generation for the probe-fed and electromagnetically coupled patches can be seen in Sections IV-A and IV-B respectively. All geometrical parameters are given in terms of wavelength (λ), allowing the appropriate physical antenna dimensions to be found for any desired operating frequency and gain/bandwidth configuration.

Given an impedance bandwidth and/or minimum gain specification, the design curves allow the dimensions of the most appropriate patch antenna to be found in terms of wavelength. These values can be converted to meters given the required antenna operating frequency [23].

A. Rectangular Probe-fed Patch design

The design variables for the probe-fed patch, selected in Section III-A, are length, width, height and feed inset. The feed offset was set to 0 and the feed radius is dependant on the frequency of operation, approximately calculated as $0.1\lambda/2 \times 2.17\pi$. An approximation, which is the result of a curve fitted to the feed radius trend, was felt to be sufficiently accurate as Section III shows that little correlation is shown between the feed radius and the performance parameters. The strong correlation between the patch width and the antenna's gain characteristics, as shown in Section III, prompted an implicit implementation of the gain constraint for the probe-fed patch by optimizing the impedance bandwidth for fixed values of patch width. The resulting design curves can be seen in Figure 10.

The design curves are fairly smooth and predominantly monotonic, implying that interpolation between the given data points should yield reasonable results. This was investigated by interpolating 50 linearly spaced data points over the bandwidth range presented in Figure 10. The difference between interpolated and actual bandwidth, minimum gain and operating frequency characteristics was calculated. Over the 50 interpolated data points the bandwidth, minimum gain and operating frequency error did not exceed 2%, 1.5% and 0.5% respectively. This small error implies that good designs can be interpolated between the given data points. An example of the design curves being applied to a given problem can be seen in [23].

B. Rectangular Electromagnetically-fed Patch design

The design variables for the electromagnetically coupled patch, selected in Section III-B, are length, width, height, feed overlap, feed length and feed height. The use of these many design variables provides more design flexibility and complexity when compared to the design procedure of [4]. The feed offset was set to 0 and the feed diameter is dependant on the frequency of operation, approximately calculated as $0.1\lambda/2.4\pi$, [23]. The gain constraint for the generation of this antenna's design curves was defined explicitly in the optimization problem, as the parameter study of Section III-B indicated that the antenna gain was dependant on multiple parameters. The resulting design curves can be seen in Figures 11 and 12.

The erratic nature of the width and feed overlap parameters in the design curves may imply that the performance parameters are less sensitive to these geometrical parameters relative to the other geometrical parameters, although it could be loosely said that a larger width allows a larger minimum gain. The length also appears to be erratic but varies over a relatively small range from 0.36λ to 0.38λ, indicating that the length value is actually quite constant. The height, feed length and feed height are shown to be relatively smooth and monotonic over relatively significant ranges, implying a strong dependance of the performance parameters on these geometrical parameters.

Another possible explanation for the erratic behaviour of the electromagnetically coupled patches design curves is that, due to the antennas many parameters, multiple patch configurations can give satisfactory solutions for a particular optimization problem. The given data may consist of a variety of these configurations.

Inaccuracy in the performance characteristics may be introduced when interpolating a design between the given data points. In order to quantify this inaccuracy 50 linearly spaced data points were interpolated over the bandwidth range presented in Figures 11 and 12. The difference between interpolated and actual bandwidth, minimum gain and operating frequency characteristics was calculated. Over the 50 interpolated data points the bandwidth, minimum gain and operating frequency error did not exceed 12%, 4% and 1% respectively. This implies that reasonable designs can be interpolated between the given data points. An example of the design curves being applied to a given problem can be seen in [23].

V. CONCLUSION

The probe-fed and electromagnetically coupled patch antennas were selected for design purposes, due to their popularity in the literature. Physical examples of these antennas were constructed for measurement purposes, allowing verification that these antennas can be simulated accurately using the SUPERNEC software. A comparison of measured and simulated results yielded satisfactory results. A parameter study of the antennas was performed, via simulation, in order to establish which geometrical parameters have the most effect on, or correlation with, the antenna's performance parameters. This parameter study allowed simplification of the design process, as only the most significant parameters need be taken into account. The design process presented a trade-off between the gain and impedance bandwidth characteristics of the antennas.

The design curves presented in this paper achieve the objective of allowing an initial patch design to be quickly se-

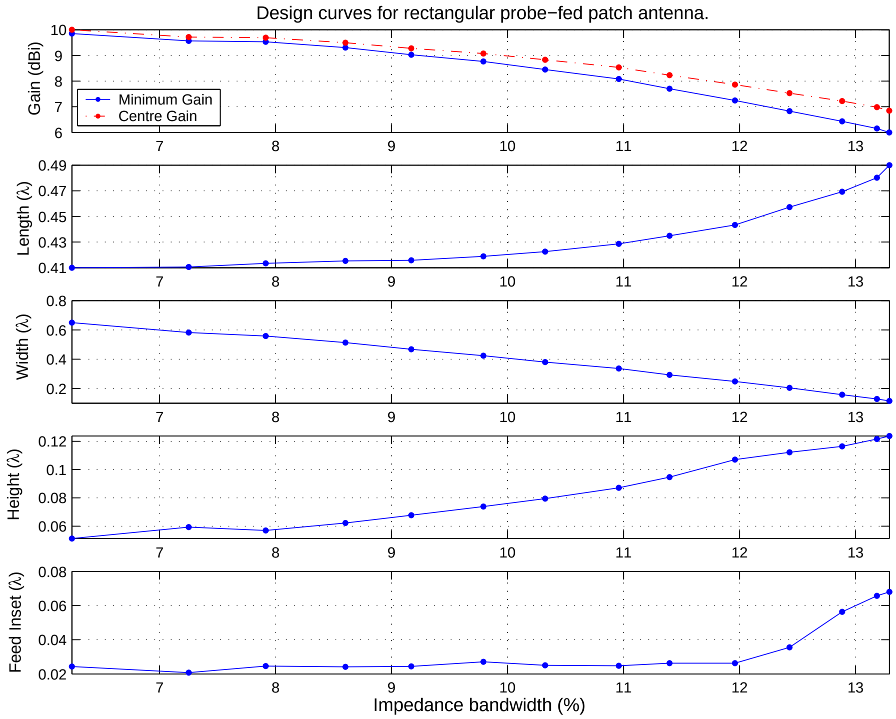

Fig. 10. Probe-fed patch design curves.

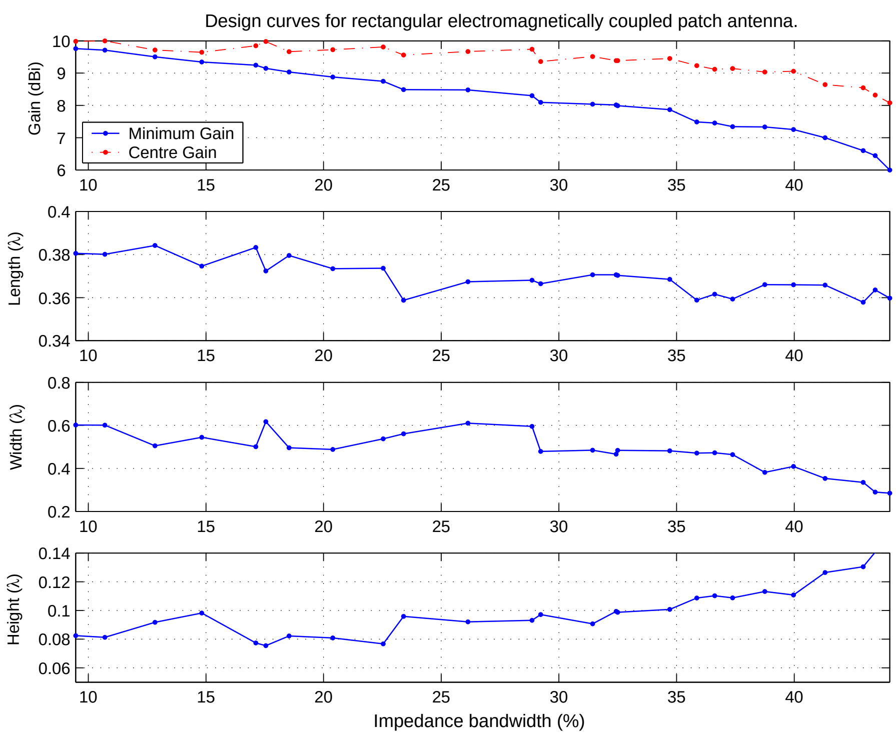

Fig. 11. Electromagnetically coupled patch design curves (gain, length, width and height characteristics).

lected, subject to certain performance requirements. However, the formulation of the design procedure is subject to certain limitations. The parameter study is limited to patch configurations with design characteristics deemed significant for this research, so parameter study results for other patch configurations may hint at different conclusions. The parameter study uses the correlation between geometrical and electrical parameters for determining which parameters are significant for design. A study of the magnitude effect of the geometrical parameters on the electrical parameters, in conjunction with the correlation study, would provide more comprehensive conclusions. The design curves are only valid for an air substrate, due to limitations of the simulation software. The shape of the antenna's radiation pattern was not investigated in detail, as operation in the TM_{10} mode with a known minimum and centre gain was assumed sufficient for the pur-

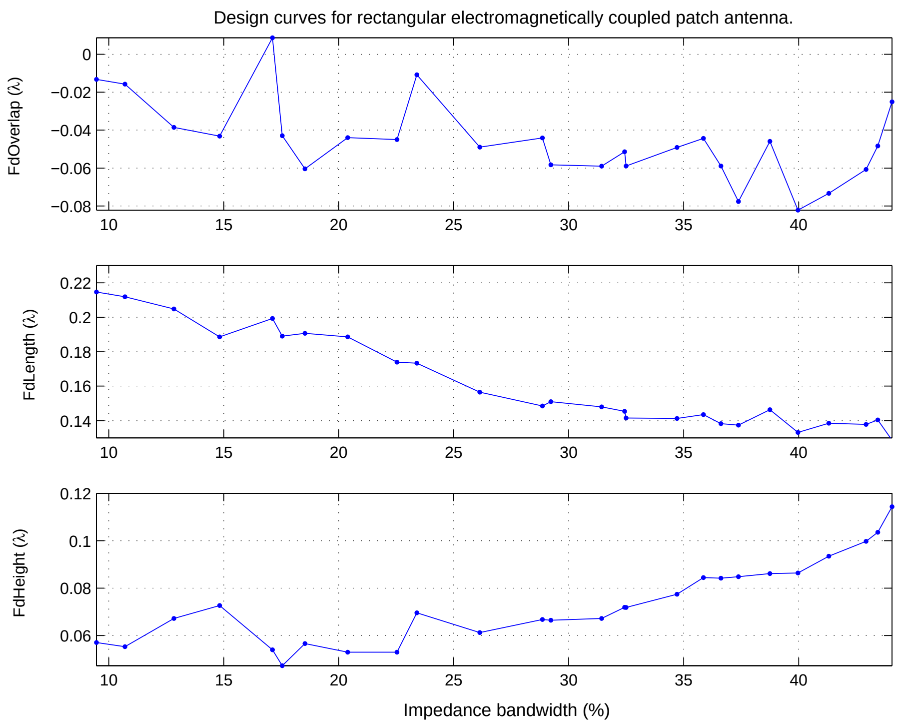

Fig. 12. Electromagnetically coupled patch design curves (feed characteristics).

poses of this paper. The design curves also assume an infinite ground plane.

Patch antenna size is often of interest, specifically the reduction of the antennas size for the purposes of installation in limited available space. Thus the design of a patch antenna could have a secondary objective of minimizing the antenna size. Future investigation of patch antenna design could implement this objective, the use of substrates other than air and perhaps focus on more specialised antenna configurations which have become popular for various applications. The use of various bandwidth enhancement techniques could also be added to the design procedure [5], [6], [7]. Patch antennas for dual and circular polarization could also benefit from the generation of design curves [9].

It would also take relatively little effort to combine the design curves presented in this paper into a computer program. This aid would benefit the designer by allowing initial design to be found rapidly with no human calculation error. This type of design interface is recommended in [8].

References

[1] Kumar, G, Ray, K, "Broadband Microstrip Antennas", *Artec House*, Boston, London, 2003.

[2] Carver, K.R, Mink, J.W, "Microstrip Antenna Technology", *IEEE Transactions on Antennas and Propagation*, vol.AP-29, pp2–24, Jan 1981.

[3] Schaubert, D.H, "Microstrip Antennas - A Review of Some Microstrip Antenna Characteristics", *Institute of Electrical Engineers*, New York , pp59–67, 1995.

[4] Splitt, G, Davidovitz, M, "Guidelines for Design of Electromagnetically Coupled Microstrip Patch Antennas on Two-Layer Substrates", *IEEE Transactions on Antennas and Propagation*, vol.AP-38, pp1136–1140, July 1990.

[5] Pozar, D.M, "Microstrip Antennas - A Review of Bandwidth Enhancement Techniques for Microstrip Antennas", *Institute of Electrical Engineers*, New York , pp157–166, 1995.

[6] Pues, H.F, Van De Capelle, A.R, "An Impedance-Matching Techniques for Increasing the Bandwidth of Microstrip Antennas", *IEEE Transactions on Antennas and Propagation*, vol.AP-37, pp1345–1354, Nov 1989.

[7] Pozar, D.M, Kaufman, B, "Increasing the Bandwidth of a Microstrip Antenna by Proximity Coupling", *IEE Electronic Letters*, vol.3 No.8, pp368–369, April 1987.

[8] Pozar, D.M, James, J.R, "A Review of CAD for Microstrip Antennas and Arrays", *Institute of Electrical Engineers*, New York, pp51–56, 1995.

[9] Pozar, D.M, Schaubert, D.H, "Microstrip Antennas - Dual and Circularly Polarized Elements", *Institute of Electrical Engineers*, New York, pp105–106, 1995.

[10] Garg, R, Bhartia, P, Bahl, I, Ittipiboon, A, "Microstrip Antenna Design Handbook", *Artech House, Inc.*, Massachusetts, 2001.

[11] Nitch, D, Verbal communication, Poynting Innovations, Winberg, South Africa, July 2003.

[12] Schaubert, D, H, Pozar, D, M, Adrian, A, "Effect of Microstrip Antenna Substrate Thickness and Permittivity: Comparison of Theories with Experiment", *IEEE Transactions on Antennas and Propagation*, Vol.37 No.6, pp677–682, 2001.

[13] Chair, R, Luk, K, M, Lee, K, F, "Measurement and Analysis of Miniature Multilayer Patch Antenna", *IEEE Transactions on Antennas and Propagation*, Vol.50 No.2, pp244–250, 2002.

[14] Parrikar, R, P, Gupta, K, C, "Multiport Network Model for CAD of Electromagnetically Coupled Microstrip Patch Antennas", *IEEE Transactions on Antennas and Propagation*, Vol.46 No.4, pp475–483, 1998.

[15] Mak, C, L, Luk, K, M, Lee, K, F, Chow, Y, L, "Experimental Study of a Microstrip Patch Antenna with an L-Shaped Probe", *IEEE Transactions on Antennas and Propagation*, Vol.48 No.5, pp777–783, 2000.

[16] Guo, Y, X, Mak, C, L, Luk, K, M, Lee, K, F, "Analysis and Design of L-Probe Proximity Fed-Patch Antennas", *IEEE Transactions on Antennas and Propagation*, Vol.49 No.2, pp145–149, 2001.

[17] Splitt, G, Davidovitz, M, "Guidelines for Design of Electromagnetically Coupled Microstrip Patch Antennas on Two Layer Substrates", *IEEE Transactions on Antennas and Propagation*, Vol.38 No.7, pp1136–1140, 1990.

[18] Chang, E, Long, S, A, Richards, W, F, "An Experimental Investigation of Electrically Thick Rectangular Microstrip Antennas", *IEEE Transactions on Antennas and Propagation*, vol.AP-34, pp767–772, June 1986.

[19] Shaw, G.L, Appendix A: Definition of Terms, MSc dissertation titled *'Patch Antenna Design'*, University of the Witwatersrand, 2004.

[20] Shaw, G.L, Appendix B: Patch Antenna Background, MSc dissertation titled *'Patch Antenna Design'*, University of the Witwatersrand, 2004.

[21] Shaw, G.L, Appendix C: Patch Antenna Simulation Investigation,

MSc dissertation titled *'Patch Antenna Design'*, University of the Witwatersrand, 2004.

[22] Shaw, G.L, Appendix D: Patch Antenna Parameter Study, MSc dissertation titled *'Patch Antenna Design'*, University of the Witwatersrand, 2004.

[23] Shaw, G.L, Appendix E: Patch Antenna Design, MSc dissertation titled *'Patch Antenna Design'*, University of the Witwatersrand, 2004.

[24] Munson, R, E, "Conformal Microstrip Antennas and Microstrip Phased Arrays", *IEEE Transactions on Antennas and Propagation*, Vol. AP-49, pp74–78, 1974.

[25] Bhattacharyya, R, E, "Long Rectangular Patch Antenna with a Single Feed", *IEEE Transactions on Antennas and Propagation*, Vol. 38 No. 7, p987, 1990.

[26] Parrikar, R, P, Gupta, K, C, "Multiport Network Model for CAD of Electromagnettically Coupled Microstrip Patch Antennas", *IEEE Transactions on Antennas and Propagation*, Vol. 46 No. 4, pp74–78, 1998.

[27] Bokhari, S, A, Zurcher, J, Mosig, J, R, Gardiol, F, E, "A Small Microstrip Patch Antenna with a Convenient Tuning Option", *IEEE Transactions on Antennas and Propagation*, Vol. 44 No. 11, pp1521–1528, 1996.

[28] Guo, Y, Luk, K, Lee, K, "Broadband Dual Polarization Patch Element for Cellular-Phone Base Stations", *IEEE Transactions on Antennas and Propagation*, Vol. 50 No, 2, pp251–253, 2002.

[29] Poynting Innovations and Poynting Software (SUPERNEC), http://www.poynting.co.za, Last accessed 22 October 2004.

[30] The MathWorks, MATLAB, http://www.mathworks.com, Last accessed 22 October 2004.

[31] Bahl, I, J, Bhartia, P, Stuchly, S, S, "Design of Microstrip Antennas Covered with a Dielectric Layer", *IEEE Transactions on Antennas and Propagation*, Vol. AP-30, No. 2, pp314–318, 1982.

APPENDIX A: DEFINITION OF TERMS

This appendix presents the definitions of terms commonly associated with patch antennas. These terms are used throughout this dissertation and formally defined in this appendix for easy reference. Related terms have been grouped together, rather than presenting the terms in alphabetical order.

A. Resonant Frequency (F0)

For the purposes of the paper and appendices of this dissertation the resonant frequency will be defined as the frequency, in the TM_{10} mode of operation, where the imaginary part of the impedance is equal to 0. Resonance usually occurs shortly after a resistive peak, with the imaginary part of the input impedance passing through 0 with a negative slope [18]. This definition is used consistently throughout this dissertation, although resonance can occur at different modes of operation and at multiple frequencies within the same mode.

B. Resonant Resistance (R0)

The resonant resistance is the real part of the impedance at the frequency where resonance, as defined in Section A-A, occurs.

C. Frequency of Maximum Resistance (Fmax)

The literature generally uses the values of resistance and frequency at resonance in order to characterize the occurrence of the TM_{10} mode of a patch antenna. A problem with this definition is that resonance does not always occur for a given patch geometry. It is necessary to characterize the occurrence of the TM_{10} mode in a different manner so that different patches can be compared. It is proposed in [18] that the frequency of the maximum resistance, as defined in Section A-D, be used to characterize the occurrence of the TM_{10} mode. This value was referred to as the 'resonant frequency re-defined' in [18], but for clarity in this text, this value will be referred to as the frequency of maximum resistance.

D. Maximum Resistance (Rmax)

The maximum resistance is defined as the peak resistance occurring in the frequency band for which the antenna operates in the TM_{10} mode.

E. Operating Frequency (Fop)

The patch antenna operating frequency could also be described as the design or centre frequency of the patch antenna. It is logical to define the operating frequency as:

$$F_o p = \frac{f_{r2} + f_{r1}}{2} \tag{1}$$

where f_{r2} and f_{r1} are the maximum and minimum frequencies at which the antenna's VSWR characteristic is less than 2.

F. Impedance Bandwidth (BW)

Impedance bandwidth is usually defined as a percentage [18]:

$$Bandwidth = \frac{f_{r2} - f_{r1}}{F_r} \times 100 \quad (2)$$

where F_r is the resonant frequency and f_{r1}, f_{r2} are the frequencies between which the magnitude of the reflection coefficient of the antenna is less than or equal to 1/3 (VSWR $<= 2$). As resonance does not always occur, a different method for calculating bandwidth will be used. The reason for this re-definition is to allow consistent comparisons of bandwidth between both resonating and non-resonating patches. The bandwidth definition of [1] is used:

$$Bandwidth = \frac{f_{r2} - f_{r1}}{F_{op}} \times 100 \quad (3)$$

where F_{op} is the operating frequency, as defined in Section A-E.

G. Minimum Gain (MinG)

The minimum gain is the antenna's lowest gain value over the frequency band of operation (where VSWR $<= 2$). All gain values are given relative to an isotropic source.

H. Gain Variation (GV)

The gain variation defines the extent to which the gain varies from the maximum gain over the 2:1 VSWR frequency band. The average gain over the 2:1 VSWR bandwidth is compared with the maximum gain of the antenna for the recorded frequency range. This value is expressed as a percentage, where a value 100% would indicate that the maximum gain is maintained over the entire VSWR bandwidth. This quantity is calculated as follows:

$$GV = \frac{\frac{1}{N}\sum G_N}{G_{Max}} \times 100 \quad (4)$$

Where GN is the recorded gain values within the 2:1 VSWR bandwidth, N is the number of gain points recorded over the operating band and G_{Max} is the maximum gain value.

I. Patch Length (L)

The length of a patch antenna denotes the length of the non-radiating sides of the rectangular antenna. The value of the length can be both greater and less than the orthogonal width dimension.

J. Patch Width (W)

The width of a patch antenna denotes the length of the radiating sides of the rectangular antenna.

K. Patch Height (h)

The height of the patch antenna denotes the distance between the top of the ground plane surface and the bottom of the radiating patch element. This value is otherwise known as the thickness of the patch antenna substrate or dielectric medium.

L. Dielectric Constant (ε_r)

The dielectric constant refers to the relative permittivity of the dielectric medium between the patch and the ground-plane.

APPENDIX B: PATCH ANTENNA DESIGN BACKGROUND

Abstract

This appendix provides a basic introduction to patch antennas in general and the rectangular, probe-fed and electromagnetically-fed patch antennas in particular. A brief history of the patch antenna is presented and the applications, benefits and disadvantages of patch antennas are discussed. The antennas which will be designed in Appendix E are described and their selection justified. Analysis of the rectangular patch is given, which provides insight into the operation of patch antennas and how the design of a patch antenna will be effected by the antennas parameters.

A. Introduction

A patch antenna typically consists of a radiating plate suspended above a ground plane. Patch or microstrip antennas exhibit characteristics such as light weight and a low profile, which makes these antennas desirable for a variety of applications. Patch antennas have gained popularity in the aerospace industry and mobile communication systems [10]. Microstrip or patch antennas were conceptualised by Deschamps (USA) and by Gutton & Baissinot (France) in 1953. However, further studies were not reported in the literature until the early 1970's, when Munson and Howell developed practical patch antennas [1], [2]. The early work by Munson on the development of microstrip antennas for use as low-profile flush-mounted antennas on rockets and missiles showed the patch antenna concept to be practical for use in many antenna system problems, thereby giving birth to a new antenna industry [2].

B. Patch Antenna Applications

Patch antennas have become extremely popular radiators in a variety of applications as this class of antenna benefits from the following characteristics [1]:

- Lightweight, small volume and low-profile planar configuration.
- Patches can be made conformal to a host surface (eg. the cylindrical surface of a missile).
- Ease of mass production and decreased costs of fabrication using printed-circuit technology.
- Circular and linear polarization can be achieved.
- Dual and triple frequency operation can be realised.

However, patch antennas suffer from limitations when compared to conventional microwave antennas [1]:

- Narrow bandwidth
- Lower gain
- Low power-handling capacity.

Despite these shortcomings patch antennas have been used in a wide variety of applications [1]. Table III shows how the use of patch antennas has permeated many different industries, emphasizing

TABLE III

PATCH ANTENNA APPLICATIONS

System	**Application**
Aircraft and ship antennas	Communication and navigation, altimeters, blind landing systems.
Missiles and satellite communications	Domestic direct broadcast TV, vehicle-based antennas, communication
Mobile radio	Pagers and telephones, man-pack systems, mobile vehicles
Remote sensing	Large lightweight apertures
Biomedical	Applicators in microwave hyperthermia
Others	Intruder alarms, personal communication - GSM, GPS applications

the desirability of the advantages offered by this class of antenna. It is therefore not surprising that there has been extensive investigation into methods for alleviating the patch's disadvantages. In particular, many techniques for improving the bandwidth characteristics have been explored [1], [5], [6], [7].

C. Patch Antenna Analysis

The commercial application of patch antennas spurned the development of a number of mathematical patch analysis techniques to aid patch design. The methods of analysis cater for a wide variety of patch shapes, on which there have many variations and improvements over time. The most popular analytical techniques are [1]:

- The transmission line model
- The cavity model
- The multi-port network method

Other methods based on the electric current distribution on the patch conductor and ground plane include [1]:

- The method of moments
- The finite-element method
- The spectral domain method
- The finite-difference time domain method

Mathematical analysis of patch antennas is necessary for producing a first-stage antenna design in a more timely and less costly manner than using a design-by-experimentation approach, in which antenna prototypes would have to be built and their characteristics measured. The SUPERNEC electromagnetic simulation software produced by Poynting Software will be used for the purposes of patch antenna design curve data generation in Appendix E. This software allows the flexibility to simulate various user-defined antenna configurations and offers connectivity with MATLAB for the purposes of analysis, visualization, optimization and repetitive computation. The accuracy with which this software can model patch antennas is explored in Appendix C.

D. Patch Antenna Design Selection

This section presents the patch antennas for which design curves will be developed in Appendix E. Two of the most popular patch antennas found in the literature are:

- The rectangular probe-fed patch, [1] pp30–49, [10] pp16–19 , [12], [2], [3], [13].
- The rectangular electromagnetically-fed patch, [1] pp131–138, [10] p28, [14] – [17].

The rectangular probe-fed patch is possibly the simplest and most widely known form of patch antenna. It is often used for explaining patch antenna operation and for research into basic patch antenna characteristics. Although the behaviour of the probe-fed patch and the effect of it's geometrical parameters on it's electrical parameters is widely known, a formal, quantified approach to this antenna's design does not seem to have been presented in the literature. For this reason it seems appropriate to develop design curves for this, the most fundamental patch antenna.

The rectangular electromagnetically-fed patch differs from the probe-fed patch only by the feed mechanism. This antenna is fed electromagnetically by an L-shaped feed line which extends below the patch element. This method of feeding the patch allows a significant improvement in impedance bandwidth, whilst still lending itself to practical construction techniques. This antenna offers a logical design progression from the probe-fed patch due to it's improved bandwidth performance and hence will also be designed in Appendix E.

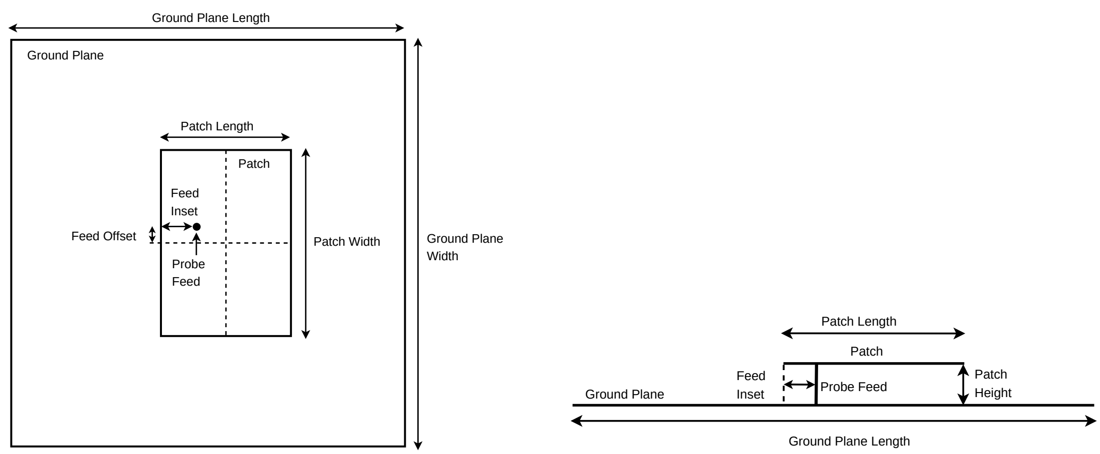

(a) Top view. (b) Side view.

Fig. 13. Rectangular probe-fed patch antenna geometry.

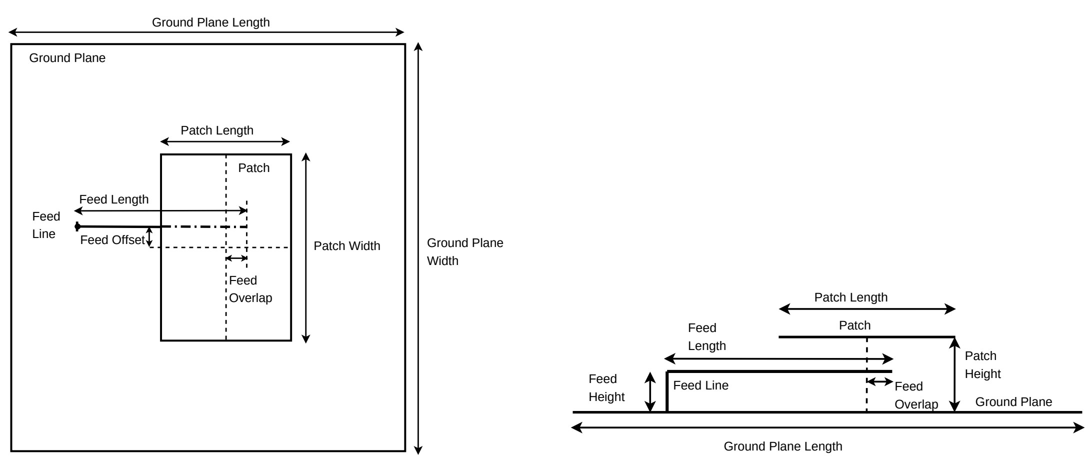

(a) Top view. (b) Side view.

Fig. 14. Rectangular electromagnetically-fed patch antenna geometry.

Figures 13 and 14 show the geometrical characteristics belonging to the two patch antennas of interest. It should be noted that the dimension of the patch element labelled "Length" denotes the dimension along which the antenna surface current distribution varies sinusoidally in the TM_{10} mode of operation (see Section B-E for more on patch antenna operation). Another geometrical factor, not presented in Figures 13 and 14, is the feed radius. This is simply the radius of the feed probe or feed line used.

E. Patch Antenna Operation

A basic understanding of how the antennas presented in Section B-D operate is helpful when analysing simulated and measured results. This section gives a brief outline of a rectangular patch antenna's operational characteristics.

The rectangular patch antenna geometry is extremely popular due to its constructional simplicity and ease of analysis, [1] p30. The probe-fed rectangular patch, as shown in Figure 13, is used in this section as an example for describing a patch antenna's fundamental mode of operation. The concepts presented in this section, regarding patch operation in the TM_{10} mode, can also be applied to the rectangular electromagnetically-fed patch antenna (Figure 14) as only the feed mechanism differs between the two patches.

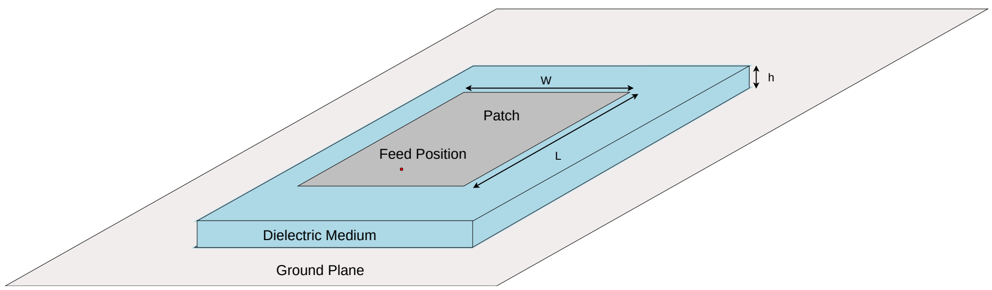

Fig. 15. Rectangular, probe-fed patch antenna.

Figure 15 provides an alternative view of the probe-fed patch geometry presented in Figure 13. The basic terminology and conventions used when describing the geometry of a patch antenna are defined in Appendix A. Analysis of this antenna, via transmission-line theory, will be presented in this section.

Transmission-line theory provides the most simple analytical description of a rectangular patch antenna. This theory describes the antenna as two parallel radiating slots [2], which are modelled by their equivalent capacitance and radiation resistance, [1] p31, as shown in Figure 16:

Analysis of the equivalent circuit of the patch antenna leads to the following approximate equation for the resonant frequency of the rectangular patch antenna, [1] p36:

$$f_0 = \frac{c}{2L_e\sqrt{\varepsilon_e}} \tag{5}$$

Where:

f_0 is the resonant frequency,
c is the speed of light,
L_e is the effective patch length:

$$L_e = L + 2\frac{h}{\sqrt{\varepsilon_e}} \tag{6}$$

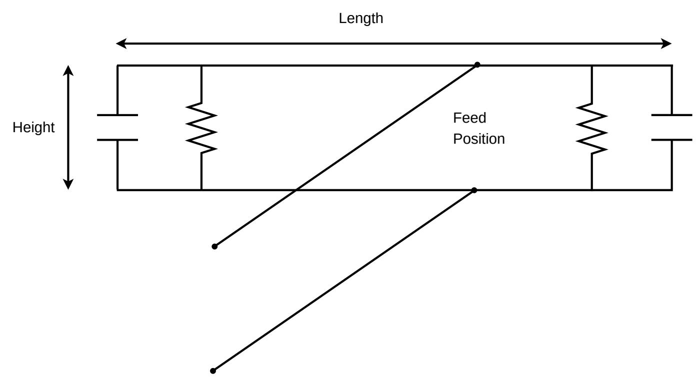

Fig. 16. Equivalent transmission-line model of a rectangilar patch antenna.

ε_e is the effective permittivity:

$$\varepsilon_e = \frac{\varepsilon_r + 1}{2} + \frac{\varepsilon_r - 1}{2}[1 + \frac{10h}{w}]^{-\frac{1}{2}} \tag{7}$$

The patch antenna radiates from the fringing fields between the periphery of the patch and the ground plane. The fringing E-field distribution is shown in Figure 17:

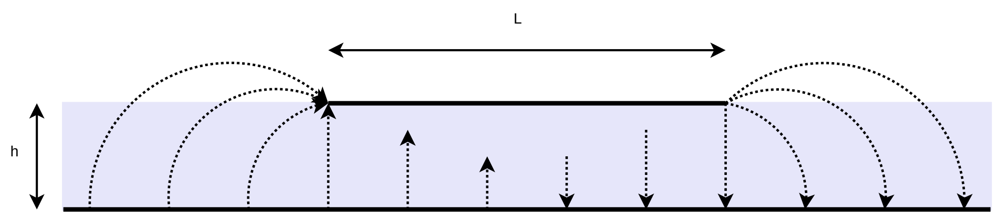

Fig. 17. TM_{10} mode E-field distribution.

Patch antennas exhibit resonant behaviour and are governed by modes of operation at which the current distribution on the patch surface dictates the radiation pattern and polarity of the radiated wave. For the fundamental Transverse Magnetic mode TM_{10} in which a broadside radiation pattern occurs, the length L should be slightly less than the wavelength in the dielectric medium at that frequency of operation (λ). λ is dependant on the effective dielectric constant (ε_e):

$$\lambda = \lambda_0 / \sqrt{\varepsilon_e} \tag{8}$$

Where λ_0 is the free-space wavelength.

ε_e is usually less than the relative permittivity of the substrate (ε_r). This is due to the effect of the fringing fields around the periphery of the patch, which are not confined in the dielectric substrate but are also spread in the air [1] p30. This effect is shown in Figure 17 and results in the length appearing electrically longer, giving an effective patch length of $\mathrm{L_e}$. Operation in the fundamental TM_{10} mode implies that the field varies one half-cycle along the length and no variation along the width.

The variation of the voltage and current along the length of the patch is shown in Figure 18. The voltage is maximum and the current minimum along the width of the patch. This is due to the open circuited ends. The resonant resistance (R_0) of a rectangular patch is greatest when the feed is placed near or on the width edge ($\mathrm{x} = 0$) as the current at the edge is at a minimum and $\mathrm{R}_0 = \mathrm{V}/\mathrm{I}$. The

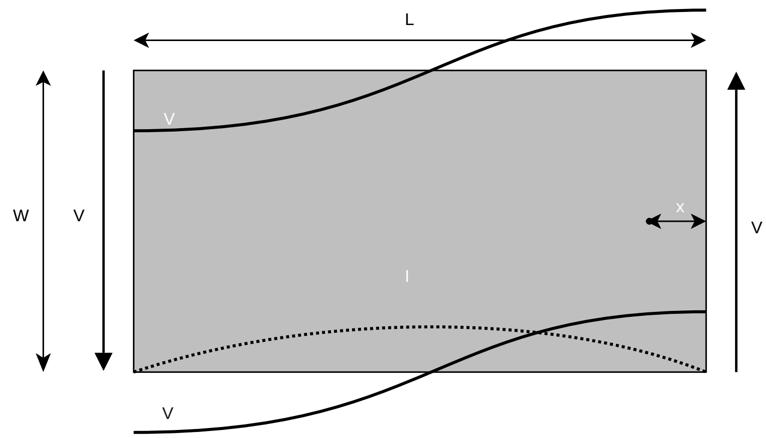

Fig. 18. Voltage and current variation on the patch antenna.

value of the resonant resistance varies as $\mathrm{R_0 \cos^2(px/L)}$ from the edge of the patch, where x is the feed position inset distance from the edge of the patch. This relationship is important for matching the patch input impedance to the feeding transmission line and maximizing impedance bandwidth.

Maximum gain results in the broadside direction due to the current distribution on the patch element surface for this mode of operation. The shape of the radiation pattern can vary for higher order modes of operation, due to the change in the current distribution on the patch element. For example, the second order or $\mathrm{TM_{20}}$ mode results in a conical radiation pattern and the third order mode yields a broadside pattern [1] pp52–55. As the radiation pattern varies with the mode of operation, this characteristic can be useful for beam shaping. Care must be taken when considering the use of higher order modes of operation due to the differing radiation properties between modes. For instance, the polarization of some of the higher order modes is different from the dominant mode [3] - and this could result in the antenna being unsuitable for its intended application.

The information presented in this section was found to be extremely valuable when sanity-checking parameter and simulation study results (Appendix C and Appendix D). Operation in the fundamental mode is also desired for design purposes in this dissertation. An understanding of the electrical characteristics exhibited by a patch antenna in the $\mathrm{TM_{10}}$ mode was vital in automating design curve data generation, as outlined in Appendix E, Section E-B.

APPENDIX C:
PATCH ANTENNA SIMULATION INVESTIGATION

Abstract

The error associated with SUPERNEC *patch antenna simulations was quantified and compared with the error resulting from other simulation/analysis techniques. This comparison showed that, although the simulation error was not insignificant,* SUPERNEC *is suitable for generating air-dielectric patch antenna design curve data.*

A. Investigation Overview

The objective of this investigation is to determine whether the SUPERNEC antenna simulation software package is suitable for generating design curve data for the rectangular, probe-fed and electromagnetically coupled, patch antennas. This can be achieved by comparing measured antenna data with corresponding SUPERNEC patch simulation results. This comparison will allow the simulation error percentage to be calculated. This error can be compared with the error calculated for other simulation methods. If the SUPERNEC simulation error is comparable to, or less than, the error encountered with the other simulation/analysis methods, and this error is practically acceptable, then it can be concluded that SUPERNEC provides sufficient accuracy for generating patch antenna design curve data. The two patch antenna configurations chosen for investigation encompass the most popular designs encountered in the literature (as presented in Appendix B):

- The rectangular probe-fed patch
- The rectangular electromagnetically-fed patch

The feed type is the distinctive characteristic that differentiates these antennas, as both exhibit a rectangular shape. Table IV provides a summary of the investigated patch configurations with their associated frequency band of interest in which the TM_{10} mode of operation occurs. The EM coupled patch antenna geometry was provided by Poynting Innovations [11] for study. The probe-fed patch geometry was constrained by the size of the available construction materials. It was nevertheless designed with a similar operating frequency to that of the EM coupled patch, which was well within the range of the network analysers used for measurements.

TABLE IV

PATCH CONFIGURATIONS USED IN SIMULATION INVESTIGATION

Patch Configuration	**Length**	**Width**	**Frequency Range**
Probe-fed patch	60mm (0.48λ)	20mm (0.16λ)	1.5GHz - 3GHz
Electromagnetically coupled patch	40mm (0.33λ)	50mm (0.41λ)	1.5GHz - 3.5GHz

In order to establish the accuracy with which a patch antenna can be simulated it is necessary to calculate the error between the measured and simulated antenna results. This error calculation is shown below:

$$\text{Error Percentage} = \frac{\text{MeasuredValue} - \text{SimulatedValue}}{\text{MeasuredValue}} \times 100 \tag{9}$$

It is required that the following antenna characteristics for the real and simulated antennas be recorded. A comprehensive investigation of the antenna simulation accuracy can be performed by comparing these measured and simulated characteristics for the antennas of interest (Appendix A provides definitions for these terms):

- Resonant resistance
- Frequency of maximum resistance
- Maximum resistance
- Impedance bandwidth
- Center frequency
- Center frequency gain

Important factors that are popularly used in the literature to characterize a patch antennas behaviour are the frequency at which resonance occurred and the input resistance at this frequency. However, resonance does not always occur for a given patch antenna configuration. In order for patch antennas to be consistently characterized, the maximum resistance in the TM_{10} mode and the frequency of maximum resistance can be recorded [18]. Antenna performance characteristics are important for antenna design purposes and thus the antenna bandwidth, operating frequency and gain are included in this investigation.

The simulation investigation is structured as follows: Section C-B presents a discussion of the reasons that may cause discrepancies between measured and simulated results. Section C-C presents the results of the rectangular probe-fed patch investigation. Section C-D presents the results of the rectangular electromagnetically-fed patch investigation. The simulation error values obtained from these investigations are compared with the errors resulting from other simulation/ analysis techniques in Section C-E and a verdict on SUPERNECs suitability for patch antenna simulation is presented.

B. Factors Influencing Correlation of Simulation and Measurement Results

Inevitably there are differences when comparing measured and simulated antenna results. There could be a wide variety of reasons for the discrepancies between measured and simulated patch antenna results, including:

- Error in simulated results due to the solving method and numerical inaccuracies [8].
- Error in the quoted value for the relative permittivity [2].
- Variations in measured results due to constructional tolerances. This topic is discussed further in Section C-B.1.
- Variations in measured results due to an in-homogenous dielectric [2]. This can be a factor even for air-dielectric patches (such as those investigated in Sections C-C and C-D) as the patch element must still be suspended above the ground-plane by double sided tape, polystyrene or another spacing element. Although the spacing material is chosen for a dielectric constant close to that of air, there will still be an effect on the measured results.
- Measurement data can be unreliable due to the measurement technique and the quality of the hardware used [11]. This topic is discussed further in Section C-B.2.
- Segmentation frequency is an item specific to SUPERNEC simulations. The frequency at which a SUPERNEC antenna assembly is segmented can also affect the nature of the simulated results. This issue is discussed further in Section C-B.3.
- Covering an antenna with a dielectric layer can affect the resonant frequency of the antenna . An example of such a cover can be seen in Figure 27 [29]. It is currently not possible to take the effect of a dielectric into account when modelling a patch antenna with SUPERNEC.

These limitations imply that perfect correlation between simulated and measured results is unlikely. Therefore the objective of using a simulation package should be defined as a mechanism for gaining a good first iteration of the antenna design parameters. By having a reasonably accurate first simulated iteration of the antenna, the number of experimental iterations necessary for optimizing the antennas performance characteristics is significantly decreased - thus saving time and money spent on construction during the experimental process.

1) Construction Tolerances: This section investigates the effect that construction tolerances can have on the agreement between simulated and measured antenna characteristics. Measured impedance data for five nominally identical electromagnetically coupled rectangular patch antennas is presented as an example in Figure 1.

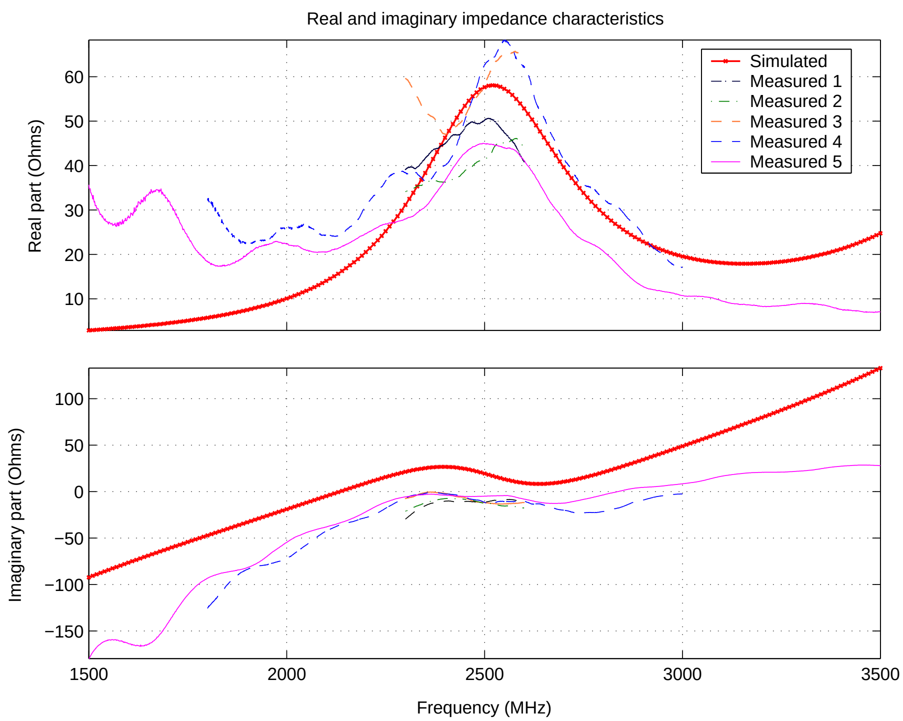

Fig. 19. Effect of construction tolerances on impedance characteristics for EM-fed patch.

It can be seen from Figure 19 that measured results for antennas made to the same geometrical specifications can vary considerably from antenna to antenna. Therefore, the agreement between the simulated and measured results also varies from antenna to antenna. This observation implies that simulated results may not be absolutely accurate due to the geometrical inaccuracies introduced by the limitations inherent in the physical construction of the antenna. The simulated results should therefore be interpreted as only a rough estimation of the antenna characteristics. This in turn affects the accuracy that one one can expect from design curves which have been generated from simulation, [10] pp299-302. The error associated with the above simulation/measurement comparison is formally quantified in Section C-D.

2) Measurement Limitations: Measurement results can also vary for the same antenna over time. This can be attributed to the measurement technique used as well as the physical properties of an antenna changing due to wear and age. Figures 20 and 21 present measured data for electromagnetically coupled patches taken at different times.

It can be seen from Figures 20 and 21 that although both sets of measurements follow similar trends, there is still a distinct difference between the two sets of measurements for each antenna. If patch antenna results vary from measurement to measurement then this implies that tolerable differences

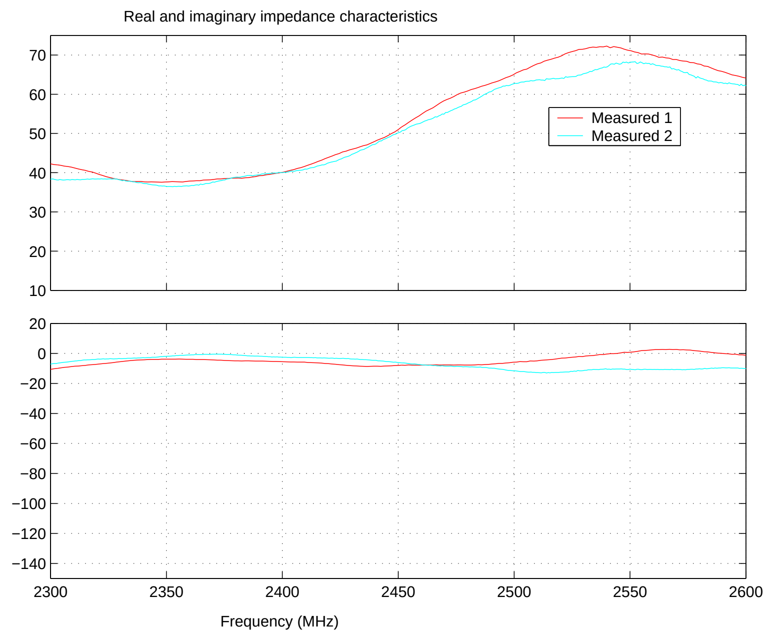

Fig. 20. Effect of measurement repeatability on impedance characteristics for EM-fed patch 4.

between simulated and measured results should be expected.

The quality of the cables, adaptors and network analyser used for the measurements will also effect the accuracy of the measured results. An example of this can be seen for the gain measurement of the electromagnetically-fed patch, as discussed in Section C-D.

3) The Effect of Segmentation Frequency: It is important to recognize that the segmentation frequency has an effect on the SUPERNEC simulation results. The frequency at which a SUPERNEC antenna assembly is segmented must be chosen such that the antenna structure is valid for all the simulation frequencies. However, there is not a unique frequency value that fulfils this requirement as over-segmentation (segmenting the structure at a frequency higher than the maximum simulation frequency) of the antenna structure can still result in, and is often required for, a valid antenna simulation structure. The effect of the segmentation frequency on the probe-fed rectangular patch antenna impedance data can be seen in Figure 22.

As the maximum simulation frequency for the probe-fed rectangular patch antenna is 2000MHz the model frequencies of 2500MHz, 3000Mhz and 3500MHz are all valid. Increasing the segmentation frequency from 3000MHz to 3500MHz results in the resonant input impedance characteristic shifting to a higher frequency (by approximately 10MHz). The input resistance increases fractionally and the imaginary part of the input impedance increases (becomes more capacitive).

Decreasing the segmentation frequency from 3000MHz to 2500MHz has the opposite effect. The resonant input impedance behaviour occurs at a lower frequency, the input resistance decreases and the imaginary part of the input impedance decreases thereby becoming more inductive. Similar behaviour can be seen for the electromagnetically coupled patch antenna in Figure 22.

In conclusion, it is generally preferable to use the lowest segmentation frequency that still results in a valid structure. The reason for this is that by using a lower segmentation frequency the simulated antenna structure will contain less MoM segments and this means that simulation time will be reduced. However, it is often necessary to over-segment an antenna structure so that a valid antenna assembly is obtained. As the results from two valid structures, segmented at different frequencies, will differ slightly, it is not obvious which is more correct (until comparison with measurements). For this

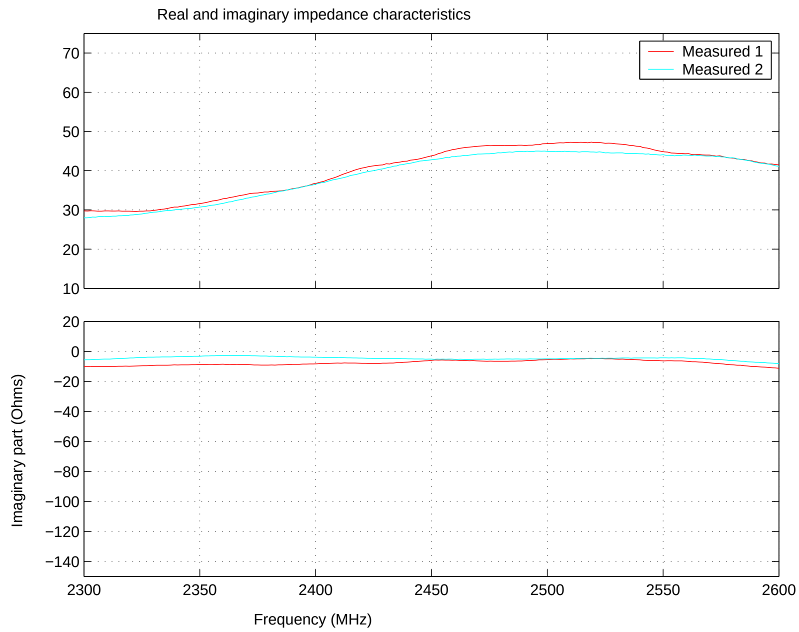

Fig. 21. Effect of measurement repeatability on impedance characteristics for EM-fed patch 5.

reason, the simulated results should be taken as a guide to range in which the antenna characteristics can be expected and 100% accuracy should not be expected.

C. Probe-fed Rectangular Patch

The objective of this section is to determine the accuracy with which a probe-fed rectangular patch can be simulated. This is achieved by quantifying the difference between simulated and measured results as an error percentage which can be compared with the error associated with other simulation/ analysis techniques.

TABLE V

GEOMETRICAL CHARACTERISTICS OF THE INVESTIGATED RECTANGULAR PROBE-FED PATCH

Parameter	**Value**
Length	60mm (0.48λ)
Width	20mm (0.16λ)
Height	9mm (0.072λ)
Feed Inset	3.5mm (0.028λ)
Feed Radius	0.4mm (0.032λ)
Feed Offset	0mm

The probe-fed rectangular patch investigated in this section has the geometrical characteristics shown in Table V. This geometry was simulated in SuperNEC using a model frequency of 4378MHz. The simulated patch characteristics were compared with four, real antennas which were constructed with the same geometry. These antennas used different construction techniques allowing the factors outlines in Section C-B.1 to be practically investigated simultaneously.

Two of these antennas (labelled A1 and A2) used a polystyrene spacing element between the patch and the ground plane. The second pair of patches (labelled B1 and B2) used double-sided tape attached to each corner of the patch as the spacing element. A photograph of Patch B1 can be seen in Figure 23. The polystyrene spacing element, used for A1 and A2, allowed a consistent patch

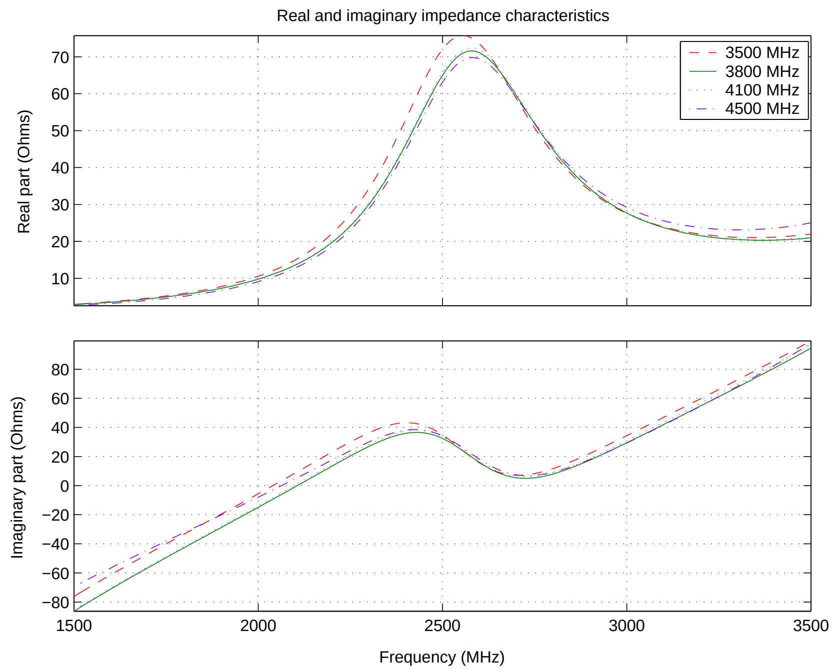

Fig. 22. Effect of segmentation frequency on electromagnetically coupled patch impedance characteristics.

height above the ground plane to be maintained. It can be expected that the polystyrene spacing element, and the glue used for attaching the ground plane and patch to the polystyrene, will effect the effective dielectric constant of the area between the patch and ground plane. As polystyrene has a relative permittivity similar to that of air, it was not expected that this would effect the comparison of measured and simulated results significantly.

The construction method employed for B1 and B2 allowed the majority of the area between the patch and ground plane to be air, which was expected to allow better agreement between measured and simulated results. However, this construction method resulted in an inconsistent patch height due to the lack of support over the entire surface of the patch.

A comparison of the impedance measurements for patches A1, A2, B1, B2 and the simulated antenna be seen in Figure 24. This figure shows that the construction method utilizing a polystyrene spacing element (patches A1 and A2) resulted in an impedance characteristic fairly close to that of the simulation. These results are re-iterated by the VSWR characteristics shown in Figure 25(a). Patches B1 and B2 resulted in an impedance characteristic that is noticeably different to the simulated impedance - this is attributed to the irregular height of the physical antenna.

A comparison of the measured and simulates gain characteristics is shown in Figure 25(b). The measured gain varies considerably from the measured gain over the displayed frequency band, although both the measured and simulated peak gains are approximately 9 dBi. The difference between measured and simulated gain may be attributed to error introduced by the measurement process, as discussed in Section C-B.2. An alternative comparison of the antennas performance characteristics can be seen in Figure 26 which allow the relationship between the gain and impedance bandwidth to be viewed.

It is immediately obvious from Figure 26 that the measured impedance bandwidth is smaller than that predicted from the simulation. The measured gain characteristic over the operating frequency band (where VSWR is less than 2) is approximately 1dBi greater the simulated gain. A quantitative comparison of the measured and simulated results can be seen in Table VI.

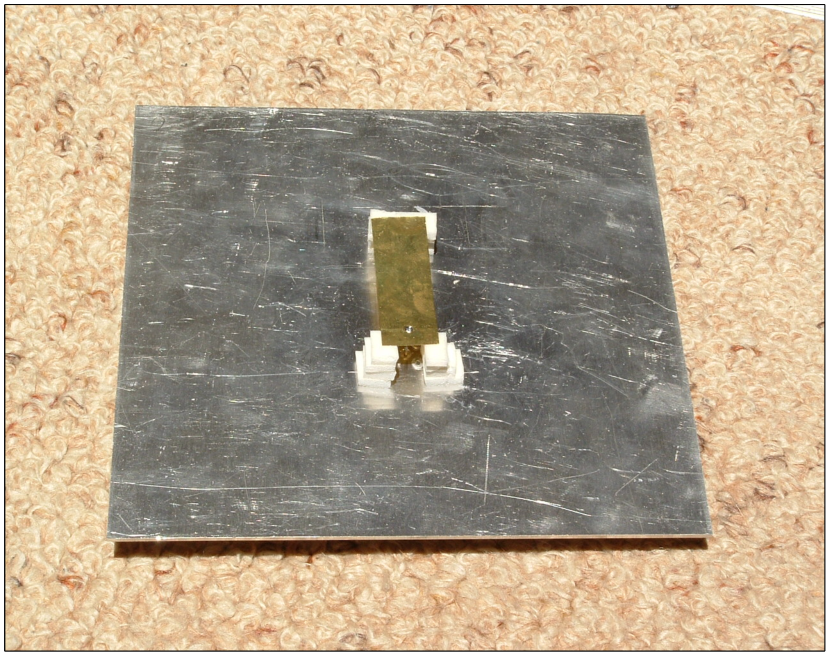

Fig. 23. Photograph of probe-fed patch ”B1” which used air spacing between the patch and ground plane.

TABLE VI

RESULTS OF RECTANGULAR PROBE-FED PATCH INVESTIGATION

Performance Parameters	**Simulated Results**	**Patch A1**	**Patch A2**	**Patch B1**	**Patch B2**
Centre Frequency (MHz)	2417	2278	2258	2344	2328
Impedance Bandwidth	11.7562 % (284 MHz)	8.6167 % (196 MHz)	8.811 % (199 MHz)	8.7017 % (204 MHz)	8.4296 % (196 MHz)
Centre Gain (dBi)	7.4	9.0	8.8	9.0	8.9
Gain Variation (%)	86.2	96.2	96.7	96.2	96.8
Resonant Frequency (MHz)	1925	1947	1947	2072	2071
Resonant Resistance (Ω)	448	408	384	303	300
Frequency of Maximum Resistance (MHz)	1911	1934	1916	2051	2022
Maximum Resistance (Ω)	457	430	417	342	345

Table VII presents the error in the simulated patch electrical parameters with reference to the measured results. The results for each electrical parameter are discussed below:

- **Centre Frequency:** The simulated and measured centre frequency values are fairly similar, with an acceptable error under 10% reported all physical patches.
- **Impedance Bandwidth:** A large error in the bandwidth (greater than 30%) is seen for all the patches. The physical antennas have a much smaller bandwidth than that predicted by the simulation. This may be attributed to the sensitivity of electrical characteristics to constructional tolerances, as described in Section A-B.1, and error introduced by the measurement process (C-B.2).
- **Centre Gain:** A large error of over 10% for the simulated centre gain was calculated for all measured antennas.
- **Gain Variation:** The gain variation is fairly similar for all measured patches, with an error of about 10% being calculated for all antennas.
- **Resonant Frequency:** The resonant frequency of all the measured patch antennas agreed well

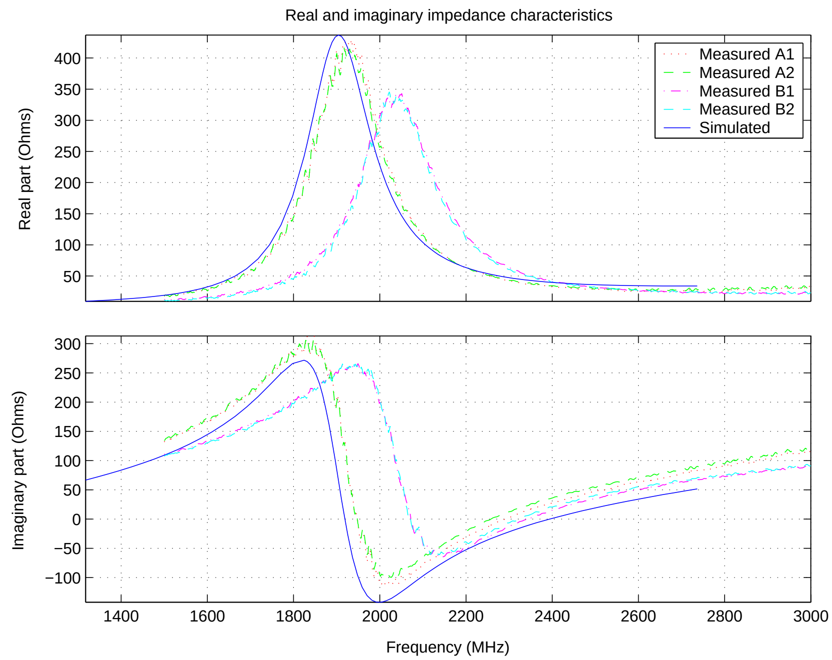

Fig. 24. Comparison of measured and simulated impedance characteristics for probe-fed patch.

TABLE VII

ERROR RESULTS FOR RECTANGULAR PROBE-FED PATCH INVESTIGATION

Electrical Parameters	**Patch A1 Error %**	**Patch A2 Error %**	**Patch B1 Error %**	**Patch B2 Error %**
Centre Frequency	6.11	7.03	3.10	3.80
Impedance Bandwidth	36.43	33.42	35.10	39.46
Centre Gain	-17.40	-15.92	-17.3326	-16.87
Gain Variation	-10.43	-10.86	-10.3936	-10.99
Resonant Frequency	-1.13	-1.15	-7.08	-7.05
Resonant Resistance	9.93	16.58	47.98	49.27
Frequency of Maximum Resistance	-1.17	-0.25	-6.81	-5.47
Maximum Resistance	6.39	9.47	33.51	32.47

with the simulation with the errors for patches B1 and B2 being under 10%, and patches A1 and A2 under 2%.

- **Resonant Resistance:** The resonant resistances exhibited by patches A1 and A2 agree fairly well with the simulation, with an error of approximately 10%. Extremely large errors (greater than 45%) were calculated for patches B1 and B2, this can be attributed to a dip in the height between the double-sided tape spacing elements (B1 can be seen in Figure 23). Appendix D shows that there is a positive correlation between the patch height and the resonant resistance. This correlation is evident here as the decreased height resulted in a decreased resonant resistance.
- **Frequency of Maximum Resistance:** The frequency of maximum resistance for all the measured patch antennas agrees well with the simulation. The errors for patches B1 and B2 are under 10%, and patches A1 and A2 are under 2%.
- **Maximum Resistance:** The maximum resistances exhibited by patches A1 and A2 agree fairly well with the simulation, being under 10%. Larger errors (greater than 30%) were calculated for patches B1 and B2, this can be attributed to the inconsistent height characteristic exhibited by these patches.

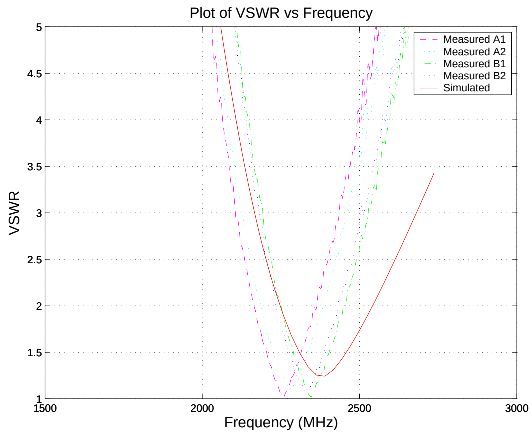

(a) Comparison of measured and simulated VSWR characteristics for probe-fed patch.

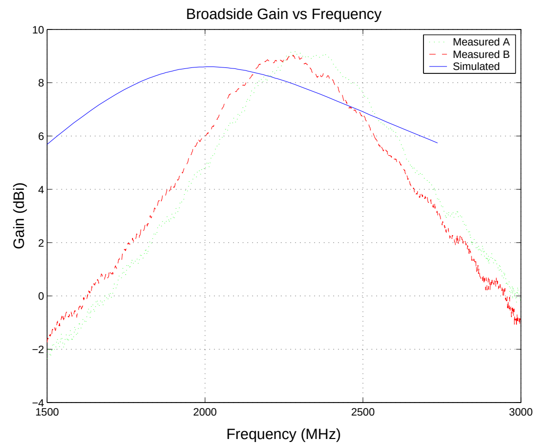

(b) Comparison of measured and simulated gain characteristics for probe-fed patch.

Fig. 25. Comparison of measured and simulated antenna characteristics.

D. *Electromagnetically-coupled Rectangular Patch*

The objective of this section is to determine the accuracy with which an electromagnetically coupled rectangular patch can be simulated. This is achieved by quantifying the difference between simulated and measured results as an error percentage. This error can be compared with the error associated with other simulation/analysis techniques. Two rectangular electromagnetically-fed patch antennas were provided by Poynting Innovations for measurement in this investigation. These antennas were presented as patches 4 and 5 in Section C-B.1, this section will use the same reference names.

TABLE VIII

GEOMETRICAL CHARACTERISTICS OF THE INVESTIGATED RECTANGULAR ELECTROMAGENTICALLY COUPLED PATCH

Parameter	**Value**
Length	40mm (0.33λ)
Width	50mm (0.41λ)
Height	11.2mm (0.093λ)
Feed Length	23mm (0.19λ)
Feed Overlap	-14.5mm (0.12λ)
Feed Height	7mm (0.058λ)
Feed Diameter	2mm (0.017λ)
Feed Offset	0mm

The antenna investigated in this section exhibits the geometrical characteristics shown in Table VIII. A photograph of the electromagentically coupled patch can be seen in Figure 23 [29]. It is currently not possible to take the effect of the dielectric cover into account when modelling a patch antenna with SUPERNEC. Typically the dielectric cover would decrease the resonant frequency [31]. However, resonance (as defined in Appendix A) was not encountered in the measured and simulated results, so this behaviour was not verified. This geometry was simulated in SUPERNEC using a model frequency of 3500MHz.

It can be seen from Figure 28 that the real part of the measured antenna impedance varies greatly for both of the physical antennas. Patch 4 exhibits a larger peak resistance than the simulated patch. In contrast Patch 5 exhibits a peak resistance smaller than that of the simulated patch. This behaviour emphasizes the concepts mentioned in Section C-B on factors influencing the agreement of measured and simulated results.

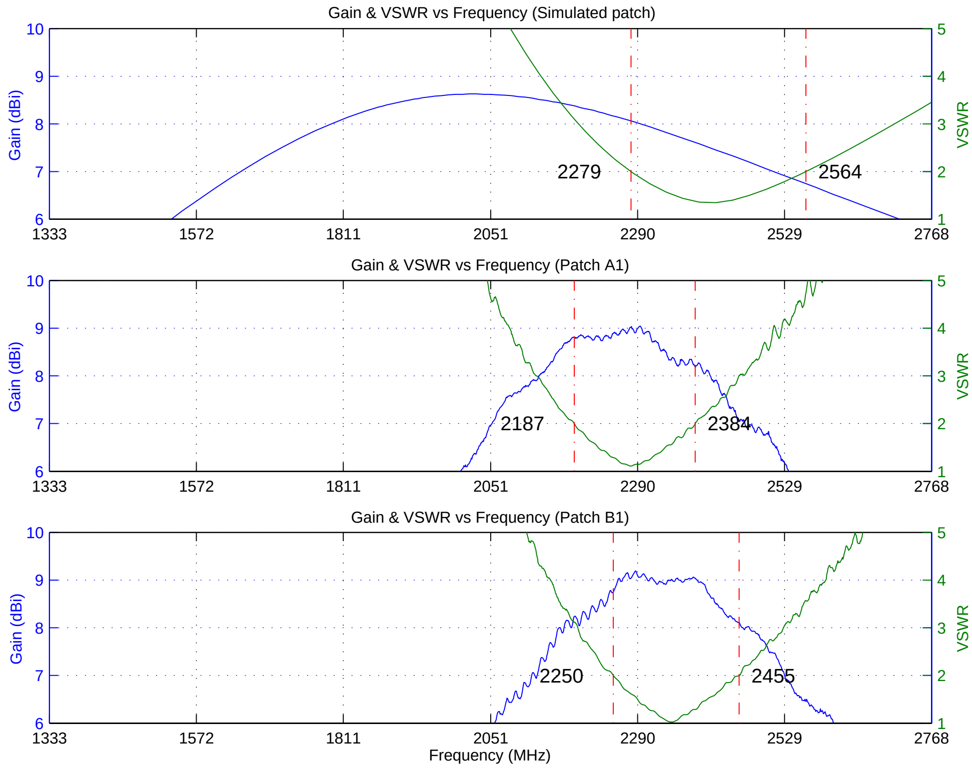

Fig. 26. Comparison of measured and simulated gain and VSWR characteristics for probe-fed patch. Top: Simulated results. Middle: Patch A1. Bottom: Patch B1.

Figure 29(a) shows that the VSWR characteristics of the measured antennas are fairly similar to that of the simulation, even though the measured impedance characteristics tended to fluctuate around the simulated results. This implies that the simulation is useful for predicting an antennas VSWR characteristics even if the measured and simulated impedance values are not totally in agreement. in agreement.

The gain characteristics of the measured and simulated antennas is presented in Figure 29(b). The measured gain is seen to be approximately 1dBi less than that of the simulated antenna over the operating frequency band where the antennas VSWR is less than 2. This may be due to measurement inaccuracies resulting from the Network Analyzer amplifier not providing a sufficiently powerful signal for accurate two-antenna gain measurements. The measured gain characteristic

An alternative representation of the measured and simulated antennas' gain and VSWR characteristics is shown in Figure 30. It can be clearly seen from Figure 30 that the physical antennas exhibit a similar operating frequency to that of the simulated antenna. The impedance bandwidth of Patch 5 is comparable to that of the simulation, whereas Patch 4 exhibits a an impedance bandwidth greater than the simulation.

Table VI shows the values of the electrical characteristics for the measured and simulated antennas. The antenna did not resonate as defined in Appendix B, hence no data is presented for this characteristic. However, the antenna can still be characterised by its peak resistance value. This behaviour shows the importance of the decision made in Section C-A to record both resonance and maximum resistance characteristcs for the purpose of characterizing a patch antennas behaviour.

Table X presents the error in the simulated patch electrical parameters with reference to the measured results. The results for each electrical parameter are discussed below:

Fig. 27. Photograph of electromagentically coupled patch.

TABLE IX
RESULTS OF RECTANGULAR ELECTROMAGNETICALLY-FED PATCH INVESTIGATION

Performance Parameters	**Simulated Results**	**Patch 4**	**Patch 5**
Centre Frequency (MHz)	2600	2440	2517
Impedance Bandwidth	19.0% (478.1 MHz)	25.7% (656.3 MHz)	18.4% (457.0 MHz)
Centre Gain (dBi)	8.9	7.4	7.9
Gain Variation (%)	95.9	91.9	92.5
Resonant Frequency (MHz)	-	-	-
Resonant Resistance (Ω)	-	-	-
Frequency of Maximum Resistance (MHz)	2520	2552	2496
Maximum Resistance (Ω)	53.9	68.2	45.0

- **Centre Frequency:** The simulated and measured centre frequency values are fairly similar, with an acceptable error under 10% reported for both physical patches.
- **Impedance Bandwidth:** A large error in the bandwidth resulted for Patch 4, with the physical patch exhibiting a much larger bandwidth than the simulation predicted. In contrast, the bandwidth of Patch 5 was quite similar to that predicted by the simulation.
- **Centre Gain:** A large error of over 10% for the simulated centre gain was calculated for both the measured antennas. This discrepancy is attributed to the network analyser used for measuremnts, as described earlier in this section.
- **Gain Variation:** The gain variation is very similar for both the measured patches, with an error of less than 5% being calculated for both antennas.
- **Resonant Frequency and Resistance:** Resonance did not occur as predicted by the simulation. However, it can be seen from Figure 7 that both measured results did not resonate due to the inductive characteristic of the impedance whereas the simulated impedance did not resonate due to a capacitive impedance. Frequency of Maximum Resistance: The predicted frequency of maximum resistance was extremely accurate, with an error of under 2% calculated for both

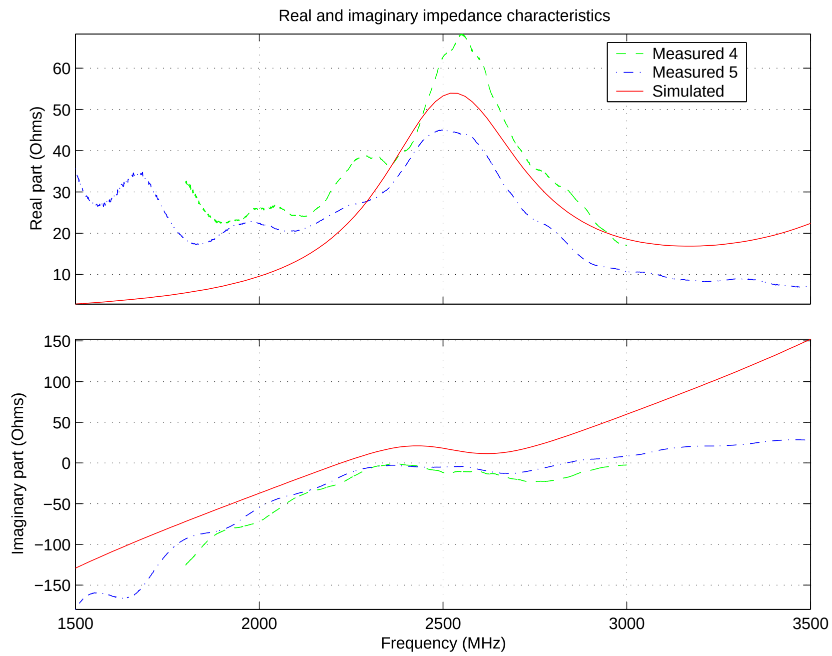

Fig. 28. Comparison of measured and simulated impedance characteristics for EM-fed patch.

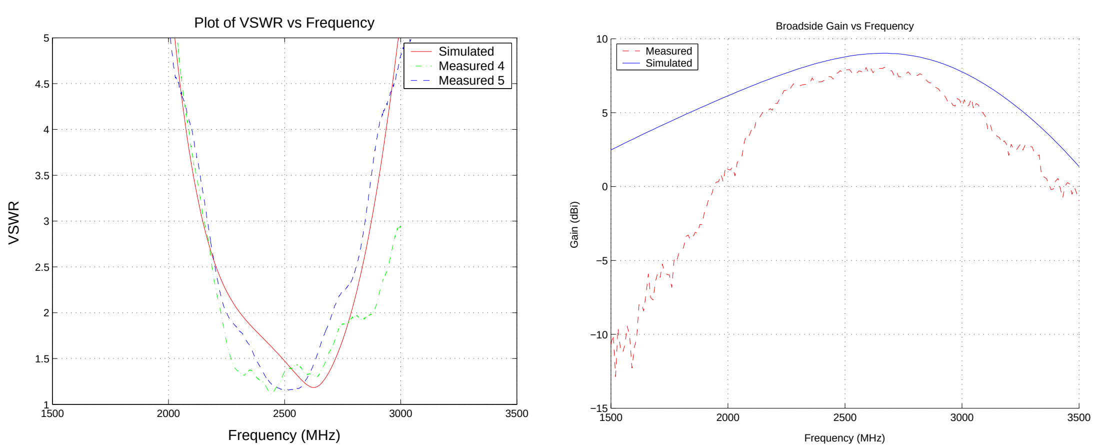

(a) Comparison of measured and simulated VSWR characteristics for EM-fed patch.

(b) Comparison of measured and simulated gain characteristics for EM-fed patch.

Fig. 29. Comparison of measured and simulated antenna characteristics for EM-fed patch.

antennas measured.

- **Maximum Resistance:** A large error in the maximum resistance was recorded for both measured antennas. This result should not be taken as an indication that the simulation was inaccurate as the measured results varied dramatically from each other. It is more likely that constructional tolerances, as discussed in Section C-B.1, account for this discrepancy.

E. Conclusion

In order to make a verdict on whether the accuracy of the patch antenna simulations presented in this appendix are satisfactory, it is necessary to compare the error associated with SuperNEC patch

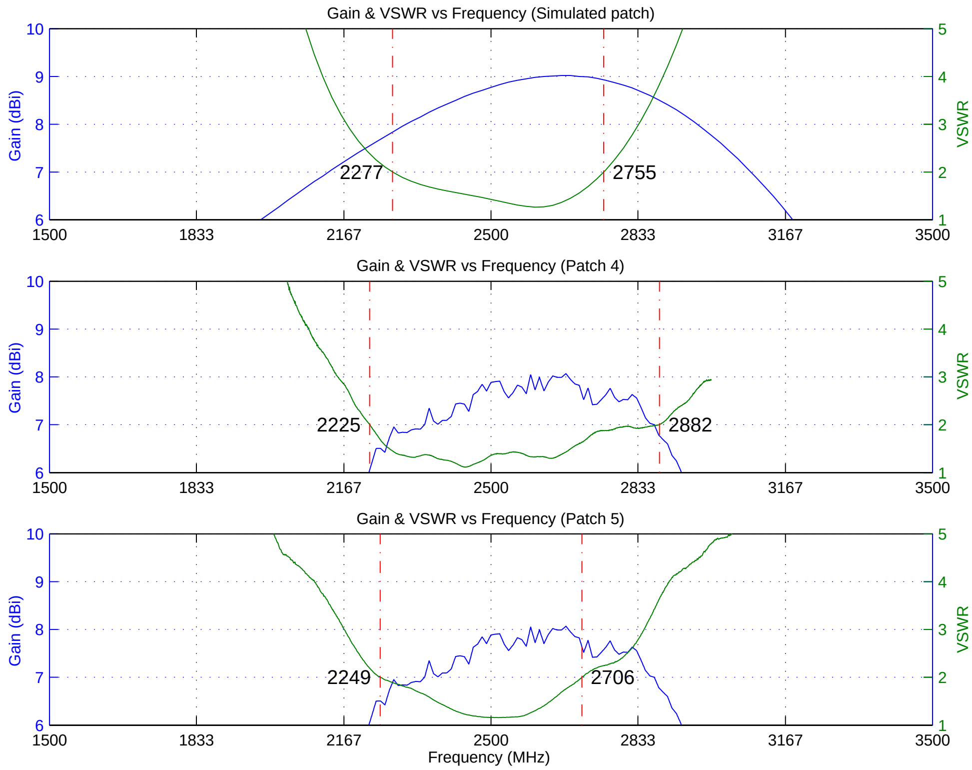

Fig. 30. Comparison of measured and simulated gain and VSWR characteristics for electromagnetically-fed patch Top: Simulated results. Middle: Patch 4. Bottom: Patch 5.

TABLE X
ERROR RESULTS FOR RECTANGULAR ELECTROMAGNETICALLY-FED PATCH INVESTIGATION

Performance Parameters	**Patch 4 Error %**	**Patch 5 Error %**
Centre Frequency	6.53	3.27
Impedance Bandwidth	-26.05	3.02
Centre Gain	20.98	13.55
Gain Variation	4.39	3.73
Resonant Frequency	-	-
Resonant Resistance	-	-
Frequency of Maximum Resistance	-1.26	0.94
Maximum Resistance	-21.02	19.82

antenna simulations with the error reported for other methods of simulation and analysis. Table XI shows the simulation errors calculated for various patch antenna configurations investigated in [12]. It should be noted that the third simulation method makes use of MoM, as does SuperNEC . Unfortunately the study presented in Table XI only gives the error in the resonant characteristics of the antennas. However this information can still be compared to the resonant characteristics error calculated in this appendix. Table XI presents the data for three different patch antenna cases.

The error in resonant frequency reported in Table XI is under 10% for all the investigated antennas. The same is true of the resonant frequency error calculated in Section C-C. The antennas investigated in Section C-D did not resonate, but the error in these antennas maximum resistance characteristics can be used as an alternative method of comparison. The error of the maximum resistance frequency for these antennas is also under 10%.

TABLE XI

COMPARISON OF MEASURED AND SIMULATED RESULTS

	Cavity Model 1		**Cavity Model 2**		**Moment Method**	
Case	**Frequency % Error**	**Resistance % Error**	**Frequency % Error**	**Resistance % Error**	**Frequency % Error**	**Resistance % Error**
1a	-2.6	-26	-1.3	31	-0.4	4.4
1b	-2.6	-21	-1.3	67	0.9	17.6
1c	-2.6	19	-1.3	153	1.3	-10.7
2a	-1.8	-41	-0.5	43	1.6	3.2
2b	-3.1	-9	-0.9	216	2	41.5
2c	-6.5	20	-1.5	320	1.3	25
3a	0	-44	2.3	18	6.9	15.7
3b	-2.7	-43	-0.5	102	2.2	-6.2
3c	-2.2	32	0	376	2.7	17.6
4a	-	-	-	-	-	-
4b	-	-	-	-	-	-
4c	-7.8	144	0.7	2122	6.4	300
5a	-2	-21	-0.3	-11	0	-4.4
5b	-2.5	-7.8	-0.8	10	-1.3	13
5c	-2.5	32	-0.8	58	-1.3	-11
6a	-1.8	-34	0.5	-40	0.5	5.2
6b	-3	-22	-0.1	-8	-0.5	31
6c	-3.1	54	-0.3	82	-0.7	16
7a	-2.9	-15.9	-0.5	-	-0.5	20
7b	-3.4	-11	-0.5	5.7	-0.8	45
7c	-2.9	75	0	109	-0.3	31
8a	-7.8	15.9	-	-	0.39	110
8b	-		-	-	-	
8c	-		-	-	-	

The error in resonant resistance reported in Table XI varies considerably from antenna to antenna, with a minimum reported error of 3.2% and a maximum error of 300% (ignoring the 2122% outlying error). In comparison, the error values reported for Section A-C varied from 9.93% to 49.27%, showing that these results did not achieve the minimum accuracy found in [12] but were also not as inaccurate for certain cases. The maximum resistance characteristics reported in C-D exhibited errors of 21.02% and 19.82%. This result is not considered accurate, but is nevertheless still on the order of the errors shown in Table XI.

A more comprehensive study would require error data for the gain and bandwidth characteristics of the patches investigated using other simulation and analysis techniques. This error could be compared with the error in gain and bandwidth presented in this study, and a more definitive verdict on SUPERNEC's patch antenna simulation accuracy made.

The effect of constructional tolerances (and other factors that can influence the agreement of measured and simulated results - as outlined in Section C-B) plays a large part in determining the errors presented. This was emphasized by the discrepancy between measured results for similar antennas, constructed using the same geometrical specification. It can thus be stated that not all the error should be attributed to the method of analysis/simulation alone.

Even though the SUPERNEC patch antenna simulations were not in total agreement with the measured results, the simulation error is comparable to that of other simulation and analysis techniques. It can be concluded that the simulation accuracy of SUPERNEC is acceptable for producing a first iteration of a practical antenna. Design curve data generated using SUPERNECwill thus also allow the antenna designer to get a good initial patch antenna design.

Appendix D: Patch Antenna Parameter Study

Abstract

This appendix presents a parameter study of the rectangular probe-fed and electromagnetically coupled patch antennas. The objective of the parameter study is to establish which geometrical parameters affect the antennas' electrical parameters most significantly. A large data set of patch antenna electrical characteristics was generated for a variety of patch configurations. The configurations were derived from designs exhibiting optimized impedance bandwidth, for various gain constraints. Effectively, this is a study of initial design curve data, thus giving results which are significant for the objective of this dissertation - patch design. From this data set the correlation between the antennas' geometrical and electrical characteristics was calculated and the most significant geometrical characteristics were identified. This knowledge allows simplification of the patch antenna design process for the investigated antennas, as only the most important geometrical characteristics need to be actively used in the design process.

A. Parameter Study Objective

Probe-fed and electromagnetically coupled patch antennas have many geometrical parameters. Varying the value of these geometrical parameters effects the electrical characteristics, and hence performance characteristics, of the antenna. The objective of the formal parameter study presented in this section is to ascertain which, if any, geometrical parameters have significant correlation with the antenna's performance parameters. The more geometrical parameters which are actively used in a design, the more complex and time consuming it is to generate design curve data for the design. The parameter study knowledge will allow a simplified patch antenna design procedure to be formulated in Appendix E. This simplification is possible by taking only the most significant geometrical parameters into account when developing the design process. Simplification of the design process is desirable given the large number of geometrical parameters belonging to a patch antenna.

B. Parameter Study Approach

Although parameter studies already exist in the literature, [1] pp39–49, 138–145, it was felt that these studies were somewhat limited, as the relative effect of the geometrical parameters of the electrical parameters was not formally quantified and only the geometrical characteristics of a single, nominal patch were varied in these studies. Rather than focusing on the behaviour of a single, nominal patch antenna geometry when it's geometrical parameters are varied, this study analyzes the data generated from a number of nominal antenna configurations which exhibit significantly different performance characteristics. The nominal configurations were selected from preliminary design curve data generated by solving an impedance bandwidth optimization problem, subject to a particular gain constraint. This design curve data was refined further following the parameter study, as outlined in design process described in Appendix E.

This study entails every geometrical parameter belonging to a nominal patch configuration being varied from it's nominal value to values 10% greater and 10% smaller than the nominal value. Data was also recorded for the variation of every parameter when the antenna's other parameters were varied simultaneously. This required the generation of data for 2^{N} cases of the antenna for each nominal geometry studied, where N is the number of geometrical characteristics belonging to the antenna. The SUPERNEC simulation software was the mechanism by which the study data sets were generated.

The parameter study data sets are analysed by the calculation of the correlation coefficient between all the parameters. A large, positive correlation coefficient (value is close to one) between two variables indicates that the two variables move together; if one increases then so does the other. A large negative correlation coefficient (value is close to negative one) between two variables indicates that the two variables move in opposite directions; if one increases then the other decreases. A correlation coefficient close to zero indicates that there is no significant correlation between two variables.

This study only discusses the performance parameters; operating frequency, bandwidth and gain characteristics [2], as they are the parameters most relevant for design. The other electrical parameters have been reported for consistency with the classical analysis of patch antennas which appears in the literature [18]. The electrical parameters of interest belonging to the studied antennas are:

- Operating frequency
- Impedance bandwidth
- Gain (minimum and centre)
- Gain variation
- Resonant frequency
- Resonant resistance
- Frequency of maximum resistance
- Maximum resistance

The definitions of these parameters can be seen in Appendix A. The efficiency was not reported as all configurations make use of an air dielectric which has little loss, and hence the efficiency is consistently 100% for the TM_{10} mode of operation investigated.

Sections D-C and D-D present the parameter studies for the probe-fed rectangular patch and the electromagnetically-fed rectangular patch respectively. Section D-E summarizes the major conclusions and recommendations derived from this investigation.

C. Probe-fed Rectangular Patch Antenna Parameter Study

This section presents an analysis of how the variation of the probe-fed rectangular patch antenna's geometrical parameters effect this antenna's electrical characteristics. The parameter study of the probe-fed rectangular patch antenna involves the variation of fifteen nominal patch cases' geometrical parameters. The performance characteristics of these nominal cases can be seen in Table XII and the geometries are given in Table XIII. As the probe-fed patch has six geometrical parameters, each case consists of 2^6 variations of the nominal patch and the nominal patch which results in a total of 65 observations per case. Data for $15 \times 2^6 = 960$ variations of the nominal patches was generated, resulting in a data set of $960 + 15 = 975$ observations for the study in total. The geometrical values for each observation in the data set can be seen in Figure 31. The nominal geometry values for each case are marked by red circles.

The corresponding electrical characteristics for the configuration geometries shown in Figure 31 can be seen in Figure 32. As expected, the data from the parameter study varies about the nominal values for each case. It should be noted that resonance did not occur for the first three nominal cases, and hence certain variations of these antennas also did not resonate. This can be seen in the plots of resonant resistance and resonant frequency in Figure 32, where non-resonating data is omitted from the plots.

TABLE XII

PERFORMANCE PARAMETERS OF ANTENNAS STUDIED

Nominal Case	Bandwidth (%)	Minimum Gain (dBi)
1	6.2439	9.96
2	6.5801	9.8
3	7.2513	9.68
4	7.915	9.64
5	8.6019	9.41
6	9.1698	9.15
7	9.792	8.9
8	10.325	8.57
9	10.959	8.25
10	11.397	7.83
11	11.961	7.45
12	12.43	6.98
13	12.885	6.63
14	13.184	6.39
15	13.291	6.28

TABLE XIII

NOMINAL GEOMETRIES OF ANTENNAS STUDIES

Nominal Case	Length (m)	Width (m)	Height (m)	Feed Inset (m)	Feed Offset (m)	Feed Radius (m)
1	0.03	0.047	3.70e-3	1.75e-3	0	1.15e-3
2	0.03	0.046	3.83e-3	7.54e-4	0	1.15e-3
3	0.03	0.042	4.28e-3	1.50e-3	0	1.15e-3
4	0.03	0.04	4.08e-3	1.76e-3	0	1.14e-3
5	0.03	0.036	4.44e-3	1.72e-3	0	1.13e-3
6	0.03	0.033	4.83e-3	1.74e-3	0	1.13e-3
7	0.03	0.030	5.22e-3	1.91e-3	0	1.12e-3
8	0.03	0.026	5.58e-3	1.75e-3	0	1.11e-3
9	0.03	0.023	6.03e-3	1.71e-3	0	1.10e-3
10	0.03	0.020	6.46e-3	1.79e-3	0	1.08e-3
11	0.03	0.016	7.17e-3	1.76e-3	0	1.06e-3
12	0.03	0.013	7.29e-3	2.31e-3	0	1.03e-3
13	0.03	0.010	7.38e-3	3.57e-3	0	1.01e-3
14	0.03	0.008	7.54e-3	4.0e-3	0	0.988e-3
15	0.03	0.007	7.53e-3	4.13e-3	0	0.968e-3

The correlation between all the electrical and geometrical parameters was calculated, giving the correlation coefficient matrix displayed in Figure 33. The polarity of each correlation coefficient is represented by a '+' or '-' sign on the figure. The correlation between the performance parameters and the geometrical parameters is discussed below.

- *Frequency of operation:* The operating frequency shows a strong correlation with the patch length of -0.82. This correlation is evident in Figure 34, where increasing the patch length of a particular configuration results in the TM_{10} mode of operation, characterised by the behaviour of the impedance (the resistive peak), occurring at a lower frequency. Figure 35 shows how the frequency at which the antenna operates is affected, with the $\mathrm{VSWR} < 2$ characteristic occurring at lower frequencies as the length increases. This result is consistent with that expected in the literature [1] p30.
- *Bandwidth:* The bandwidth shows strongest correlation with the patch width (-0.64) and the patch height (+0.48). These results are expected from the literature [1] p42–44. Figure 36 shows how increasing the patch width of a particular configuration decreased the bandwidth from 2.4% to 2.0%. Figure 37 shows how increasing the patch height increased the bandwidth from 2.3% to 2.7%. The results shown in Figures 36 and 37 reflect the negative correlation between the bandwidth and patch width and the positive correlation between bandwidth and patch height. As the feed position has a direct effect on the matching of the antenna, this

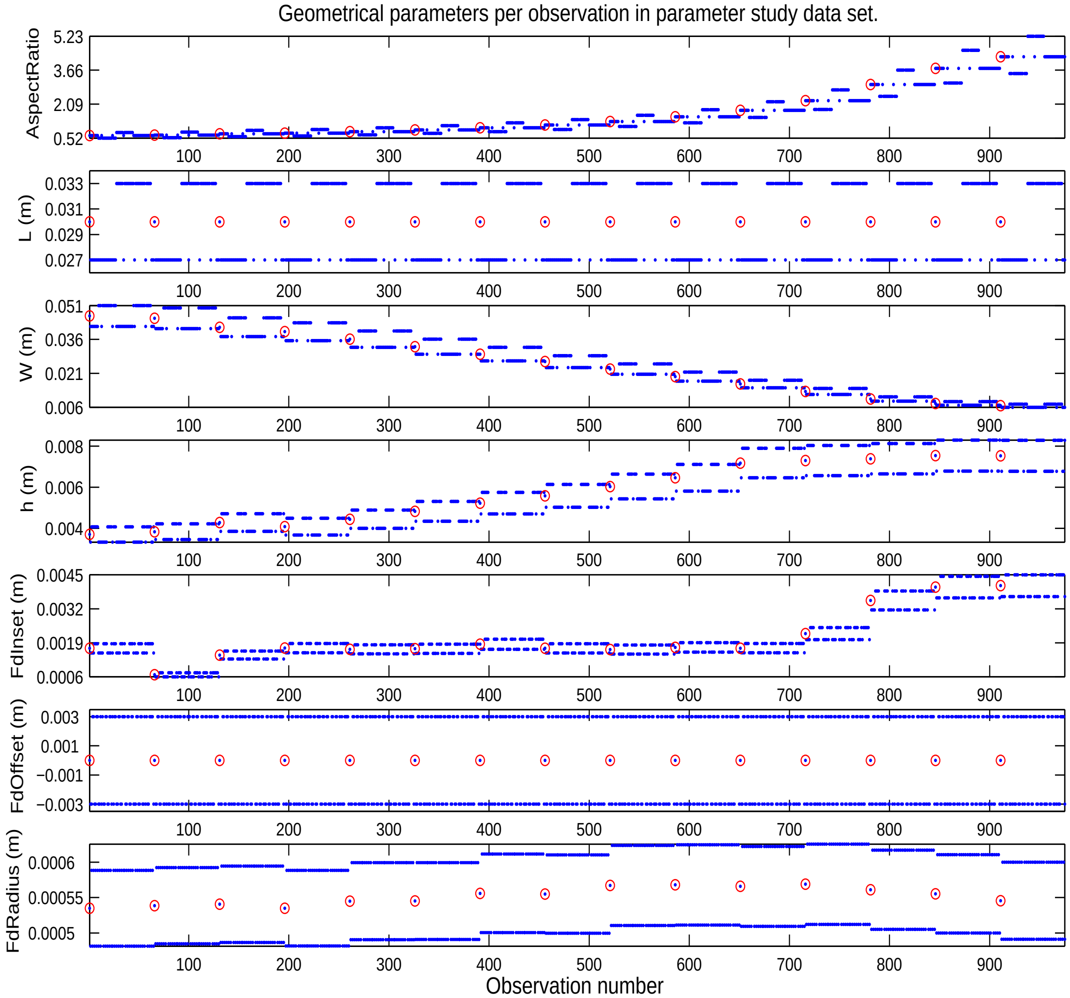

Fig. 31. Geometrical data for each observation in the probe-fed patch parameter study. Nominal data points are circled.

parameter is also important even though significant correlation with the bandwidth was not reported. Significant correlation was shown between the resonant and maximum resistance parameters and the feed inset, which implies an effect on the bandwidth.

- *Center gain and Minimum gain:* Both the center and minimum gain showed strong correlation with the patch width (0.97) and the patch height (-0.91). These results are expected from the literature [1] p42–44. Figure 36 shows how increasing the patch width increased the centre gain from 9.5dBi to 10dBi and the minimum gain from 9.3dBi to 9.8dBi for a particular configuration. Figure 37 shows little variation in the gain characteristics due to changing the patch height, implying that a study of single nominal patch does not provide a comprehensive study of an antenna's behaviour. In contrast Tables XV and XII, which present the characteristics of the multiple configurations investigated in this study, show that the minimum gain decreased from 9.96dBi to 6.28dBi as the patch height increased from 3.7mm to 7.5mm over the nominal cases considered.
  The negative correlation between the gain (both minimum and center) and the patch height is a function of the nominal patch configurations investigated, as it is expected from the literature that increasing the patch height should result in more radiated power [10] p265. This emphasizes the fact that a combination of parameters is responsible for the antenna's resulting characteristics.
- *Gain variation:* The gain variation shows strongest correlation with the aspect ratio (-0.98). As the aspect ratio is a ratio of the length to the width this implies that increasing the width

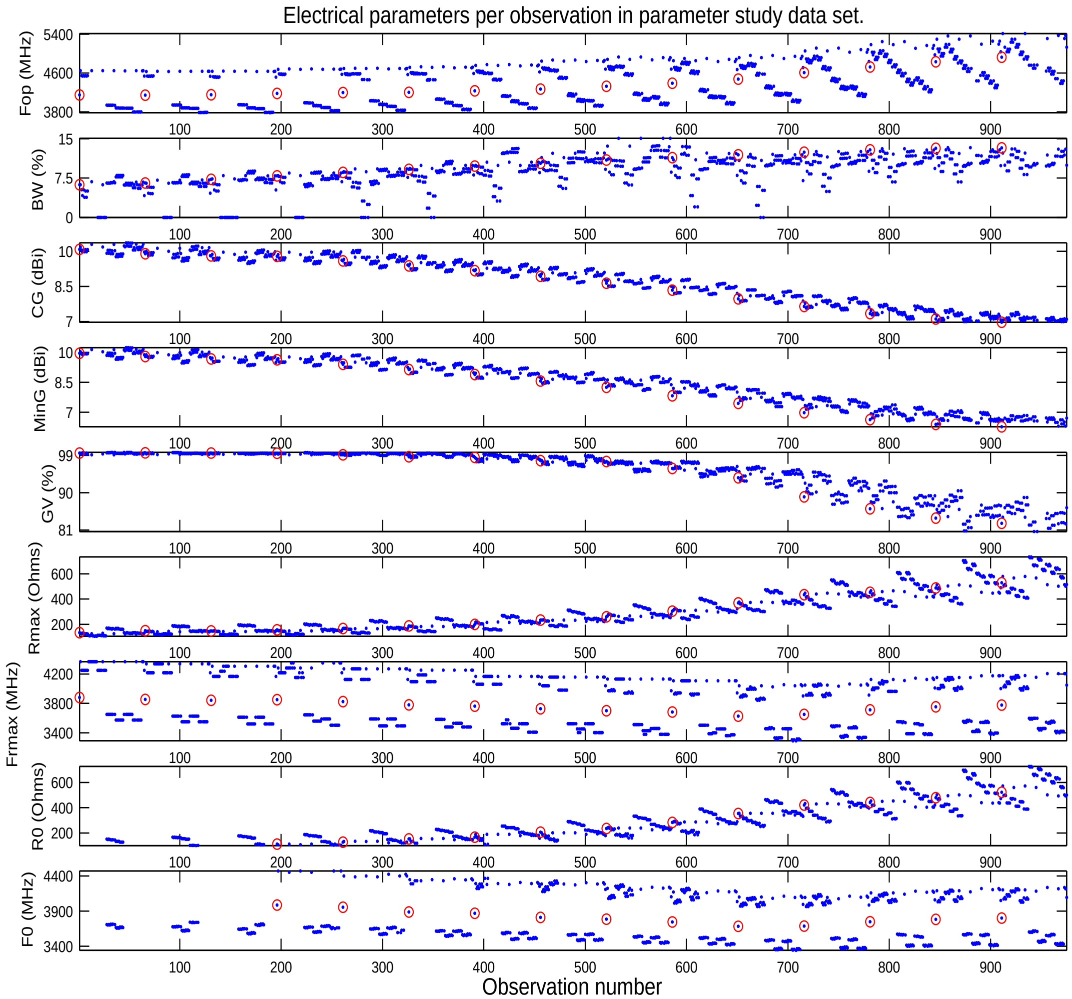

Fig. 32. Electrical data for each observation in the probe-fed patch parameter study. Nominal data points are circled.

increases the gain variation percentage and indeed there is a strong correlation of +0.86 between the width and the gain variation. Figure 38 shows how the gain in Case 1 (width = 0.047m) varies very little over the frequency band of operation (where $\mathrm{VSWR} < 2$), depicted by the dotted lines, with a gain variation of 97%. In contrast Case 15 (width = 0.007m) shows a large variation of the gain over the frequency band of operation (a gain variation of 82%). The frequency band of operation is also larger for Case 15, giving the gain a greater frequency range over which to vary. This characteristic is expected when noting the negative correlation between gain variation and bandwidth - the larger the bandwidth, the smaller the gain variation percentage which implies a more varying gain over the operating frequency band.

Figure 33 shows that variation of the feed offset and feed radius seem to have little correlation with the antenna's electrical characteristics. For this reason these two parameters will not be actively part of the probe-fed patch design. The length, width, height and feed inset showed significant correlation with the performance parameters and will be used actively in the patch antenna design.

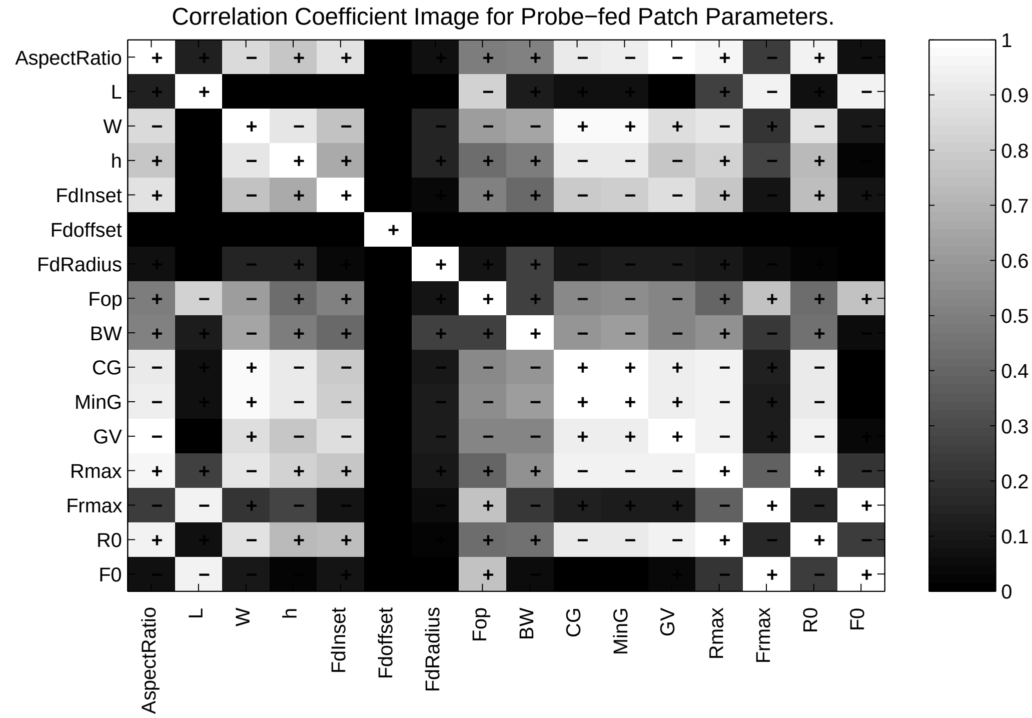

Fig. 33. Correlation coefficient matrix for entire probe-fed patch parameter study data-set.

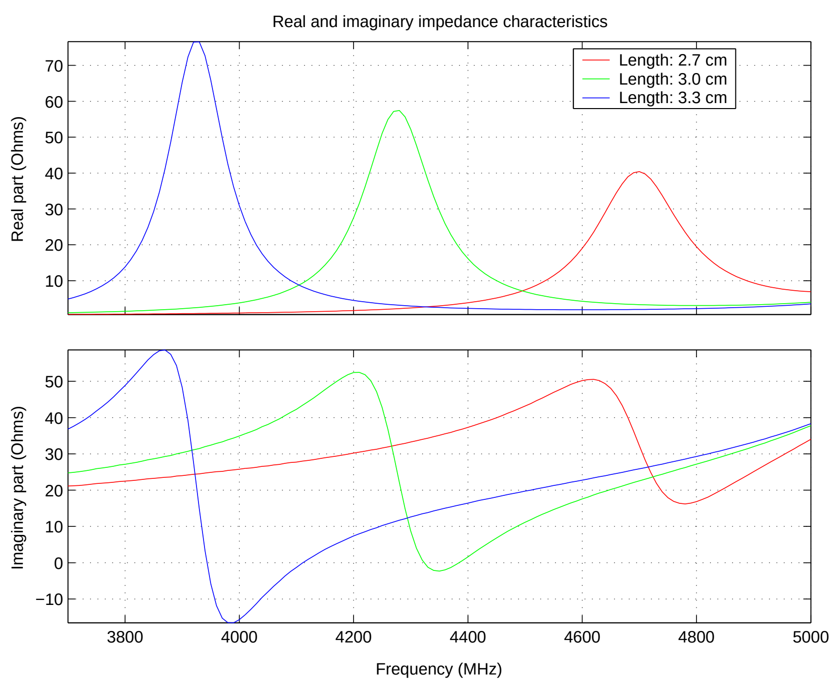

Fig. 34. Effect of patch length on the probe-fed patch impedance characteristics.

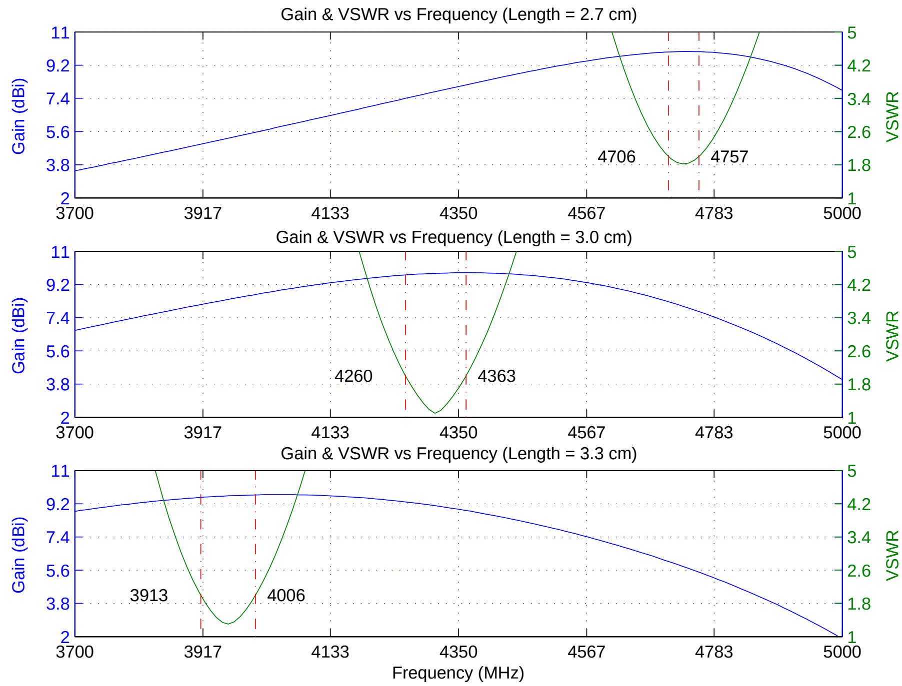

Fig. 35. Effect of patch length on the probe-fed patch gain and VSWR characteristics.

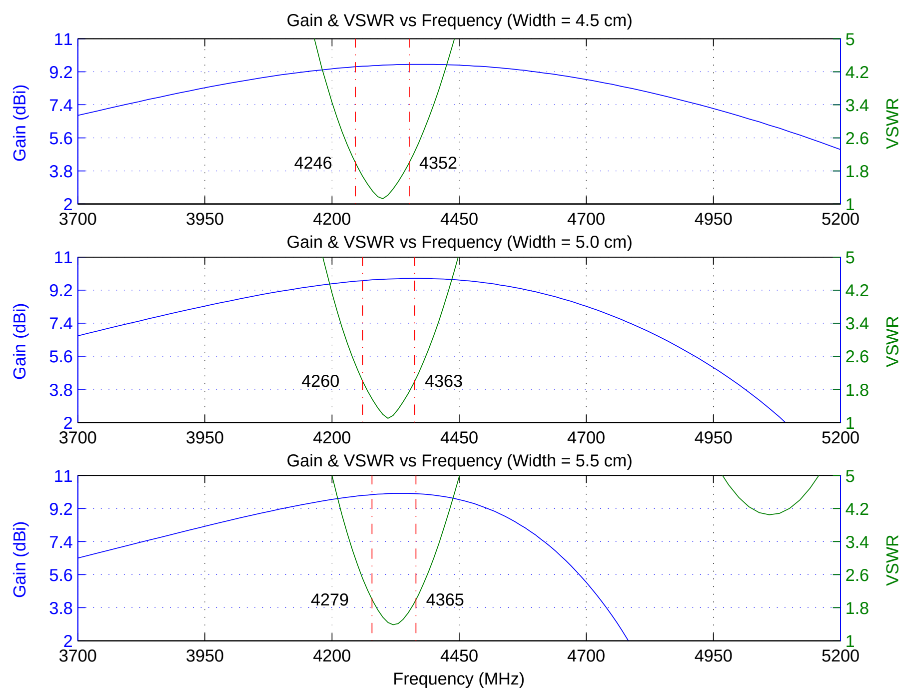

Fig. 36. Effect of patch width on the probe-fed patch gain and VSWR characteristics.

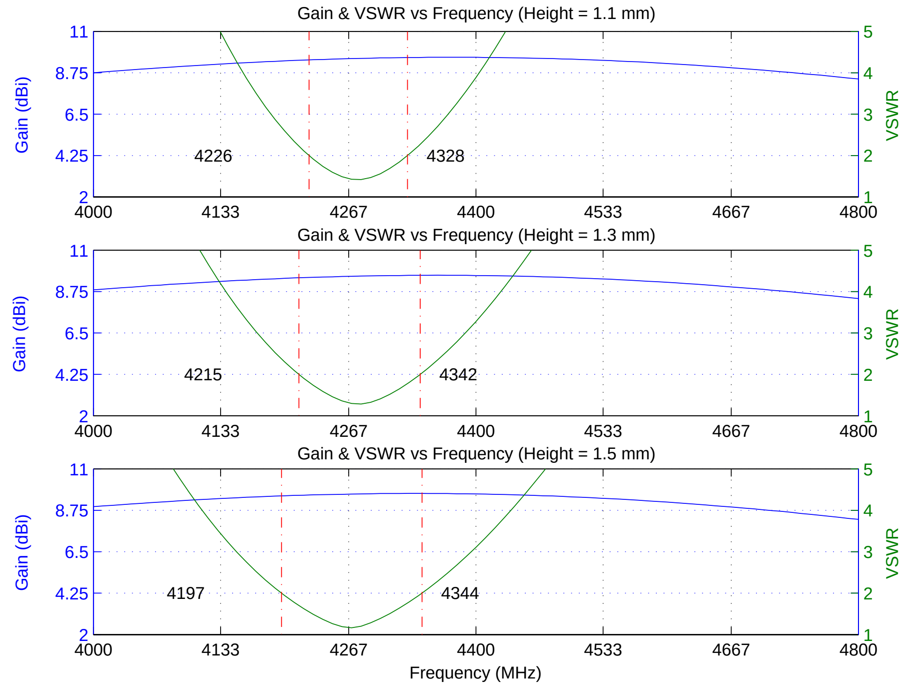

Fig. 37. Effect of patch height on the probe-fed patch gain and VSWR characteristics.

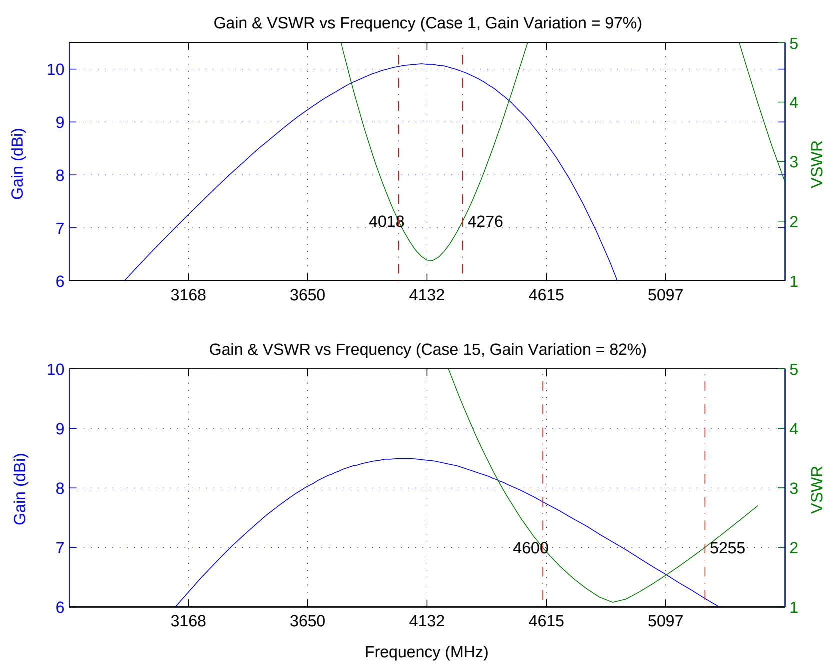

Fig. 38. Overlay of gain and VSWR data for gain variation investigation.

D. Electromagnetically Coupled Rectangular Patch Antenna

This section presents an analysis of how the variation of the electromagnetically-fed rectangular patch antenna's geometrical parameters, to values 10% greater and smaller than the nominal value, effects this antenna's electrical characteristics. Fourteen nominal patch cases' geometrical parameters are considered. The performance characteristics of these nominal cases can be seen in Table XIV and the geometries are given in Table XV. As this patch has eight geometrical parameters, each case consists of 2^8 variations of the nominal patch plus the nominal patch which results in a total of 257 observations per case. Data for $14 \times 2^8 = 3584$ variations of the nominal patches was generated, resulting in a data set of $3584 + 14 = 3598$ observations for the study in total. The geometrical values for each observation in the data set can be seen in Figure 39. The nominal geometry values for each case are marked by red circles.

TABLE XIV
PERFORMANCE PARAMETERS OF NOMINAL ANTENNA CASES STUDIED

Nominal Case	Bandwidth	Minimum Gain
1	7.35	9.622
2	10.02	9.24
3	16.18	9.05
4	18.53	9.03
5	20.39	8.88
6	22.53	8.75
7	26.13	8.48
8	31.43	8.04
9	32.49	7.99
10	36.62	7.46
11	37.37	7.35
12	39.97	7.25
13	42.92	6.6
14	43.43	6.45

TABLE XV
NOMINAL GEOMETRIES OF ANTENNA CASES STUDIED

Nominal Case	**Length (m)**	**Width (m)**	**Height (m)**	**Feed Overlap (m)**	**Feed Length (m)**	**Feed Height (m)**	**Feed Offset (m)**	**Feed Diameter (m)**
1	0.03	0.0392	0.0061	-0.002	0.0191	0.0036	0	1.042e-3
2	0.03	0.0308	0.0065	6.64E-04	0.0191	0.0033	0	1.040e-3
3	0.03	0.0387	0.0062	-0.0036	0.0162	0.0036	0	1.042e-3
4	0.03	0.0392	0.0065	-0.0048	0.0151	0.0045	0	1.004e-3
5	0.03	0.0392	0.0065	-0.0035	0.0152	0.0043	0	1.062e-3
6	0.03	0.0431	0.0062	-0.0036	0.014	0.0043	0	1.062e-3
7	0.03	0.0498	0.0075	-0.004	0.0128	0.005	0	1.110e-3
8	0.03	0.0392	0.0073	-0.0048	0.012	0.0054	0	1.043e-3
9	0.03	0.0392	0.008	-0.0048	0.0115	0.0058	0	1.113e-3
10	0.03	0.0392	0.0091	-0.0049	0.0115	0.007	0	1.147e-3
11	0.03	0.0387	0.0091	-0.0065	0.0115	0.0071	0	1.144e-3
12	0.03	0.0335	0.0091	-0.0067	0.0109	0.0071	0	1.124e-3
13	0.03	0.0281	0.0109	-0.0051	0.0116	0.0084	0	1.144e-3
14	0.03	0.0239	0.0116	-0.004	0.0116	0.0085	0	1.144e-3

The corresponding electrical characteristics for the configuration geometries shown in Figure 39 can be seen in Figure 40. As expected, the data from the parameter study varies about the nominal values for each case. It should be noted that resonance did not occur for the first two nominal cases, and hence certain variations of these antennas also did not resonate. This can be seen in the plots of resonant resistance and resonant frequency in Figure 40, where non-resonating data is omitted from the plots.

The correlation between all the electrical and geometrical parameters was calculated, giving the

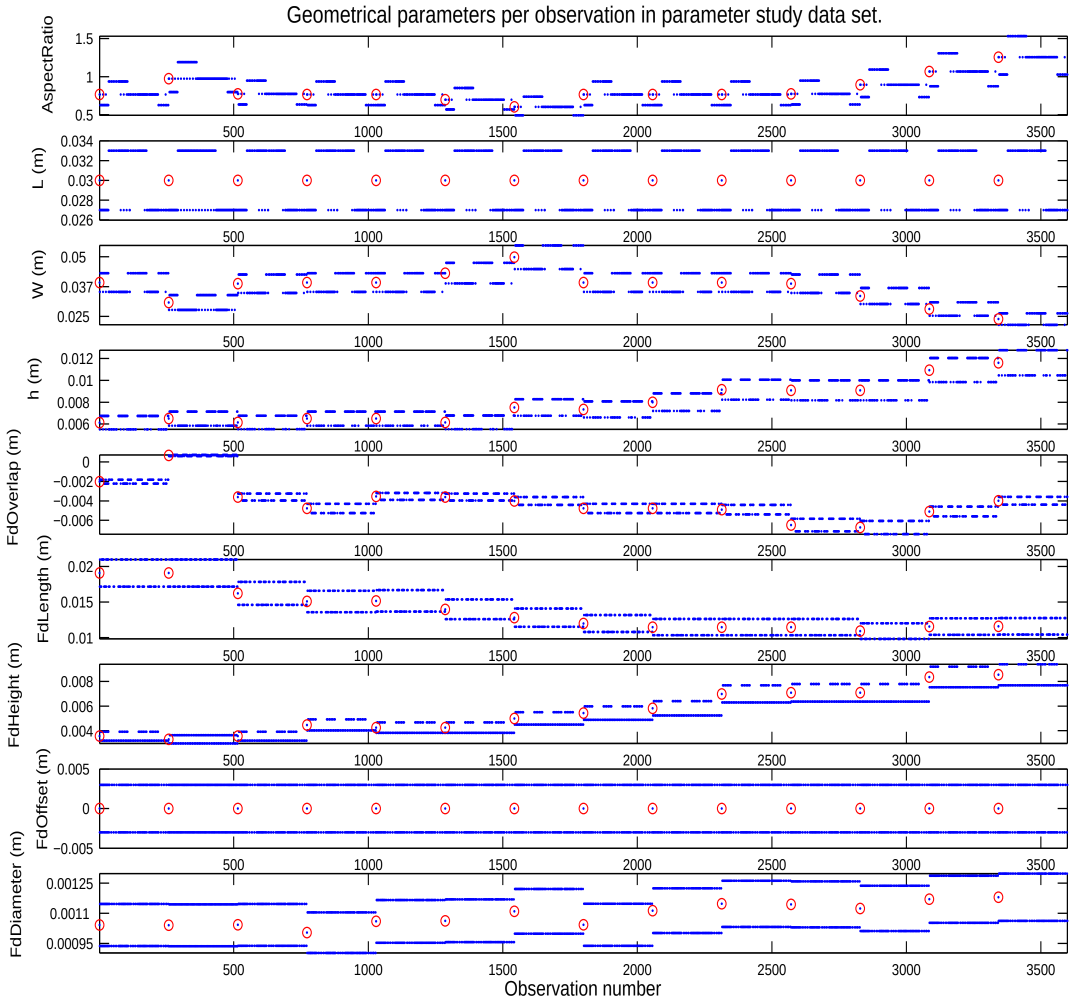

Fig. 39. Geometrical data for each observation used in the EM-fed patch parameter study. Nominal data points are circled.

correlation coefficient matrix displayed in Figure 41. The polarity of each correlation coefficient is represented by a '+' or '-' sign on the figure. The correlation between the performance parameters and the geometrical parameters is discussed below.

- *Frequency of operation:* The operating frequency shows a strong correlation with the patch length of -0.76. This correlation is evident in Figure 42, where increasing the patch length results in the TM_{10} mode of operation occurring at a lower frequency. Figure 43 shows how the frequency at which the antenna operates is affected, with the $\mathrm{VSWR} < 2$ characteristic occurring at lower frequencies as the length increases. This result is consistent with that expected in the literature [1] p30.
- *Bandwidth:* The bandwidth did not show strong correlation with any particular geometrical parameter. This implies that the bandwidth may be dependant on a combination of geometrical parameters. However, strongest correlation occurred with the patch height (+0.41), feed length (-0.44) and feed height (+0.46). This correlation is expected from the literature as [1] pp134–136 and can be seen in Figure 44, where the bandwidth and gain characteristics of the two configurations for cases 7 and 14 can be compared. Figure 44 shows that the height and bandwidth both increase from 7.5mm and 26% (case 7) to 11mm and 43% (case 14) respectively. This behaviour implies that there is a positive correlation between the height and bandwidth, as expected. The negative correlation between the feed length and bandwidth is shown by the feed length decreasing from 12mm to 11mm as the bandwidth increases. The feed height shows the

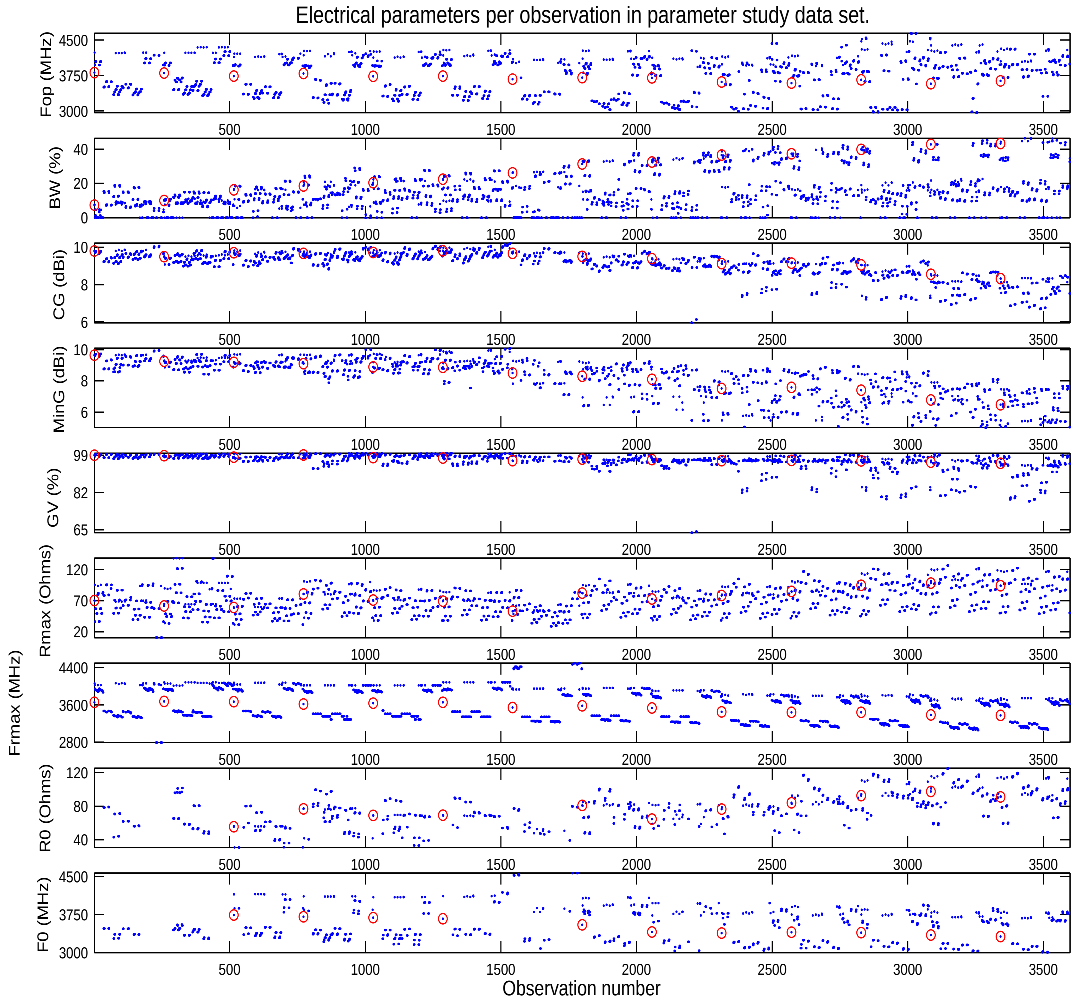

Fig. 40. Electrical data for each observation in the EM-fed patch parameter study. Nominal data points are circled.

expected positive correlation, increasing from 5mm to 8.5mm as bandwidth increases.

- *Center gain:* The center gain showed strong correlation with the aspect ratio (-0.64) which is reflected in the width (+0.62). The patch height (-0.84) and the feed height (-0.77) also showed significant correlation. These results are exemplified in Figure 44 where the positive correlation between the width and center gain can be seen, with both the width and center gain decreasing from 49mm and 9.7dBi (case 7) to 23mm and 8.4dBi (case 14) respectively. The negative correlation between the patch height and the center gain is shown with these parameters changing from 7.5mm and 9.7dBi (case 7) to 11mm and 8.4dBi (case 14). Similar behaviour is seen between the feed height and the center gain with these parameters changing from 5mm and 9.7dBi (case 7) to 8.5mm and 8.4dBi (case 14).
  The negative correlation between the gain (both minimum and center) and the patch height is a function of the nominal patch configurations investigated, as it is expected from the literature that increasing the patch height should result in more radiated power [10] p265. This emphasizes the fact that a combination of parameters is responsible for the antenna's resulting characteristics.
- *Minimum gain:* The center gain showed strong correlation with the patch height (-0.84), the feed length (+0.67) and the feed height (-0.77). In contrast to the results for the center gain, the minimum gain showed little correlation with the patch width (0.36). This indicates a distinct difference between the behaviour of the electromagnetically-fed and probe-fed patches, which showed strong correlation between the minimum gain and the patch width. This result implies

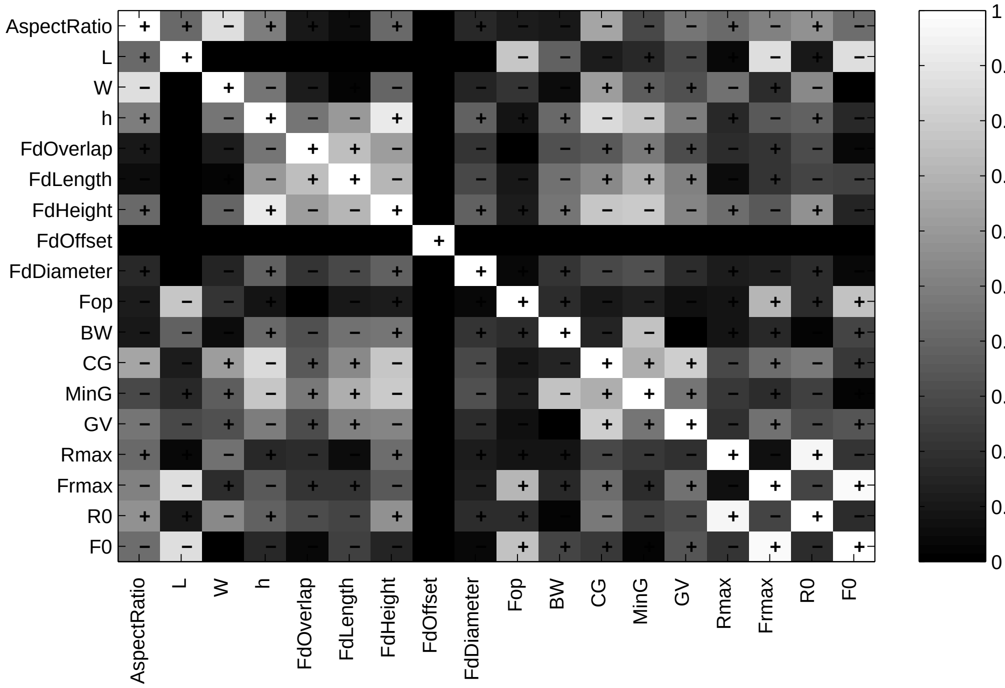

Fig. 41. Correlation coefficient matrix for entire EM-fed patch parameter study data-set.

that different design procedures will apply to each configuration if a certain minimum gain is required. A comparison of cases 1 and 14 in Figure 44 shows that as the patch height and feed height increase from 7.5mm and 5mm to 11mm and 8.5mm respectively, the minimum gain decreases from 8.4dBi (case 7) to 6.45dBi (case 14). An expected negative correlation between the patch height, feed height and the minimum gain is thus evident. A positive correlation between the feed length and minimum gain is also noted in Figure 44 as the feed length and minimum decrease from from 12mm and 8.4dBi (case 7) to 11mm and 6.45dBi (case 14) respectively.

- *Gain variation:* The gain variation showed little correlation with any particular geometrical parameter. This is expected when viewing the nominal gain variation data in Figure 40 which shows the gain variation to be fairly constant for the nominal configurations investigated. The gain variation did, however, appear to vary more for the cases that exhibited smaller gain characteristics and increased bandwidth (after observation 2000). As with the bandwidth, this implies a dependency on multiple geometrical parameters.

Figure 41 shows that variation of the feed offset and feed radius seem to the geometrical parameters with the least correlation with the antenna's electrical characteristics. For this reason these two parameters will not be actively part of the electromagnetically coupled patch design. The length, width, height and feed overlap, feed length and feed height showed significant correlation with the performance parameters and will be used actively in the patch antenna design.

E. Conclusion

This appendix presented parameter studies for the probe-fed and electromagnetically coupled rectangular patch antennas. The correlation between geometrical and electrical the parameters was calculated, providing insight into which geometrical parameters are most significant for patch design purposes. For the probe-fed patch the following geometrical parameters were selected for design:

- Patch length - strong correlation with operating frequency.

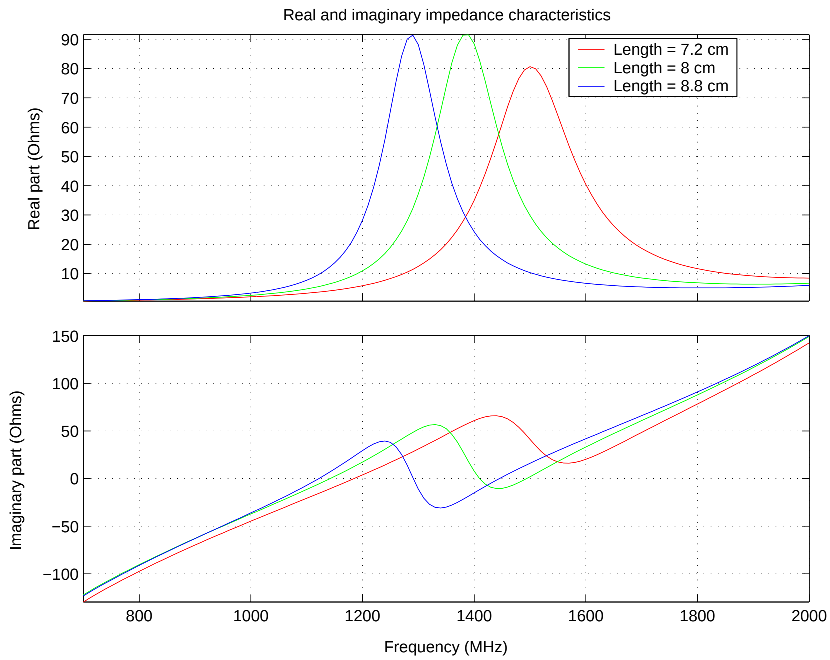

Fig. 42. Effect of patch length on the electromagentically coupled patch impedance characteristics.

- Patch width - correlation with bandwidth and gain.
- Patch height - correlation with bandwidth and gain.
- Feed inset - correlation with gain and necessary for achieving matching due to it's effect on the input impedance.

For the electromagnetically coupled patch the following geometrical parameters were selected for design:

- Patch length - strong correlation with operating frequency.
- Patch width - no strong correlation with any particular electrical parameter, but there was small, but not insignificant, correlation with gain.
- Patch height - correlation with bandwidth and gain.
- Feed overlap, length and height - the combination of feed characteristics allows impedance matching to occur. These particular characteristics showed small correlation with all the electrical parameters other than operating frequency.

The results and conclusions derived from any parameter study are obviously dependant on the data set analysed. The nominal cases used in the parameter study were generated by the use of bandwidth optimization routines given a particular minimum gain constraint, thus this data can be seen as preliminary design curve data. The data chosen for the studies presented in this Appendix is thus highly relevant to patch design, as outlined in Appendix E. It is impractical to study a complete range patch data where infinite configurations can occur, so limiting the data set to data relevant to the design process was seen as an acceptable compromise, although the conclusions may not be generally applicable to all patch configurations. The parameter study presented in this section focuses on the correlation between geometrical and electrical parameters. Analysis of the results showed good agreement with the literature for the probe-fed patch. The magnitude of the effect of the geometrical parameters on the electrical parameters has not been investigated. It is felt that establishing the correlation between parameters is sufficient for the purposes of this study, as the process of generating the design data by optimization should implicitly take the magnitude of the geometrical parameters effect into account.

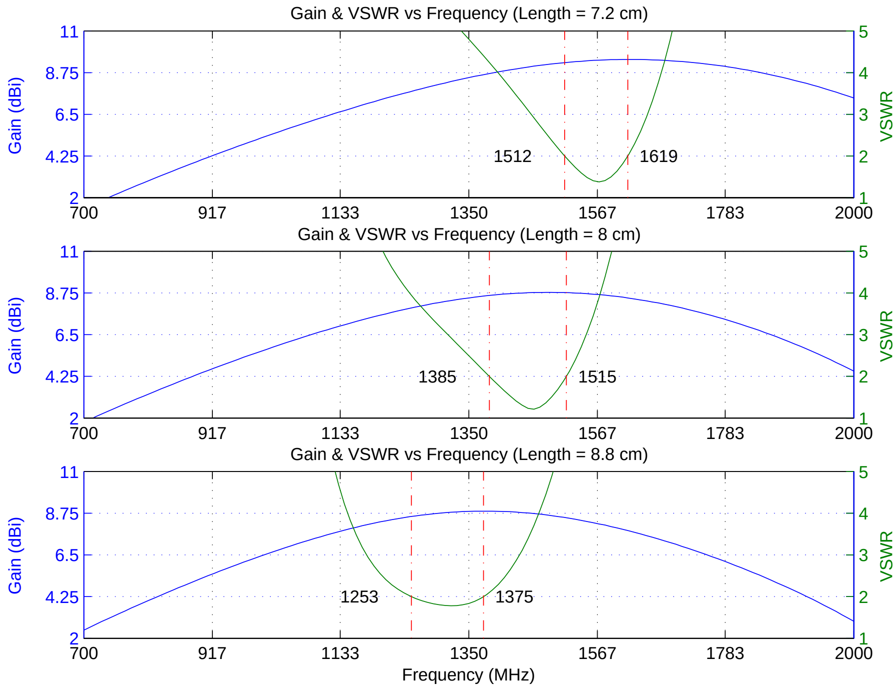

Fig. 43. Effect of patch length on the electromagentically coupled patch gain and VSWR characteristics.

The implication of this parameter study on the design of the probe-fed patch and electromagentically coupled patch is the ability to simplify the design curves. Simplification is desirable for generating design curve data rapidly, as well as allowing a user of the design process to find an appropriate antenna configuration with minimum effort. This simplification is achieved by justifying the reduction of the number of variables which are actively used in the design process, as concluded in Sections D-C and D-D.

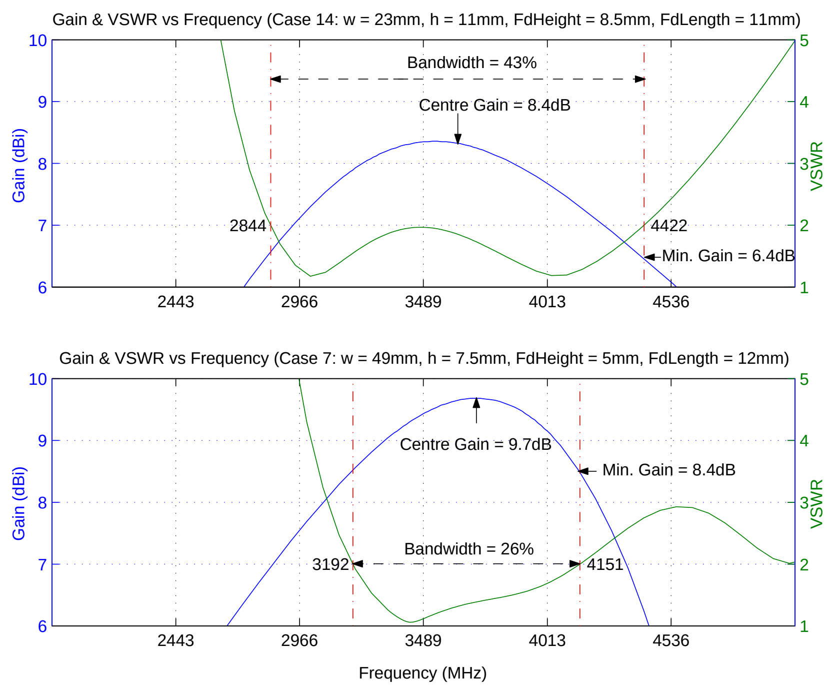

Fig. 44. Comparison of gain and VSWR characteristics for case 7 and case 14.

APPENDIX E:
PATCH ANTENNA DESIGN

Abstract

This appendix describes the generation of design curves for the rectangular, probe-fed and rectangular, electromagnetically coupled patch antennas. The design procedure involves the selection of the patch antenna geometrical characteristics such that an acceptable tradeoff between the gain and impedance bandwidth offered by the antenna exists. The design curves given in this appendix allow a practical first iteration of the desired patch antenna design, with a given performance requirement, to be rapidly found. The bandwidth and minimum gain configurations for design of the probe-fed patch range from 6.2% and 9.9dBi to 13.2% and 6.1dBi. The bandwidth and minimum gain configurations for design of the electromagentically coupled patch patch range from 9.5% and 9.7dBi to 44% and 6.0dBi.

A. Introduction to Patch Antenna Design

Few patch antenna design procedures have been presented in the literature [2], [4], implying that practical patch antenna design is still limited to the design-by-simulation approach or the iteration of a physical prototype. These approaches require the designer to have a broad knowledge of patch antenna operation in order to produce a successful design. In practice, tolerances in construction and material characteristics play a significant role in determining the performance of an antenna. For this reason any theoretical design should be viewed as the first, ideal iteration in the antenna development process. This reality should be noted by the designer, who should accept that a software design package is an aid and not a substitute for experience and understanding the fundamentals [3]. However, a formal design procedure, as presented in this Appendix, can aid the designer in gaining a good first iteration of the patch antenna with minimum time and effort required.

A design strategy proposed in [3] is to use design curves for obtaining a starting point in the design process and then iterate the design using a CAD model, followed by experimental iteration. The objective of this Appendix is to present the formulation of the first design stage involving the generation of design curves. The benefit of having design curves for an antenna of interest would be the rapid progression to finding a suitable initial design. There could possibly be another constraint on the design, not taken into account by the design curves (for example beam width or antenna size). Specialization of this initial design could then take place via further parameter tuning, or other geometrical alteration, in a simulation environment before the design enters the experimental stage. The design process presented in this Appendix involves the selection of patch antenna geometrical characteristics subject to a trade-off between the antenna's minimum gain (over the impedance bandwidth) and the size of the impedance bandwidth. Increasing the antenna's minimum gain implies a reduction in impedance bandwidth and vice versa.

In general the design curve data was generated by solving a bandwidth optimization problem subject to a specified gain constraint. The optimization problem was setup in MATLAB which used SUPERNEC for simulating the antenna configuration's characteristics. This process is outlined in Section E-B. The results of the design curve generation for the probe-fed and electromagnetically coupled patches can be seen in Sections E-C and E-D respectively. All geometrical parameters are given in terms of wavelength (λ), as calculated in Equation 10, allowing the appropriate physical antenna dimensions to be found for any desired operating frequency and gain/bandwidth configuration.

$$\lambda = \frac{c}{F} \tag{10}$$

Where c is the speed of light and F would be the desired frequency of operation of the antenna. Actual usage of the design curves is described in Section E-E.

The electrical parameters which define the basic performance of the antenna are:

- Operating frequency
- Impedance bandwidth
- Minimum gain

The performance requirements of the antenna to be designed are specified by defining these parameters.

B. Design Curve Data Generation

This section describes the process of generating data for use in design curves. As optimal impedance bandwidth is desired for most patch antennas [5] – [7], the design curve data was generated by solving a number of impedance bandwidth optimization problems. Each impedance bandwidth optimization problem was subject to a particular minimum gain constraint. These gain constraints ranged from approximately 9dBi to unconstrained optimization routines which generally resulted in a minimum gain of 6dBi being realised. Design curves can be constructed from these patch configurations which offer optimal impedance bandwidth for a variety of minimum gain values. This implies that an aspect of the design curves will be the relationship between gain and impedance bandwidth for a variety of patch configurations, and indeed this can be seen in the resulting design curves shown in Figures 46, 49 and 50. The process of generating this data required the solution of a number of sub-problems to be coded in MATLAB [30]. These sub-problems, which are outlined below, allow the automation of the extremely time-intensive procedure required for generating design curve data. Knowledge of the expected operation of the patch antenna in the desired TM_{10} is vital for implementing an automated optimization program (see Appendix B for more information the TM_{10} mode of operation).

When a patch antenna optimization routine is executed, it is necessary for the optimization routine to iteratively evaluate a variety of different patch antenna models automatically. The optimization routine uses the results of evaluating the different patch models in order to determine how the antenna's geometrical characteristics should be modified, such that a more optimal design is achieved in the next optimization routine iteration. The ability to automate the simulation of any patch antenna configuration in SUPERNEC is required for an optimization problem to be solved programmatically. Although a SUPERNEC simulation can be initiated via a command in MATLAB, there are simulation parameters, such as the SUPERNEC model frequency and the range and resolution of the simulation frequencies, that still need to be setup automatically. The `singlesim` function was coded in order to implement this functionality (See Appendix F for more information on the code structure). The automated simulation process is described below.

1) The patch antenna geometrical characteristics are the inputs to the simulation program.
2) The frequency range over which the antenna is to be simulated must be calculated automatically while the optimization program is running. An initial guess of the antenna's operating frequency in the TM_{10} mode was calculated using the transmission line theory for a patch antenna's resonant frequency as shown in Equation 5 of Appendix B, Section B-E.

3) The antenna was then simulated over a frequency range from 30% greater to 30% smaller than the predicated resonant frequency, with 30 frequency steps in this range. The SUPERNEC antenna model was segmented at 1.6 times the highest frequency of simulation, as this was found to result in a valid model structure. The results of this initial simulation are used for defining a more appropriate frequency range of simulation.
4) A more refined frequency range over which the patch will be simulated can now be found by analysing the radiation pattern data from the initial simulation. As the current distribution on the antenna surface in the TM_{10} mode takes the form of half a period of a sine wave, an example of which can be seen in Figure 45(a), it is expected that the radiation pattern will follow a similar shape, as shown in Figure 45(b). The gain characteristics for each of the 30 frequency steps simulated previously are analysed and the frequencies at which the antenna's broadside gain is greater than any other gain value in the plane parallel to the antenna's length is recorded. The frequency at which the largest broadside gain occurred in this set is used as the centre frequency for the next simulation. This code can be seen in lines 82 – 93 of the `singlesim` function and predicted a satisfactory simulation frequency range for both the probe-fed and electromagnetically coupled patches.

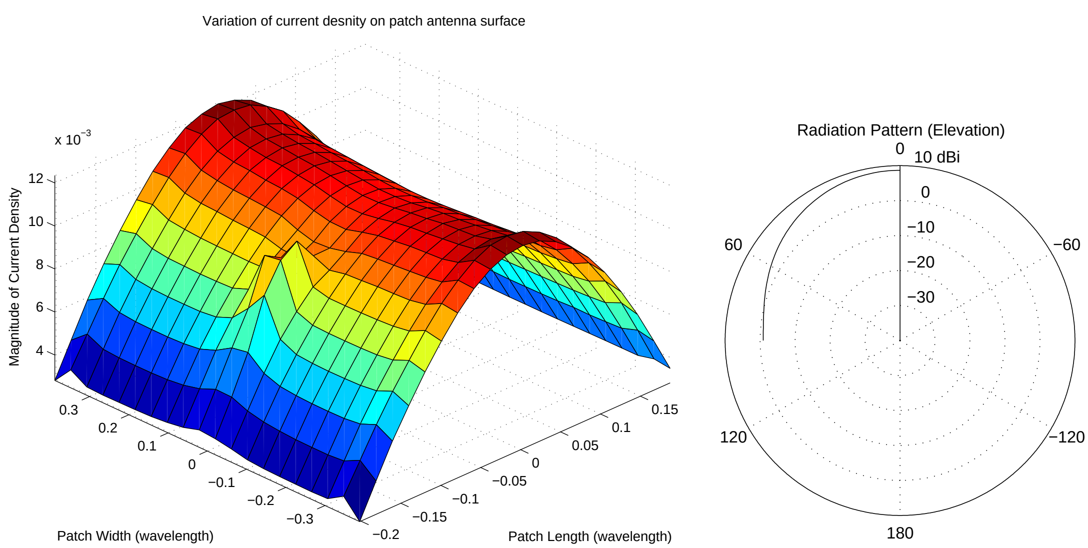

(a) Patch antenna current distribution in TM_{10} mode.

(b) Patch antenna radiation pattern in TM_{10} mode.

Fig. 45. Current distribution and radiation pattern characteristics for patch antenna operation in the TM_{10} mode..

5) A final simulation is then run over the frequency range from 45% less than the new simulation centre frequency to 45% greater than the new simulation frequency. There are 65 frequency steps in this range. Once again, the SUPERNEC antenna model was segmented at 1.6 times the highest frequency of simulation. The gain and impedance data over all the simulation frequencies is returned from this patch simulation program for analysis in the optimization program .

A genetic algorithm based optimization approach was ultimately chosen for the purposes of optimizing an antenna's performance characteristics. Although some initial success was achieved using a gradient-based, Gauss-Newton algorithm approach to the optimization, it was found that the nature of the objective function lent itself to a genetic algorithm solution.

The following description of the genetic algorithm is quoted from The MathWork's Genetic Algorithm and Direct Search Toolbox accompanying documentation [30]: *"The genetic algorithm is a method for solving optimization problems that is based on natural selection, the process that drives biological evolution. The genetic algorithm repeatedly modifies a population of individual solutions.*

At each step, the genetic algorithm selects individuals at random from the current population to be parents and uses them produce the children for the next generation. Over successive generations, the population "evolves" toward an optimal solution. You can apply the genetic algorithm to solve a variety of optimization problems that are not well suited for standard optimization algorithms, including problems in which the objective function is discontinuous, non-differentiable, stochastic, or highly nonlinear."

The programs which implement the optimization for the probe-fed patch and electromagnetically coupled patches are called `pbgabwoptimization` and `emgabwoptimization` respectively. The desired gain constraint for the optimization is setup in these functions and the bandwidth and minimum gain is calculated from the information returned by the `singlesim` program. This gain constraint was implemented implicitly for the probe-fed patch, by fixing the width value with which the optimization was performed. This implicit implementation of the gain constraint is justified by noting the strong correlation between the gain and impedance bandwidth exhibited in the probe-fed patch parameter study (D, Section D-C). The gain constraint for the electromagnetically coupled patch was implemented explicitly, as no clear correlation between the gain and a particular geometrical parameter was noted in the parameter study. The implicit gain constraint was implemented by penalizing an optimization iteration's score if the resultant minimum gain was under the minimum gain constraint. The severity of the penalty depended on the square of the difference between the actual and required minimum gain values, if the actual gain was less than the required gain. Otherwise the score was not penalized. This means that it was possible to find a patch configuration for which the bandwidth was optimized and the minimum gain actually exceeded the constraint. The constraint can therefor be seen as a lower bound for the minimum gain.

When the optimization terminates these programs return the impedance, gain and geometrical characteristics of the best patch configuration which can be saved to disc for later incorporation into design curves. More information on these programs can be found in Appendix F.

The feed radius for both the probe-fed and electromagnetically coupled patches is dependant on the antennas operating frequency. In order to produce a valid SUPERNEC structure, each segment in the SUPERNEC model must have a radius calculated by:

$$SegmentRadius = \frac{SegmentLength \times \lambda_{seg}}{2 \times \pi} \tag{11}$$

Where:

$SegmentLength$ is the length of the segment, in terms of wavelength, and equal to 0.1 for these models.
λ_{seg} is the wavelength of the frequency at which the model is segmented.

The radius of the feed is calculated in the same manner (the electromagnetically coupled patch arbitrarily uses the diameter of the feed instead of the feed radius as a parameter). This means that Equation 11 can be expressed in terms of the wavelength of the operating frequency for each patch, as shown in Equations 12 and 14.

Equation for the feed radius of the probe-fed patch:

$$FeedRadius = \frac{0.1 \times \lambda_{op}}{2 \times FS \times \pi} \tag{12}$$

Where:

λ_{op} is the wavelength of the antenna's operating frequency.
FS is the factor by which the operating frequency must be scaled in order to equal the SUPERNEC model's segmentation frequency. The frequency of segmentation varied between 2.45 and 1.73 times the patch antenna operating frequency for the probe-fed patch, depending on the bandwidth configuration chosen. The mean value for this factor is 2.17 but a more accurate value can be found via the polynomial shown in Equation 13, which was fitted to the frequency scaling factors over the entire bandwidth range.

$$FS = -0.01Bandwidth^2 + 0.096Bandwidth + 2.218 \tag{13}$$

Where $Bandwidth$ is the impedance bandwidth, selected from the design curves of Section E-C, for which the antenna will be designed.

Equation for the feed diameter of the electromagnetically coupled patch:

$$FeedDiameter = \frac{0.1 \times \lambda_{op}}{FS \times \pi} \tag{14}$$

Where:

$$FS = -63 \times 10^{-5}Bandwidth^2 + 0.036Bandwidth + 2.238 \tag{15}$$

FS ranges between 2.588 and 2.119 with a mean value of 2.4 for the electromagnetically coupled patch .

The approximate nature of these equations is justified by the small effect the feed radius/diameter has on the patch electrical characteristics, as shown in Appendix D. Examples in which Equations 13 and 15 are used can be seen in Section E-E.

C. Probe-fed Rectangular Patch Design Curves

The design variables for the probe-fed patch, selected in Section D-C of Appendix D, are:

- Length
- Width
- Height
- Feed inset

The feed offset was set to 0 and the feed radius is dependant on the frequency of operation, approximately calculated as shown in Equation 12. The strong correlation between the patch width and the antenna's gain characteristics, as shown in Section III, prompted an implicit implementation of the gain constraint for the probe-fed patch by optimizing the impedance bandwidth for fixed values of patch width. Fixing the patch width reduces the number of variables actively varied in the optimization problem. Reducing the variables in the optimization problem provides the benefit faster convergence to an optimal solution. The resulting design curves can be seen in Figure 46.

The x-axis for all the design curve plots represents the percentage impedance bandwidth that a particular patch antenna design can offer. The minimum gain (and centre gain) corresponding to a particular bandwidth percentage can be read off the top-most graph. Given the required antenna impedance bandwidth, the length, width, height and feed inset geometrical antenna characteristics,

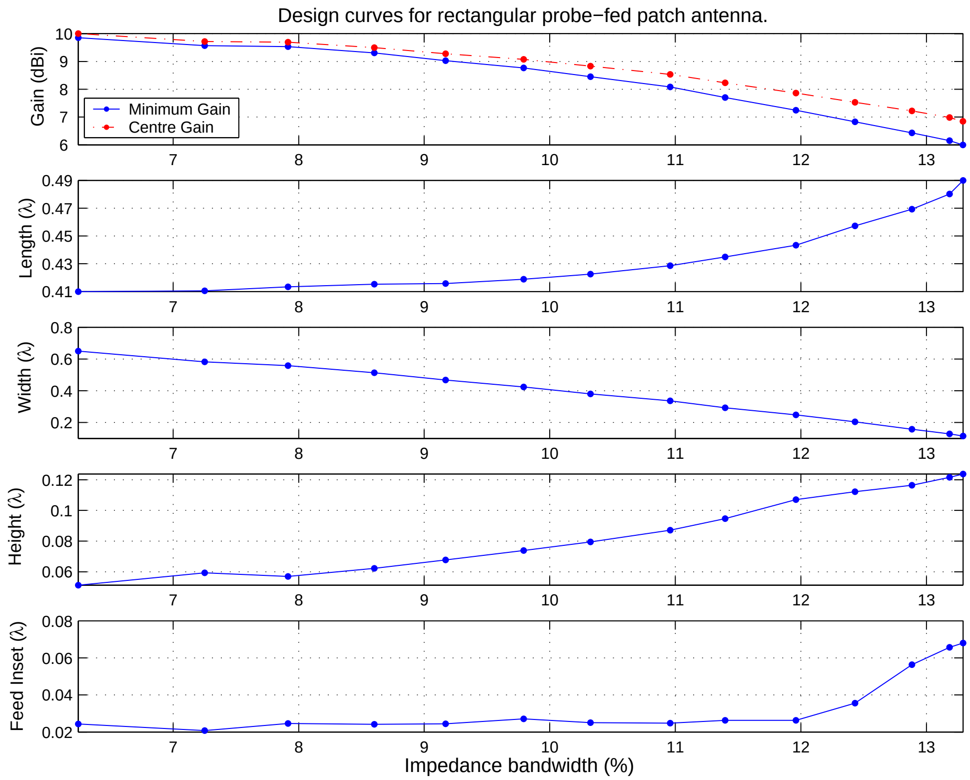

Fig. 46. Probe-fed patch design curves.

given in wavelength, can similarly be read off the plots following the gain vs. bandwidth plot. These curves allow a designer to find the geometrical characteristics of an antenna with a particular gain and bandwidth performance.

Plots of the performance characteristics verses frequency for the configurations used in the design curves can be seen in Figure 47, where a patch of length 30mm is used to exhibit the cases. The transition from higher gain, lower bandwidth characteristics to lower gain higher bandwidth characteristics can be seen as the plots move form left to right, top to bottom of the figure.

When viewing the design curve of length vs. bandwidth in Figure 46 it is apparent that a longer patch length is required for probe-fed patches operating at a specific frequency but requiring larger bandwidth. This behaviour is evident in Figure 47 where operating frequency increases from 4159MHZ to 4917MHz, as the same length value of 30mm is used for all the cases.

The design curves are fairly smooth and monotonic, implying that interpolation between the given data points should yield reasonable results. This was investigated by interpolating 50 linearly spaced data points over the bandwidth range presented in Figure 10. The difference between interpolated and actual bandwidth, minimum gain and operating frequency characteristics were calculated. The bandwidth, minimum gain and operating frequency error did not exceed 2%, 1.5% and 0.5% respectively over the 50 interpolated data points. This implies that accurate designs can be interpolated between the given data points.

Use of these design curves is outlined in Section E-E.

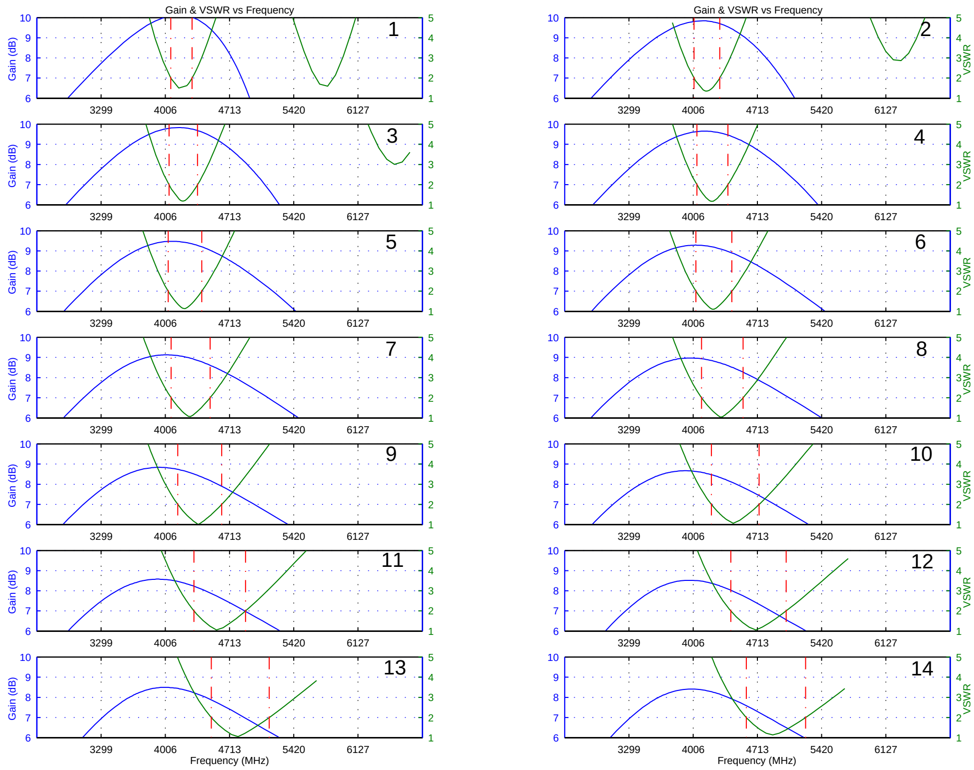

Fig. 47. Probe-fed patch Design curve cases for a length of 30mm. The designs increase in bandwidth and decrease in minimum gain from left to right, top to bottom (case 1 – case 14).

D. Electromagnetically Coupled Patch Design Curves

The design variables for the electromagnetically coupled patch, selected in Section D-D of Appendix D, are:

- Length
- Width
- Height
- Feed overlap
- Feed length
- Feed height

The feed offset was set to 0 and the feed diameter is dependant on the frequency of operation, as shown in Equation 14.

The gain constraint for the generation of this antenna's design curves was defined explicitly in the optimization problem, as the parameter study of Appendix D, Section D-D indicated that the antenna gain was dependant on multiple parameters. The gain constraint was implemented by penalizing the optimization result with a value dependant on the difference between the actual and required minimum gain. The resulting design curves can be seen in Figures 49 and 50.

The x-axis for all the design curve plots represents the percentage impedance bandwidth that a particular patch antenna design can offer. The minimum gain (and centre gain) corresponding to a particular bandwidth percentage can be read off the top-most graph. Given the required antenna impedance bandwidth, the length, width, height and feed overlap, feed length and feed height geometrical antenna characteristics, given in wavelength, can similarly be read off the plots following

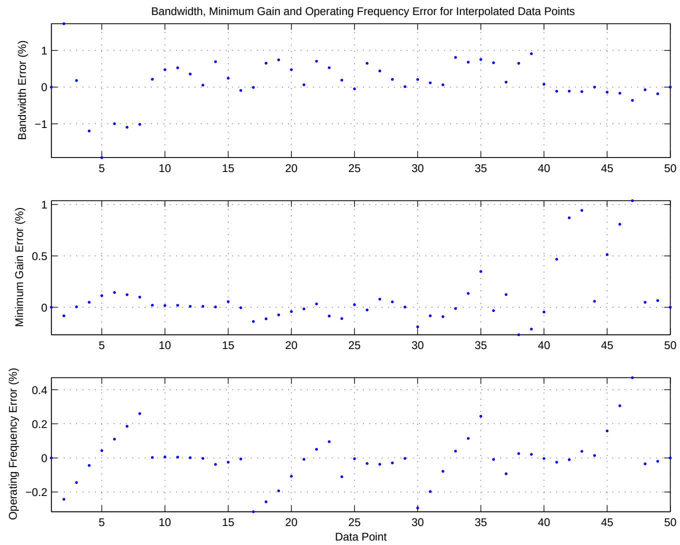

Fig. 48. Interpolation error for the probe-fed patch design curves.

the gain vs. bandwidth plot. These curves allow a designer to find the geometrical characteristics of an antenna with a particular gain and bandwidth performance.

The erratic nature of the width and feed overlap parameters in the design curves may imply that the performance parameters are less sensitive to these geometrical parameters, relative to the other geometrical parameters, although it could be loosely said that a larger width allows a larger minimum gain. The length also appears to be erratic but varies over a relatively small range from 0.36λ to 0.38λ, indicating that the length value is actually quite constant. The height, feed length and feed height are shown to be relatively smooth and monotonic over relatively significant ranges, implying a strong dependance of the performance parameters on these geometrical parameters.

Another possible explanation for the erratic behaviour of the electromagnetically coupled patches design curves is that, due to the antennas many parameters, multiple patch configurations can give satisfactory solutions for a particular optimization problem. The given data may consist of a variety of these configurations. The resulting performance characteristics of the configurations used in the design curves can be seen in Figure 51, which uses a patch of length 30mm to exhibit the cases. The transition from higher gain, lower bandwidth characteristics to lower gain higher bandwidth characteristics can be seen as the plots move form left to right, top to bottom.

As expected, the operating frequency remains relatively constant for the cases shown in Figure 51 with a mean value of 3694MHz, a maximum value of 3840MHz and a minimum value of 3576MHz.

Inaccuracy in the performance characteristics may be introduced when interpolating a design between the given data points. In order to quantify this inaccuracy 50 linearly spaced data points were interpolated over the bandwidth range presented in Figure 49. The difference between interpolated and actual bandwidth, minimum gain and operating frequency characteristics were calculated and the results can be seen in Figure 52. The bandwidth, minimum gain and operating frequency error did not exceed 12%, 4% and 1% respectively over the 50 interpolated data points. This implies that reasonable designs can be interpolated between the given data points.

The 50th data point shown in Figure 52 corresponds to the error between the final data point in the design curves and the final interpolated data point. The small error between the interpolated data and the design curve data seen here is thus unexpected. This unexpected error is attributed to the fact that the simulation frequency range, and hence segmentation frequency, was extended by a small amount during the design curve data generation process. It was necessary to extend the simulation

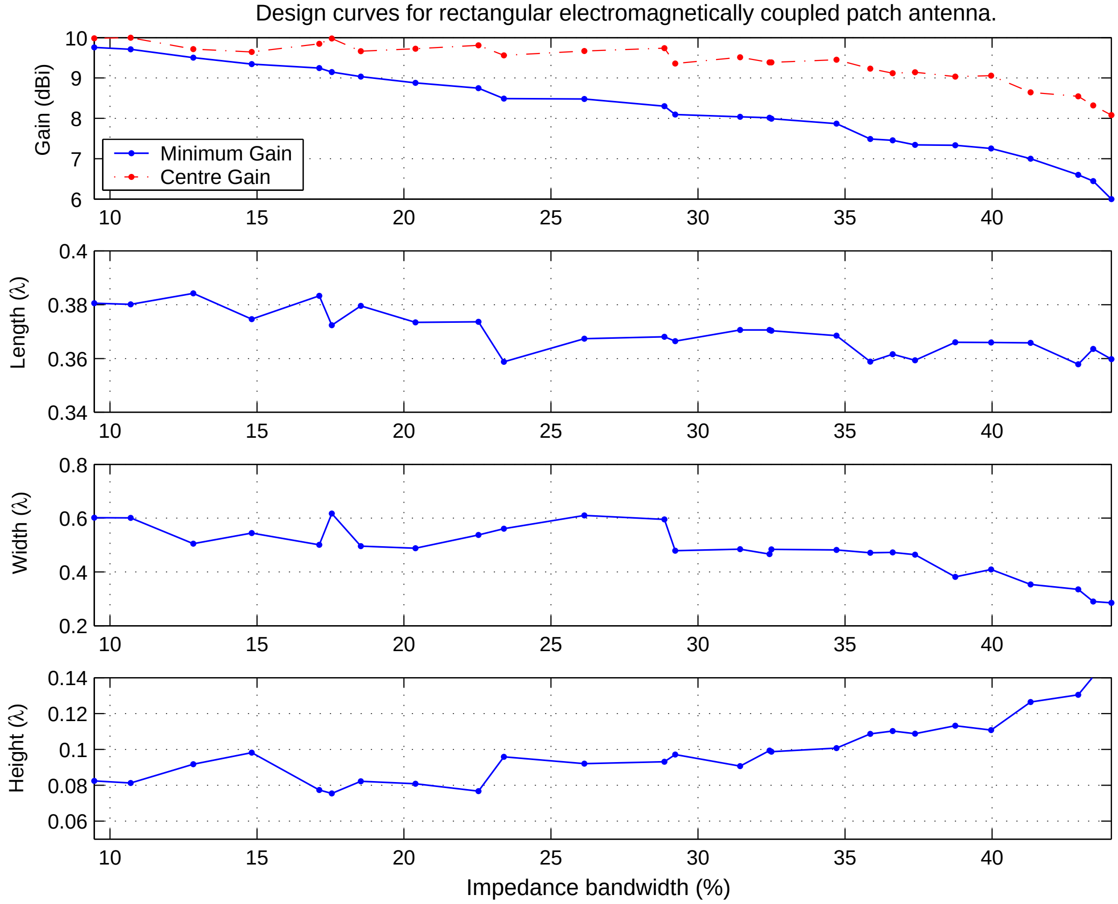

Fig. 49. Electromagnetically coupled patch design curves (gain, length, width and height characteristics).

frequency range in order to realise valid SUPERNEC models for certain gain constraint values. The entire interpolated data set is generated using the extended frequency range. This change of segmentation frequency has a small effect on the results, as discussed in Appendix C Section C-B. A change in the simulation frequency range was not required for the probe-fed patch, which shows perfect agreement between the final design curve data point and interpolated data point in Figure 48.

Use of these design curves is outlined in Section E-E.

E. Using Design Curves

The design curves shown in Sections E-C and E-D are used to select the patch geometrical characteristics given specifications for the operating frequency, minimum gain and impedance bandwidth requirements for the application. The gain at the centre frequency is also shown in these design curves and could be used for design purposes if appropriate. This section shows two examples of how the design curves could be used during the design process. The first examples makes use of the design curves for the probe-fed patch and the second examples makes use of the design curves for the electromagnetically coupled patch.

Example 1: A probe-fed patch must be designed for operation at 5GHz and provide a minimum gain of 9dBi over it's frequency range of operation. The antenna should operate between 4750MHz and 5250MHz.

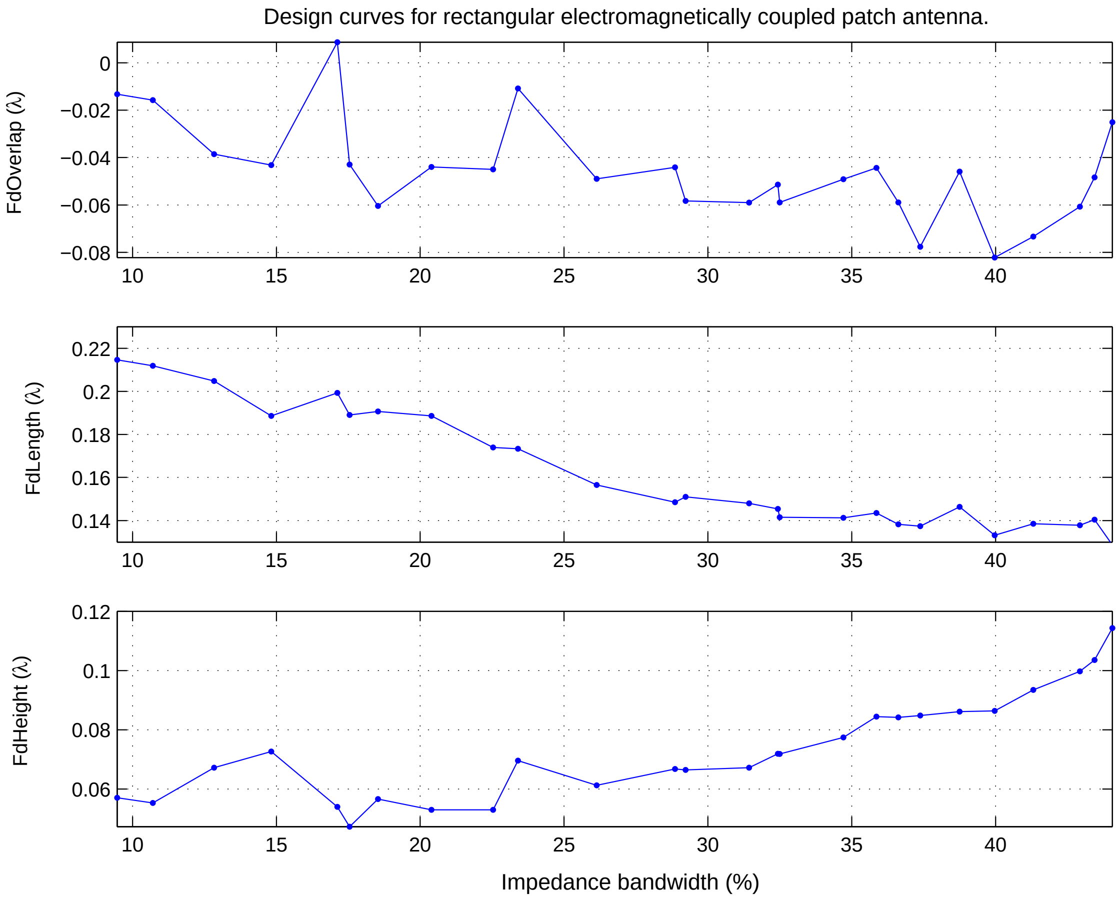

Fig. 50. Electromagnetically coupled patch design curves (feed characteristics).

The specified frequency range of operation requires the antenna to have a bandwidth of 500MHz or 10%. When viewing Figure 46 it is apparent that a bandwidth of 10% requires the minimum gain to be limited to 8.6dBi. It is therefore not possible to meet the specification with the basic probe-fed patch configuration as given in the design curves. In this case a preliminary design could be chosen from the design curves and enhanced further via specialised simulation iterations. The preliminary design, which reaches a compromise between the required bandwidth and minimum gain, exhibits a bandwidth of 9.5% and minimum gain of 8.8dBi. The design for an impedance bandwidth of 9.5% can be read off Figure 53 by finding the value at which the curves cut the 9.5% impedance bandwidth line.

The antenna's geometrical values, which correspond to the desired impedance bandwidth value, are read off the design curves in terms of wavelength. These geometrical parameters can then be multiplied by the wavelength corresponding to the desired operating frequency (see Equation 10) and thus converted into distance. Using Equation 10, the wavelength for this example is found to be $\lambda_{\mathrm{op}} = 300/5000$ which results in $\lambda_{\mathrm{op}} = 0.06\mathrm{m}$. The required geometrical parameters, in terms of wavelength and meters, are shown below:

- Length = $0.425\lambda_{op}$ (0.0255m).
- Width = $0.415\lambda_{op}$ (0.0249m).
- Height = $0.0752\lambda_{op}$ (0.0045m).
- Feed inset = $0.0266\lambda_{op}$ (0.0016m).

The feed radius can be calculated using Equations 12 and 13:

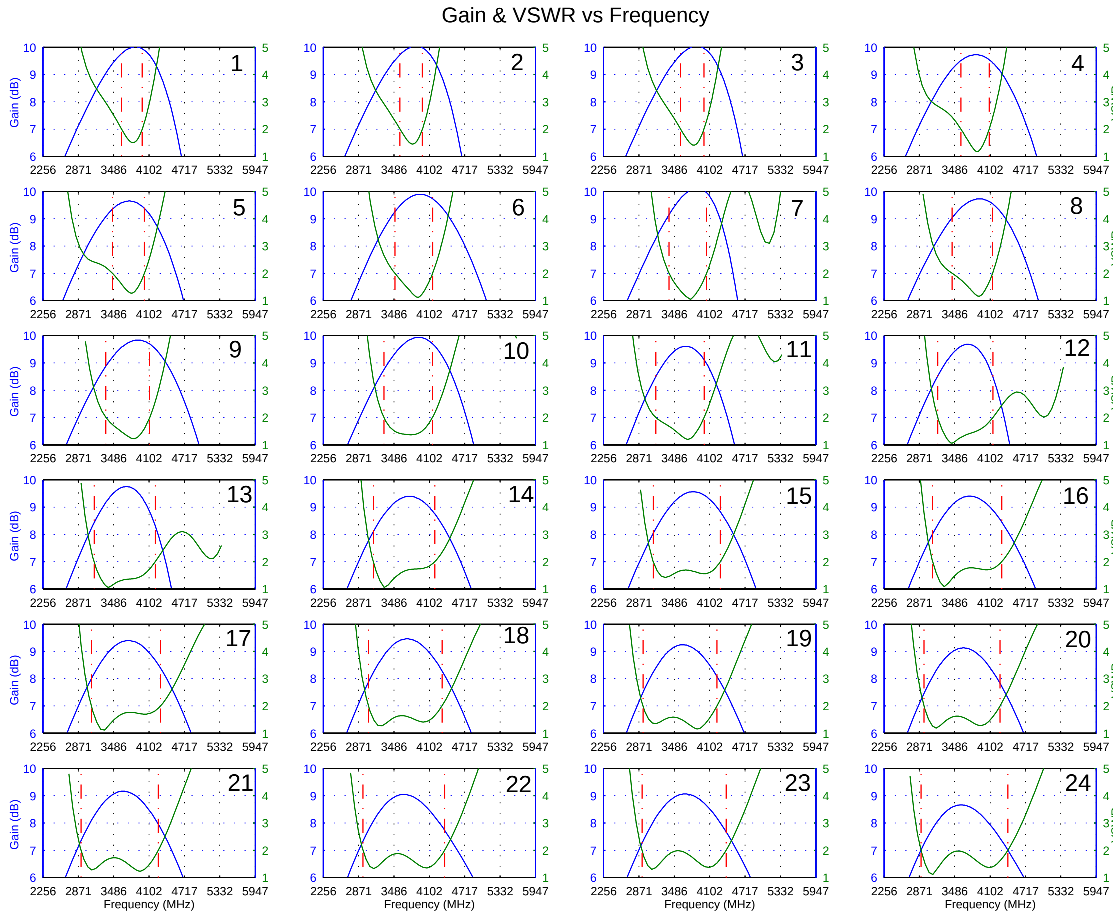

Fig. 51. Electromagnetically coupled patch design curve cases for a length of 30mm. The designs increase in bandwidth and decrease in minimum gain from left to right, top to bottom (case 1 – case 24).

Using Equation 13:

$$FS = -0.01(9.5)^2 + 0.096(9.5) + 2.218$$
$$FS = 2.2275$$

Using Equation 12:

$$FeedRadius = \frac{0.1 \times 0.06}{2 \times 2.2275 \times \pi}$$

$$FeedRadius = 4.28 \times 10^{-4} m$$

Example 2: An antenna must be designed for a bandwidth of at least 30% with an operating frequency of 2GHz.

The probe-fed patch is not suitable for an application with the specified bandwidth requirement, as this patch can offer a maximum of just over 13% bandwidth. An electromagnetically coupled patch will therefore be designed for this application, as this configuration offers a bandwidth of up to 44%. In order to eliminate interpolation error, the actual design curve data point which exhibits a gain of 8dBi and impedance bandwidth of 31% will be used. This design can be read off the electromagnetically coupled patch design curves, as shown in Figures 54 and 55, by finding the value at which the curves cut the 31% impedance bandwidth line.

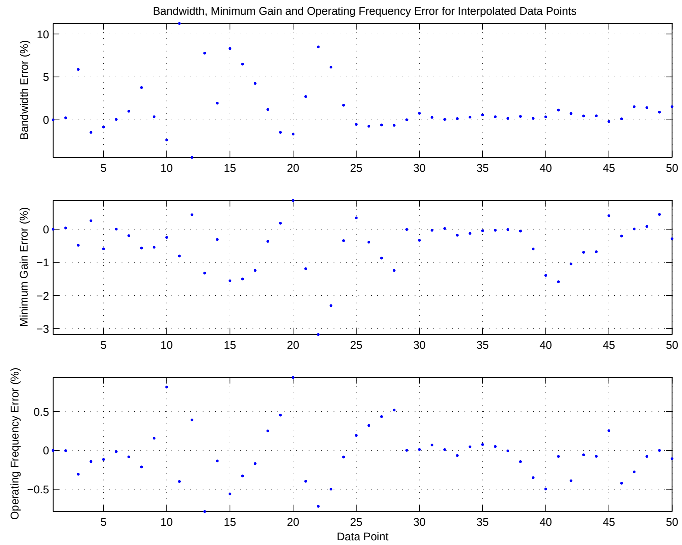

Fig. 52. Interpolation error for the electromagnetically coupled patch design curves.

Using Equation 10 the wavelength for this example is found to be $\lambda_{op} = 300/2000$ which results in $\lambda_{\mathrm{op}} = 0.15\mathrm{m}$. The required geometrical parameters, in terms of wavelength and meters, are shown below:

- Length = $0.370\lambda_{op}$ (0.0555m).
- Width = $0.484\lambda_{op}$ (0.0726m).
- Height = $0.0906\lambda_{op}$ (0.0136m).
- Feed overlap = $-0.0589\lambda_{op}$ (-0.0088m).
- Feed length = $0.147\lambda_{op}$ (0.0220m).
- Feed height = $0.0671\lambda_{op}$ (0.0101m).

The feed radius can be calculated using Equations 14 and 15:

Using Equation 15:

$$FS = -63 \times 10^{-5}(31)^2 + 0.036(31) + 2.238$$
$$FS = 2.7486$$

Using Equation 14:

$$FeedDiameter = \frac{0.1 \times (0.15)}{2.7486 \times \pi}$$

$$FeedDiameter = 0.0017m$$

F. Conclusion

This appendix presented the formulation of design curves for basic, rectangular probe-fed and electromagnetically coupled patch antennas. The design curve data was generated by solving an impedance bandwidth optimization problem, as outlined in Section E-B, in which the minimum gain over the antenna's frequency band of operation was constrained. That is, a sequence of optimization routines were performed which maximized the impedance bandwidth subject to a different minimum gain constraint. The gain constraint varied from 9dBi to an unconstrained optimization,

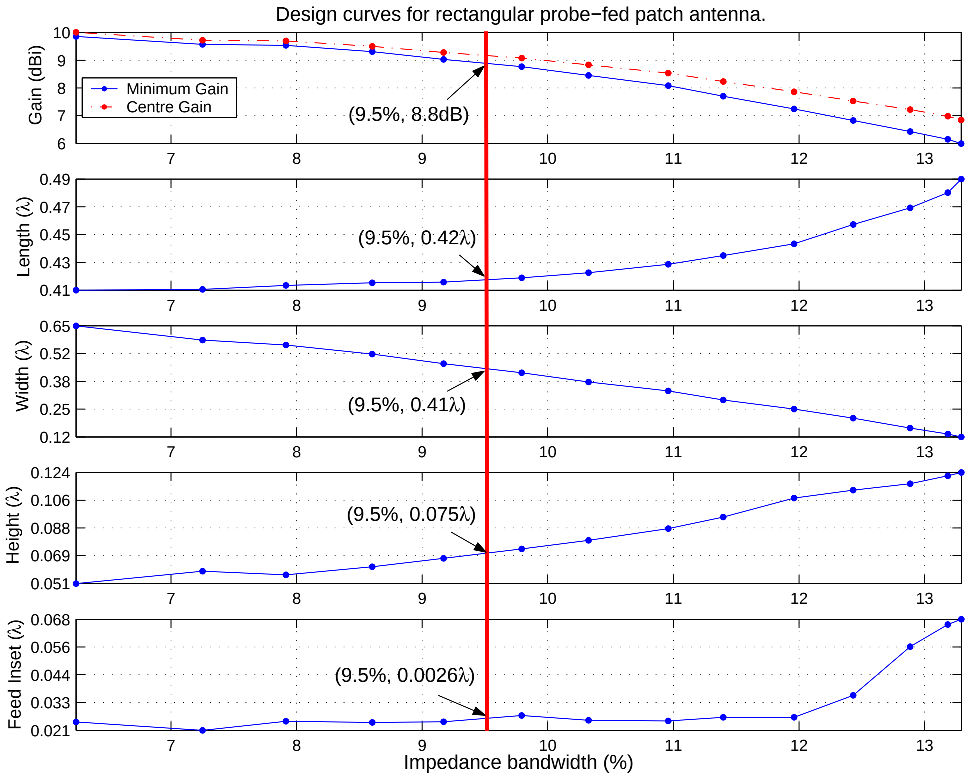

Fig. 53. Example 1: Using probe-fed patch design curves.

which resulted in a 6dBi minimum gain.

The gain constraint was implemented implicitly for the probe-fed patch, by fixing the width value with which the optimization was performed. The gain constraint for the electromagnetically coupled patch was implemented explicitly by penalizing the optimization's score, the severity of the penalty depended on the square of the difference between the actual and required minimum gain values. The results of the design curve generation for the probe-fed and electromagnetically coupled patches were shown in Sections E-C and E-D respectively. Reasonably small errors resulted from interpolation between the given data points on the design curves in general, although errors of up to 12% in bandwidth resulted for the electromagnetically coupled patch due to the erratic nature of this antenna's curves. Examples of using the design curves to find an initial design were shown in Section E-E.

It could be argued that if a patch antenna optimization program is available, then design curves are unnecessary. The optimization approach alone may be suitable for once-off, specialized antennas whose performance parameters are not required to vary in future designs. However, the optimization routine can be time consuming. The more design parameters that need to be varied during the optimization, the longer the routine takes. The optimization of a single electromagnetically fed patch, with 5 actively varied geometrical parameters, would take 3 to 4 days (on a P4 3GHz machine). Once design curves are available it takes a couple of minutes to find an appropriate design. Obviously the initial generation of the design curves takes a considerable amount of time and processing power, but once available allow a substantial reduction in design time.

Limitations of the design curves presented in this appendix are summarized below:

- Due to limitations of the simulation software, the design curves are only valid for an air substrate. However, when the simulation software supports the use of dielectrics with various

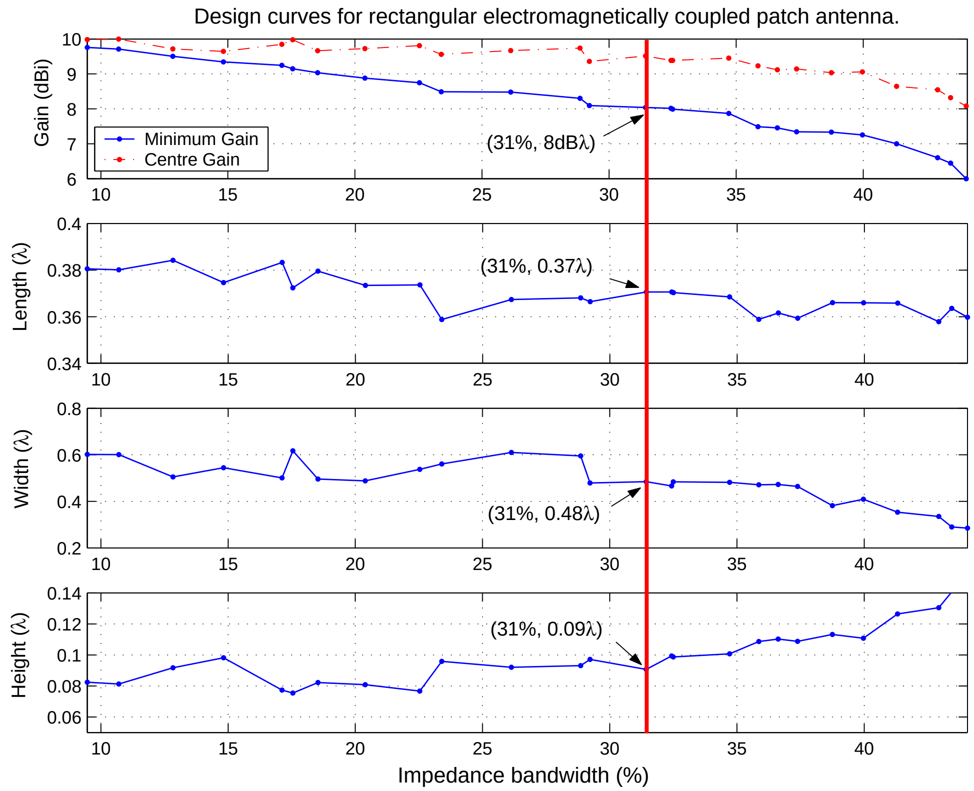

Fig. 54. Example 2: Using electromagnetically coupled patch design curves (gain, length, width and height characteristics).

relative permittivities, the optimization code could be re-used for generating design curve data given a specified substrate. As, practically, the available substrates that are suitable for patch antennas are limited, a set of design curves for the most popular substrates could be generated.

- The shape of the antenna's radiation pattern was not investigated in detail, as operation in the TM_{10} mode with a known minimum and centre gain was assumed sufficient for the purposes of this paper. The radiation pattern could form part of the optimization problem's objectives or constraints if this was found necessary for a particular application.
- The parameter study is limited to patch configurations with design characteristics deemed significant for this research, so parameter study results for other patch configurations may hint at different conclusions.
- The design curves assume an infinite ground plane. If a small ground-plane with a length of less than three times the patch length is used, then the recommended design approach would be to select the appropriate patch configuration from the design curves and simulate this configuration with the limited ground-plane. The antennas parameters can then be tuned in the simulation environment.

Patch antenna size is often of interest, specifically the reduction of the antennas size for the purposes of installation in limited available space. Thus the design of a patch antenna could have a secondary objective of minimizing the antenna size. Future investigation of patch antenna design could implement this objective, the use of substrates other than air and perhaps focus on more specialized antenna configurations which have become popular for various applications.

Although the design curves have been presented graphically in this appendix, the ideal form and use of the curves would be via a computer program. It would take little effort to create a program which allows interpolation/selection of designs and implements all the necessary calculations, given the required operating frequency of the design. This would allow an initial design to be rapidly realized with little opportunity for human error.

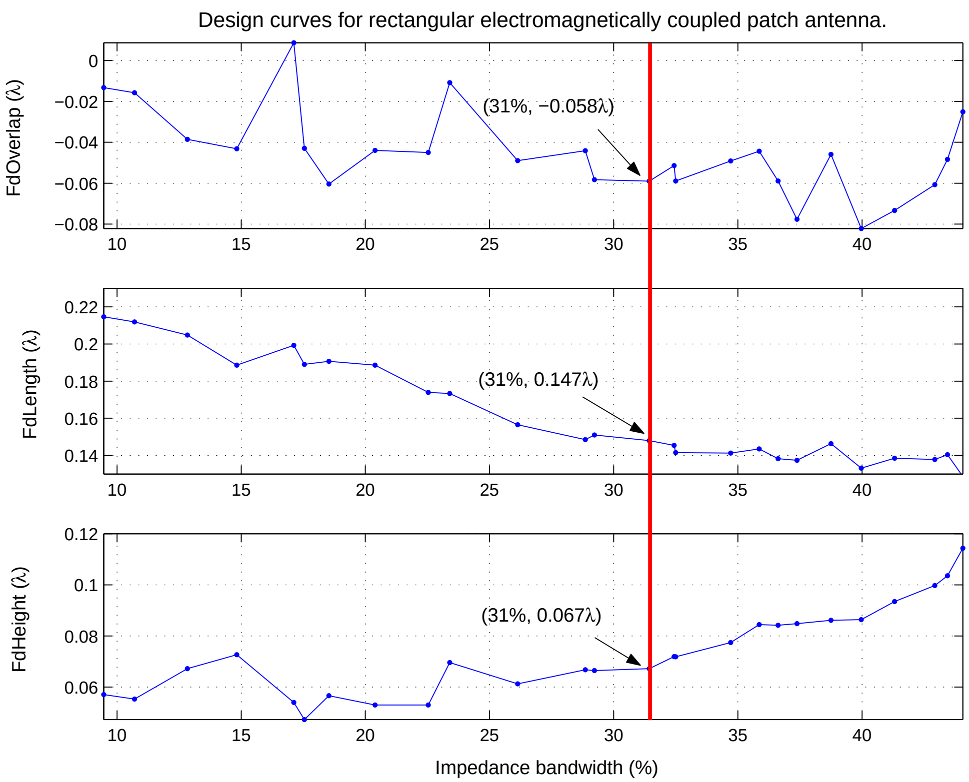

Fig. 55. Example 2: Using electromagnetically coupled patch design curves (feed characteristics).

APPENDIX F:
PATCH ANTENNA DESIGN CD CONTENTS

A. CD Contents

The CD provided with this dissertation contains all the code and documentation relevant to this MSc. A basic outline of the CD directory structure is presented below:

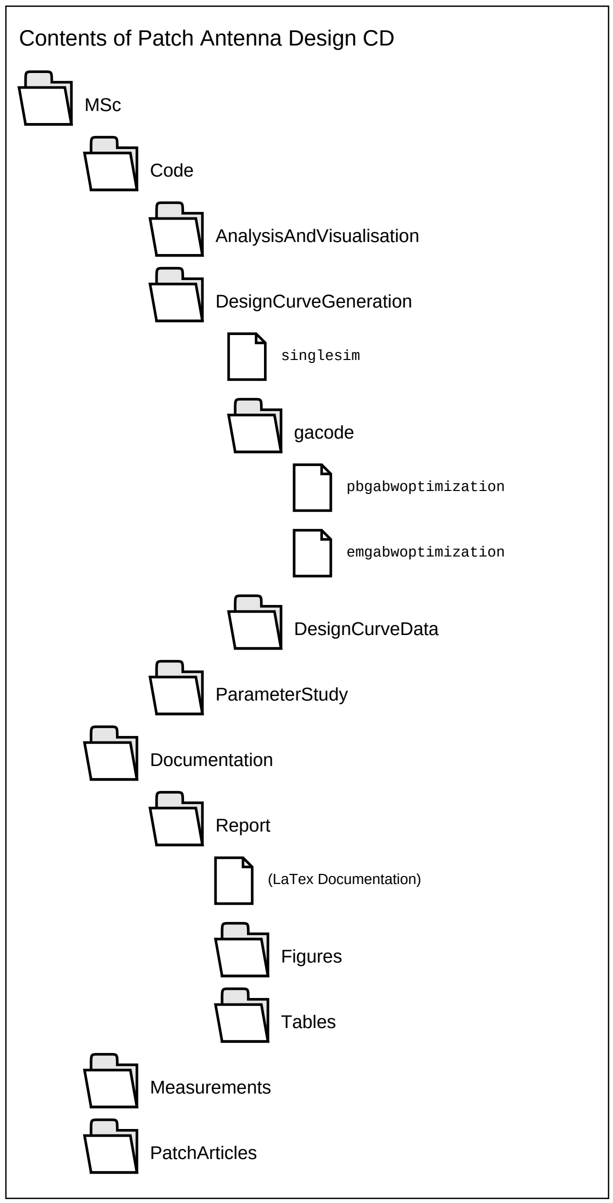

Fig. 56. Directory structure of Patch Antenna Design dissertation CD.